

Instituto Nacional de Matemática Pura e Aplicada

Organizing structures in the Riemann solution for
thermal multiphase flow in porous media.

Estruturas de organização na solução de Riemann para
escoamentos multifásicos térmicos em meios porosos.

Julio Daniel M. Silva

Orientador: Dan Marchesin (IMPA)

Co-orientador: Johannes Bruining (TU-Delft)

August – 2011

Abstract

The aim of this work is to construct the solution to a nonlinear system of conservation laws arising in petroleum engineering for a model that describes the injection of a mixture of gas and oil, in any proportion, into a porous medium filled with a similar mixture, at different temperatures. The model allows the existence of fluids in three thermodynamical configurations, namely: a single phase gas configuration, a single phase liquid configuration and a two-phase configuration. The solutions are constructed around two organizing structures. The first is a singular point, intrinsically associated to most bifurcations in the Riemann solutions for this class of models. The second is the interface between the two-phase configuration and the single-phase liquid configuration in state space; the change of thermodynamical configuration introduces a new pattern in the Riemann solutions.

Resumo

O objetivo deste trabalho é construir soluções para um sistema de leis de conservação proveniente da engenharia de petróleo, para um modelo que descreve a injeção de uma mistura de gás e óleo, dados em quaisquer proporções, em um meio poroso preenchido com outra mistura semelhante. Ele permite a existência de fluidos em três diferentes configurações termodinâmicas, a saber: uma configuração monofásica onde há somente gás, uma configuração monofásica onde há somente líquido e uma configuração bifásica. As soluções são construídas em torno de duas estruturas de organização. A primeira é um ponto singular, intrinsecamente associado à maioria das bifurcações nas soluções de Riemann, nesta classe de modelos. A segunda é a interface entre a configuração bifásica e a configuração monofásica onde há apenas líquido; a mudança de configuração termodinâmica nesta interface introduz um novo tipo de padrão nas soluções de Riemann.

Agradecimentos

Escrever um agradecimento é muito difícil. Não há idioma apto a expressar os sentimentos de quem escreve nem papel grande o suficiente para conter todos que merecem ser lembrados. Deixo minha impressão aqui, incompleta. Temo que ao completá-la não sobraria espaço para o texto que segue.

Agradeço à minha esposa Clarissa. Sua simplicidade me ilumina e inspira: é o modelo que um dia, rogo, ser capaz de alcançar. Agradeço aos meus pais Nelma e Norival e ao meu irmão André Felipe. Eles são a base sólida que sustenta o que sou hoje. Aos meus familiares muito obrigado.

Agradeço aos amigos que fiz no IMPA, cuja nobre companhia tornou estes tempos memoráveis. Carlo Pietro, Maria, Emílio, Cristina, Ives, Fernando Marek, Tertuliano, Marcelo Hilário, Marcelo Cicconet, Fábio Simas, Fábio XP, Adriana Neumann, Patricia Cirilo, Augusto, Daniel Valesin, Guilherme, Carlos, Gabriela, Renato, Laura e Ítalo: muito obrigado! Agradeço aos amigos que ouviram muitas besteiras em seminários intermináveis: Grigori, Pablo, Panters, Helmut, Vítor e Wanderson.

Agradeço aos orientadores Dan e Hans. Muito obrigado pela disposição e boa vontade! Este trabalho nada seria sem vocês. Ao Dan que tanto tentou me ensinar, muito mais do que matemática: espero não ter sido teimoso demais.

Agradeço aos professores André, Cido, Fred, Eduardo e Christian. Ao André, Cido e Fred que foram parte da banca e muito contribuíram com suas sugestões. A eles também por tudo que contribuíram antes de serem integrantes da banca. Ao Christian que me apresentou ao IMPA: muito obrigado.

Agradeço aos funcionários do IMPA e ao ensino sempre dispostos a ajudar.

Agradeço aos funcionários do FLUID, aptos a resolver todos aqueles problemas que eu sequer desconfiava que tinha. Obrigado Sérgio, Ankie e Sami: acho que perturbei a vocês mais do que aos outros.

De todos estes, bem como daqueles não citados, espero ter sido digno da honra que foi tê-los como amigos.

Ao fim, mas não menos importante, agradeço ao IMPA pelo excelente ambiente e à ANP pelo auxílio financeiro.

Contents

1	Introduction	1
1.1	Foundations	2
1.2	Current theory of multiphase flow	4
2	Preliminaries	8
2.1	General theory	8
2.1.1	Self-similar solutions	9
2.2	The Riemann problem	12
2.2.1	Shock waves	13
2.2.2	Rarefaction waves	15
2.2.3	Admissibility criteria	15
2.2.4	Wave groups and nomenclature	18
2.3	Bifurcation manifolds	20
2.3.1	Coincidence locus	20
2.3.2	Inflection locus	21
2.3.3	Self-intersection and secondary bifurcation loci	21
2.3.4	Double contact locus	22
2.3.5	Extension locus	23
2.4	On notation	24
3	Physical model	25
3.1	Flow of fluids and qualitative behavior	25
3.2	Thermodynamic fundamentals	25
3.2.1	Two-phase behavior	26
3.3	Darcy's law for two-phase flow	28
3.4	Balance equations	29
3.4.1	Mass balance equations	30
3.4.2	Energy balance equations	31

3.4.3	The main state space and state variables	31
3.5	Configurations in thermodynamical equilibrium	32
3.5.1	Single phase gaseous region (SPG)	32
3.5.2	Single phase liquid region (SPL)	34
3.5.3	Two-phase region (TP)	35
3.5.4	On notation	37
4	Basic facts on the two phase region	38
4.1	Characteristic speeds and eigenvectors	38
4.1.1	Calculations	39
4.2	Elementary wave curves	43
4.2.1	Rarefaction curves	43
4.2.2	Shock curves	45
4.3	Triple Shock Rule and properties of the Darcy speed	48
4.4	The Bethe-Wendroff Theorem	51
4.5	Bifurcation manifolds in TP	52
4.5.1	Coincidence locus	52
4.5.2	Inflection locus	55
4.5.3	The self-intersection set	57
4.5.4	Double contact locus	63
5	Riemann problem I in TP	64
5.1	Bifurcations in the Riemann solution	64
5.2	Region A	66
5.2.1	Riemann solutions with increasing temperatures	68
5.2.2	Riemann solutions with decreasing temperature	70
5.3	Region A'	73
5.3.1	Riemann solutions with decreasing temperature	74
5.4	Region B	75
5.4.1	Riemann solutions with decreasing temperatures	77
5.4.2	Riemann solutions with increasing temperatures	78
5.5	Region C	81
5.5.1	Riemann solutions	82
6	Intermezzo	85
6.1	Riemann solutions in TP	85
6.1.1	The influence of the exceptional locus on Riemann solutions	87

6.1.2	Riemann solutions near the pure oil boundary	88
6.2	Elementary waves in the SPL	91
6.3	Shock waves between regions	93
6.3.1	Shock waves from TP to SPL	94
6.3.2	Shock waves from SPL to TP	97
7	Riemann Problem II between TP and SPL	99
7.1	Riemann solutions for L in SPL	99
7.2	Riemann solutions for L in TP	104
A	Physical quantities	115
A.1	Physical quantities, symbols and values	115
A.1.1	Temperature dependent variables.	116

Chapter 1

Introduction

The aim of this work is to construct the solution for a nonlinear system of conservation laws arising in petroleum engineering. Our interest is two-fold. First, this system models proposed enhanced heavy oil recovery techniques. Second, it presents a unique combination of mathematical structures that elegantly determine the solutions. We postpone the discussion of the mathematical aspects of our work, and we focus on its application now.

Steam drive recovery of oil continues to be an economical way of producing heavy oil and is used world wide. The main challenges are to improve sweep efficiency and to improve recovery from the steam swept zone. Our interest focuses on the latter issue. In the late seventies, Dietz proposed to add small amounts of volatile oil to the steam. His view was that the volatile oil co-injected with the steam would displace the dead oil ahead of the steam condensation front leaving no oil behind in the steam swept zone. The stability of the steam displacement would guarantee an even distribution of volatile oil along the steam condensation front. Experiments investigating the mechanism are described in Bruining et al. [5], [6]. Similar ideas were put forward independently by Farouq Ali and Abad [18].

In this work, we pursue the analysis of the model in Bruining and Marchesin [4]. Their approach was to simplify the model equations in such a way that the essential elements are retained while avoiding the complexities of solving the pressure equation. The long term objective is the full Riemann solution for this model. We will soon enter into the details of Riemann solutions, for now it is sufficient to know that our interest hinges in its constructive nature. Once the Riemann solution is given, the full set of possible injection scenarios can be analyzed in a comprehensive manner.

The problem proposed by Bruining and Marchesin is very difficult in a different way. It adds thermodynamics and phase transitions to a problem already well known for its difficulty, namely the immiscible three-phase flow problem in porous media. We have no

hope of obtaining this solution right away: there is too much concurrent dynamics going on. Instead, in this work we set and solve the following subproblem: volatile oil in the form of gas is injected in a reservoir containing a mixture of the same volatile oil and dead oil. This is not only a necessary step, because it introduces thermodynamical behavior, which has been systematically neglected in the literature of multi-phase flow theory until very recent works of Bruining, among others.

We provide more details of the background for the theory of conservation laws in the next section, then proceed with multiphase flow theory. It is remarkable that one of the fundamental pieces in the Riemann solution, discontinuous solutions or shocks, were first understood during the century old struggle to understand gas flow in a tube. The main tool to settle the issue was Thermodynamics.

1.1 Foundations

An early reference to singular solutions is due to Stokes [47], in 1848. He was the first to characterize the jump conditions that a discontinuous solution must satisfy to guarantee conservation of a physical quantity when it flows. Stokes did this in the context of conservation of mass and momentum, in rectilinear isothermal flow of an ideal gas. His idea, however, was criticized: his discontinuous solutions failed to conserve mechanical energy. Convinced that a physical solution must conserve mechanical energy, Stokes abandoned his theory. The world had to wait the development of Thermodynamics for almost half a century, when the task of determining the jump conditions that express energy conservation in the presence of discontinuities was undertaken by Rankine [40] and Hugoniot [24], independently. Nowadays these jump conditions, which any weak solution of conservation laws must satisfy, bear their name.

A landmark in the theory of conservation laws was constructed by Riemann [42]. Riemann considered the one-dimensional flow of gas dictated by the Euler equations. He solved the initial value problem that nowadays bears his name, in which an initial jump in the state variables is generally resolved into an wave fan with a forward and a backward wave, either of which are allowed to be a (smooth) rarefaction wave or a (discontinuous) shock wave. He rediscovered the jump conditions satisfied by discontinuities in mass and momentum (without any mention to energy) and emphasized that only compressive shocks should be physically admissible, on the grounds of stability.

The observation that physically admissible discontinuous solutions must satisfy other restrictions besides the Rankine-Hugoniot jump conditions soon became a major concern. Both Stokes [47] and Hugoniot [24] were aware that heat conductivity would smear shocks.

This “vanishing viscosity” result was first formalized by Duhem [17]. Subsequent work, still in the context of polytropic gases, was done independently by Rayleigh [41] and Taylor [49], characterizing the structure of shocks.

The Second World War focused the attention of many top scientists on the conservation laws of gas dynamics. An important issue at time was the behavior of real gases, at high temperatures and pressure, far beyond the limits of the polytropic gas model. The work of Bethe [3] pointed out that the conditions used at the time to select physically admissible shocks were not sufficiently stringent: they may select unstable solutions, especially in the case of strong shocks. At the same time the work of Weyl [53] extended the aforementioned work on shock structure, noticing that the existence of a particular shock was related to a repeller-saddle connection in an underlying system of ordinary differential equations. The definitive treatment of this problem was provided two years later by Gilbarg [21]. Concurrent work was done independently by Courant and Friedrichs [12] and Gel'fand [20].

In the fifties, the area of partial differential equations experienced a change of trend: the qualitative theory and well posedness of the Cauchy problem became a major topic. The works of Hopf [23] and Cole [9] established the well posedness of weak solutions in the large for the the Burgers equation. Later, the work of Lax [32] became a new landmark. He extended the work of Hopf, solving the Cauchy problem for the general case of scalar conservation laws with convex flux. Convexity was the key point, allowing one to select admissible shocks on the sole ground of compressibility. With the Euler equations in mind, Lax crafted the concept of genuine nonlinearity, and showed that for systems it generalizes convexity for scalar equations. Genuine nonlinearity together with strict hyperbolicity are the main concepts needed to define what is nowadays known as the Lax conditions. Lax provided a general construction of shock and rarefaction wave curves as tools to solve Riemann problems, setting the direction of modern research in the Riemann solution, using gas dynamics as a prototype. All this work culminated in the seminal contribution of Glimm [22], who was able to guarantee well posedness in the large for Cauchy solutions with “small” initial datum, using Riemann solutions as building blocks. Glimm was able to show that, under certain hypotheses, all wave interactions in the Cauchy problem for systems can be resolved in terms of Riemann solutions. His work hinged on the same hypotheses of genuine nonlinearity and strict hyperbolicity, the very hypotheses that are violated in our model.

These are the early foundations of the theory for hyperbolic conservation laws. Later more general equations began to be considered, such as flow in porous media. They failed to fulfill one or both of these hypotheses. The result was chaos: even existence

and admissibility of solutions raise thorny issues. Wave fans began to display unusual structures and wave interactions became a major problem: the existence of resonance in wave speeds led to new amplifications both in the size as in the variation of solutions. As a result, a fully encompassing theory is not available yet. Instead, one interested in those phenomena nowadays should focus on specific systems arising from continuum physics. These systems have showed so far a common feature: they remain solvable, despite of the oddities. The quest to discover the properties that distinguish solvable from unsolvable general models is still open.

1.2 Current theory of multiphase flow

The theory of multiphase flow in porous media, as an application of conservation laws theory, has its roots in the work of Buckley and Leverett [8], in the context of immiscible two-phase oil displacement by either gas or water. We will not elaborate on the implications of this work in the engineering community, but refer the reader to the book of Lake [27]. Immiscible three-phase flow models were proposed in the works of Stone [48] and Corey et al. [11]. In three-phase flow systems of conservation laws, both genuine nonlinearity and strict hyperbolicity fail to such a degree that subtleties of the theory still require active work today. A comprehensive survey on mathematical theory of Riemann problems relevant for multi-phase flow in porous media can be found in Marchesin and Plohr [36].

Genuine nonlinearity is related to monotonicity; its role is to generate separate compression and rarefaction waves. In the former gradients increase in the solution while in the latter gradients decrease. One of the effects of lack of genuine nonlinearity is the existence of “middle ground” waves, for example contact waves which are neither compression nor rarefaction waves. When genuine nonlinearity fails, the compression requirement alone is typically insufficient to select physically admissible shocks. Models with such behavior were an early concern to the Russian school. The fact that the “vanishing viscosity” argument can be applied to general systems is due to Gel’fand [20]. Courant and Friedrichs [12] also mention an analogous result in the context of gas dynamics with reactions. Unfortunately the viscous profile criterion, used to select physically admissible shocks, is too difficult to be used systematically. The work of Oleřnik [39] identified a simple criterion (which bears her name today) equivalent to the viscous profile criterion in the restricted scope of scalar equations; this set of ideas was advanced independently in the Engineering community, giving rise to the “Fractional Flow Theory”, see *e.g.* Lake [27]. In the West, Liu [33], [34] was able to extend the work of Oleřnik to systems and

override some of the difficulties imposed by loss of genuine nonlinearity. The equivalence of the Liu criterion and the viscous profile criterion was established later in certain cases, see Conlon [10] and Majda and Pego [35].

Loss of strict hyperbolicity is a more serious problem and history has shown that the current results tend to be restricted to the particular models in question. An early sign of difficulty is found in Isaacson et al. [25]. There the existence of transitional (or undercompressive) waves was established: admissible shock waves in the sense of the viscous profile that fail to be admissible under any other criterion. Their existence shows that the Liu criterion may not always be adapted to non-strictly hyperbolic systems of conservation laws.

The work of Isaacson, Marchesin, Plohr, and Temple [26] presented the Riemann solution for immiscible three-phase flow, with equal viscosities. This particular case, full of symmetries, is an insightful example of the complicated bifurcation pattern a Riemann solution may possess. This symmetry was broken in the work of de Souza [14], which let one of the viscosities be slightly different from the others – opening the door to structural stability of Riemann solutions resulting from changes in the flux function.

Structural stability for Riemann solutions with respect to their initial datum was established in the beautiful and never-aging monograph by Furtado [19] and extended to non-degenerate, non-strictly hyperbolic systems in Schechter et al. [44], [45]. The use of the viscous profile criterion led to the profound observation that unstable dynamics in the underlying EDOs, used to select admissible (transitional or undercompressive) shocks, may lead to stable behavior in the PDEs. This work was pursued by Zumbrun and Howard [54], [55] and others.

Closer to our work are thermal multiphase flow models in porous media. The typical interest is the transport of hot fluids undergoing mass transfer between phases. The work of Bruining et al. [7] brought the possibility of phase transitions to conservation laws modeling multiphase flow. They solved the Riemann problem for water-steam injection into a reservoir containing water. This work was extended by Lambert et al. [30] who solved the complete Riemann problem for the water-steam injection problem. An important part of the general theory for thermal multiphase flow was established in Lambert [28], [29] and [31].

Our work intends to address gas injection into a porous medium filled with a mixture of oil and dissolved gas. Our main objective is the solution of the Riemann problem in the neighborhood of two particular structures, namely a singular point as well as an interface between different thermodynamical configurations; the latter differ in the number or type of phases present. As in the case of previous works in thermal multiphase flow, we allow

the fluids to be in different physical configurations, in a way that will be soon explained. Those are the fundamental tools to construct the full Riemann solution in our case. “Singular point” is a name usually given to points where strict hyperbolicity fails in an egregious manner, greatly complicating the Riemann solution. Umbilic points [26] are a known example of such points. Our case, however, is more similar to those found in the works of de Souza and Marchesin [15], [16], with the remarkable difference that in our model they are not related to linear degeneracy.

This thesis is structured as follows. In Chapter 2 we give an overview of the general theory for systems of conservation laws arising in thermal multiphase flow in porous media. We state the Riemann problem in this class and present definitions and facts needed to properly describe the basic bifurcations in Riemann solutions. This chapter is fundamental for understanding the material presented later. Even specialists in three-phase flow theory should read it quickly to become aware of its subtleties. We warn the non-specialist that this review is rather concise. Unfortunately, most of this material is too new to be found in books.

Following [4], in Chapter 3 we present the model that describes the injection of a mixture of gas and oil (in any proportions) into a porous medium filled with another such mixture. Here, the oil is composed of two miscible components: a light alkane (allowed to vaporize) and a dead alkane. This model allows the existence of fluids in three thermodynamical configurations, namely: a single phase gas configuration, a two-phase configuration and a single phase liquid configuration. The two-phase configuration is the most complex and interesting of the three: it contains the singular points and is intrinsically associated to most bifurcations in the Riemann solutions. The interface between the two-phase region and the single-phase liquid region is the aforementioned interface that plays a significant role in the Riemann solutions.

In Chapter 4 we focus on the two-phase region. We set and prove the basic results needed in the chapters that follow. It includes basic wave structures, bifurcation results and some remarkable properties of this class of problems. This chapter is crucial for understanding the Riemann solutions.

In Chapter 5 we solve the Riemann problem in a neighborhood of the singular point in the two-phase region. The structure responsible for “gas condensation” appears here. Particularly interesting is the discovery of a very strong degeneracy: the Riemann solution is given by a unique wave group in a full open set of Riemann data. Another interesting result is a characterization of wave interactions induced by this singular point: changes in one variable, namely the temperature, can greatly amplify the variation of the other variable, namely the saturation.

In Chapter 6 we state the basic results and definitions needed to describe the Riemann solutions in the two-phase region together with the single-phase liquid region. Our main motivation originates from a curious observation: it is not possible to solve the Riemann problem for any pair of left and right states in the two-phase region using only waves defined within the two-phase region. Nevertheless, it is still possible to find all Riemann solutions if one is allowed to use waves from other thermodynamical configurations, in addition to those defined inside the two-phase region. A similar statement holds for the single phase liquid region.

We finalize this work in Chapter 7 describing this Riemann solution in a neighborhood of the interface between the two-phase and the single-phase liquid regions.

Chapter 2

Preliminaries

In this chapter we review the relevant theory for systems that model multiphase flow in porous media with mass interchange between phases. This theory is less than ten years old and is far from complete.

2.1 General theory

We are interested in systems of conservation laws of the form:

$$\partial_t G(\mathbf{w}) + \partial_x u F(\mathbf{w}) = 0, \quad (2.1)$$

where $(\mathbf{w}, u) \in \Omega \times \mathbb{R}$ are functions of one space variable and time, $F, G : \Omega \mapsto \mathbb{R}^{n+1}$ are smooth maps and Ω is locally a n -dimensional Euclidean space, called state space. The variable u is commonly associated to a *speed* and has a special role since it does not appear in the accumulation term.

As it is widely known, see Dafermos [13], systems of conservation laws do not, generically, possess smooth solutions in the large. It is therefore necessary to look for a weak solution, *i.e.*, a pair $(\mathbf{w}, u) \in L^\infty(\mathbb{R} \times \mathbb{R}^+; \Omega \times \mathbb{R})$ that satisfies the integral relationship:

$$\int_0^{+\infty} \int_{-\infty}^{+\infty} [G(\mathbf{w}(x, t)) \partial_t \phi(x, t) + u(x, t) F(\mathbf{w}(x, t)) \partial_x \phi(x, t)] dx dt = 0, \quad (2.2)$$

for any smooth real valued function ϕ with compact support in $\mathbb{R} \times (0, +\infty)$, ignoring the initial datum for convenience.

2.1.1 Self-similar solutions

We focus on Equation (2.2). It is invariant under a uniform scaling of coordinates $(x, t) \mapsto (\alpha x, \alpha t)$, for any positive α ; hence we expect it to admit *self-similar* solutions. These are defined in the space-time half-plane and are constant along straight line rays emanating from the origin.

If $(\mathbf{w}(x, t), u(x, t))$ is a bounded weak self-similar solution of equation (2.2), it admits the representation (with a small abuse of notation):

$$\mathbf{w}(x, t) = \mathbf{w}\left(\frac{x}{t}\right) \quad \text{and} \quad u(x, t) = u\left(\frac{x}{t}\right), \quad (2.3)$$

where now (\mathbf{w}, u) is a pair of bounded measurable functions on the real line. In the new variable $\xi = x/t$, equation (2.2) can be rewritten as (see Dafermos [13], which we follow):

$$\int_0^{+\infty} \int_{-\infty}^{+\infty} [G(\mathbf{w}(\xi)) t \partial_t \phi(\xi t, t) + u(\xi) F(\mathbf{w}(\xi)) t \partial_x \phi(\xi t, t)] d\xi dt = 0. \quad (2.4)$$

We set

$$\eta(\xi) = \int_0^{+\infty} \phi(\xi t, t) dt, \quad (2.5)$$

and after a little computation we get (the dot on η denotes the derivative of η with respect to ξ):

$$\int_0^{+\infty} t \partial_x \phi(\xi t, t) dt = \dot{\eta}(\xi) \quad \text{and} \quad \int_0^{+\infty} t \partial_t \phi(\xi t, t) dt = -\eta(\xi) - \xi \dot{\eta}(\xi). \quad (2.6)$$

Substituting equations (2.6) in equation (2.4) we get:

$$\int_{-\infty}^{+\infty} \{[u(\xi) F(\mathbf{w}(\xi)) - \xi G(\mathbf{w}(\xi))] \dot{\eta}(\xi) - G(\mathbf{w}(\xi)) \eta(\xi)\} d\xi = 0. \quad (2.7)$$

Since equation (2.7) is satisfied by any η with compact support in the real line, it states that the pair (\mathbf{w}, u) must solve the ordinary differential equation

$$\frac{d}{d\xi} [u(\xi) F(\mathbf{w}(\xi)) - \xi G(\mathbf{w}(\xi))] + G(\mathbf{w}(\xi)) = 0, \quad (2.8)$$

in the weak sense. The boundedness hypothesis on the weak solution gives in particular that the function

$$\mathcal{H}(\xi) = u(\xi) F(\mathbf{w}(\xi)) - \xi G(\mathbf{w}(\xi)), \quad (2.9)$$

is Lipschitz continuous.

We first look at the jump discontinuities of (\mathbf{w}, u) , *i.e.*, points of discontinuity of (\mathbf{w}, u) for which the lateral limits exist. For a ξ_0 at which (\mathbf{w}, u) has a jump discontinuity we write the lateral limits as $\lim_{\xi \downarrow \xi_0} \mathbf{w}(\xi) = \mathbf{w}^+$, $\lim_{\xi \uparrow \xi_0} \mathbf{w}(\xi) = \mathbf{w}^-$ (and similarly for u) and use the continuity of \mathcal{H} to obtain the *Rankine-Hugoniot* equation:

$$u^+ F(\mathbf{w}^+) - u^- F(\mathbf{w}^-) - \xi_0 (G(\mathbf{w}^+) - G(\mathbf{w}^-)) = 0. \quad (2.10)$$

When ξ is a point of differentiability of (\mathbf{w}, u) we can proceed using the chain rule in equation (2.8). After taking the derivatives we write the $(n+1) \times (n+1)$ matrix (here the D stands for the derivative):

$$J(\mathbf{w}, u; \xi) = (uDF(\mathbf{w}) - \xi DG(\mathbf{w}), F(\mathbf{w})). \quad (2.11)$$

The functions DF, DG map the state space Ω into the space of linear transformations from \mathbb{R}^n to \mathbb{R}^{n+1} . Equation (2.8) can finally be rewritten as (the superscript T denotes matrix transposition):

$$J(\mathbf{w}, u; \xi) (\dot{\mathbf{w}}(\xi), \dot{u}(\xi))^T = 0, \quad (2.12)$$

which is a generalized eigenvector problem. The solutions of the generalized eigenvalue problem:

$$\det(J(\mathbf{w}, u; \lambda)) = 0, \quad (2.13)$$

are called *characteristic speeds* of the system (2.1), which we will suppose to be real numbers. Notice that if we rewrite an eigenvalue as $\lambda \equiv u\tilde{\lambda}$ and substitute into equation (2.13) we get (for non-zero u):

$$\det(DF(\mathbf{w}) - \tilde{\lambda}DG(\mathbf{w}), F(\mathbf{w})) = 0. \quad (2.14)$$

The Inverse Function Theorem guarantees that in a neighborhood of a point $\mathbf{w}_0 \in \Omega$ where Equation (2.14) has distinct eigenvalues we can write the characteristic speeds, for $i = 1, \dots, n$, as:

$$\lambda_i(\mathbf{w}_0, u) = u\tilde{\lambda}_i(\mathbf{w}_0), \quad (2.15)$$

and choose smooth fields of right and left eigenvectors $\vec{r}_i(\mathbf{w}, u)$, $\vec{l}_i(\mathbf{w}, u)$, for $i = 1, \dots, n$:

$$J(\mathbf{w}, u; \lambda_i) \vec{r}_i(\mathbf{w}, u) = 0 \quad \text{and} \quad \vec{l}_i(\mathbf{w}, u) J(\mathbf{w}, u; \lambda_i) = 0, \quad (2.16)$$

where $\vec{r}_i(\mathbf{w}, u)$ is a column vector and $\vec{l}_i(\mathbf{w}, u)$ is a row vector. In fact, equation (2.11) together with (2.15) says a bit more about left eigenvectors since we can rewrite (2.16b)

as:

$$\vec{l}_i(\mathbf{w}, u)(uDF(\mathbf{w}) - u\tilde{\lambda}_i(\mathbf{w}_0)DG(\mathbf{w}), F(\mathbf{w})) = 0, \quad (2.17)$$

where the quantity u factors out and we readily get:

$$\vec{l}_i(\mathbf{w}, u) \equiv \vec{l}_i(\mathbf{w}). \quad (2.18)$$

A similar computation shows that right eigenvectors are written:

$$\vec{r}_i(\mathbf{w}, u) \equiv (r_1(\mathbf{w}), \dots, r_n(\mathbf{w}), u r_{n+1}(\mathbf{w})). \quad (2.19)$$

In classical theory of conservation laws a fundamental observation is that in these conditions we can solve Equation (2.12) by setting:

$$(\dot{\mathbf{w}}(\xi), \dot{u}(\xi))^T = \vec{r}_i(\mathbf{w}(\xi), u(\xi)), \quad (2.20)$$

for some $i = 1, \dots, \dim(\Omega)$, if we can find a parametrization ξ for which:

$$\xi = \lambda_i(\mathbf{w}(\xi), u(\xi)). \quad (2.21)$$

A sufficient condition to do this is to look at points in the state space where

$$\nabla \lambda_i(\mathbf{w}, u) \cdot \vec{r}_i(\mathbf{w}, u) \neq 0, \quad (2.22)$$

(where ∇ stands for differentiation) which after a suitable normalization of the right eigenvector reads:

$$\nabla \lambda_i(\mathbf{w}, u) \cdot \vec{r}_i(\mathbf{w}, u) = 1. \quad (2.23)$$

Now condition (2.21) can be easily fulfilled: it suffices to combine Equations (2.23) and (2.20) to get

$$\frac{d}{d\xi} \lambda_i(\mathbf{w}(\xi), u(\xi)) = 1, \quad (2.24)$$

and (2.21) follows by choosing $\xi_0 = \lambda_i(\mathbf{w}(\xi_0), u(\xi_0))$. These observations were first made precise by Lax in his seminal work [32] in the context of isentropic gas dynamics and here we follow suit.

Definition 2.1 *The system (2.1) is said to be **strictly hyperbolic** at states $\mathbf{w} \in \Omega$ if the generalized eigenvalue problem*

$$\det(DF(\mathbf{w}) - \tilde{\lambda}DG(\mathbf{w}), F(\mathbf{w})) = 0.$$

has n real distinct eigenvalues.

Remark 2.2 *We stress out that the variable u plays no role in concerning hyperbolicity. This should be expected since it is not an evolutionary quantity.*

Definition 2.3 *The state $\mathbf{w} \in \Omega$ is said to be a point of **genuine nonlinearity** for the i^{th} family of the system (2.1) if*

$$\nabla \lambda_i(\mathbf{w}, u) \cdot \vec{r}_i(\mathbf{w}, u) \neq 0.$$

Remark 2.4 *Genuine nonlinearity express monotonicity across a solution. Intuitively its role is to generate compression and rarefaction waves. The former renders slopes of the solution steeper, while the latter renders the slopes of the solutions gentler.*

2.2 The Riemann problem

We have so far deduced what would happen if we have a self-similar solution of equation (2.2). Of course, a very good candidate for self-similar solution is a profile with self-similar initial datum. In one spatial dimension, this initial profile must consist of distinct constant states at left and right of a jump discontinuity at the $x = 0$.

Definition 2.5 *The Riemann problem for equation (2.2) is the initial value problem with self-similar initial data:*

$$\mathbf{w}(x, 0) = \begin{cases} \mathbf{w}_L, & \text{if } x < 0, \\ \mathbf{w}_R, & \text{if } x > 0, \end{cases}$$

and

$$u(x, 0) = u_L, \quad \text{if } x < 0,$$

where $\mathbf{w}_R, \mathbf{w}_L \in \Omega$ and $u_L \in \mathbb{R}^+$ are constants.

Remark 2.6 *A crucial observation is that the Riemann problem for Equation (2.2) is not an initial value problem in the variable u . We can, indistinguishably, give its left or right value but not both. We will come back to this issue latter, but refer the reader to Lambert and Marchesin [29] for an early observation of this fact.*

Following our discussion above we shall seek a solution of the Riemann problem in the form (2.3), where (\mathbf{w}, u) satisfies the ordinary differential equation (2.8) in the parameter

$\xi \in \mathbb{R}$, together with the boundary values:

$$\lim_{\xi \rightarrow -\infty} \mathbf{w}(\xi) = \mathbf{w}_L, \quad \lim_{\xi \rightarrow +\infty} \mathbf{w}(\xi) = \mathbf{w}_R, \quad \text{and} \quad \lim_{\xi \rightarrow -\infty} u(\xi) = u_L. \quad (2.25)$$

Such solutions, called Riemann solutions, play a privileged role among the full set of solutions for general Cauchy problems. The fundamental result in this direction is due to Glimm [22] who showed how one can use the Riemann solution to construct the Cauchy solution in the large (for a genuinely nonlinear system of conservation laws) when the initial data have small variation. The same question posed in the case of more general systems remains open today. The Riemann solution is also very important as a tool to validate numerical algorithms. Due to its constructive character, the Riemann solution is a very useful tool to validate complex numerical simulators.

A Riemann solution is a concatenation of constant states and elementary waves, *i.e.*, centered rarefaction waves and centered shock waves (discontinuous solutions).

2.2.1 Shock waves

In the previous section it was shown that only certain discontinuous solutions can satisfy the self-similarity hypothesis. These are called the centered shock waves.

Definition 2.7 *A centered shock wave of speed σ connecting the pairs (\mathbf{w}^+, u^+) , (\mathbf{w}^-, u^-) is a jump discontinuity that satisfies the Rankine-Hugoniot Equation (2.10):*

$$u^+ F(\mathbf{w}^+) - u^- F(\mathbf{w}^-) - \sigma (G(\mathbf{w}^+) - G(\mathbf{w}^-)) = 0.$$

Remark 2.8 *Notice that the Rankine-Hugoniot Equation (2.10) expresses that the vectors*

$$F(\mathbf{w}^+), \quad F(\mathbf{w}^-), \quad \text{and} \quad (G(\mathbf{w}^+) - G(\mathbf{w}^-)),$$

are linearly dependent. If we require the non-degeneracy hypothesis that they are not collinear then any pair $(\mathbf{w}^+, \mathbf{w}^-)$ that solves equation (2.10) for a triple (u^+, u^-, σ) will actually solve it for a one parameter family of triples. Once u^- is given, the pair (u^+, σ) can be written as:

$$u^+ = u^- u_1^+ \quad \text{and} \quad \sigma = u^- \sigma_1, \quad (2.26)$$

where u_1^+ and σ_1 are reference values when $u^- = 1$.

Typically, our interest is to fix an initial state (w^-, u^-) and ask which is the locus of states (w^+, u^+) that satisfy the Rankine-Hugoniot equation. To this end we define the

Hugoniot function, $\mathcal{H}_{\mathbf{w}^-} : \Omega \times \mathbb{R}^+ \times \mathbb{R} \rightarrow \mathbb{R}^{n+1}$, as:

$$\mathcal{H}_{\mathbf{w}^-}(\mathbf{w}^+, u^+, \sigma) = u^+ F(\mathbf{w}^+) - F(\mathbf{w}^-) - \sigma (G(\mathbf{w}^+) - G(\mathbf{w}^-)), \quad (2.27)$$

and by Remark 2.8 it is sufficient to consider the case $u^- = 1$, since $u^+ = u^- \cdot u_1^+$ for any $u^- > 0$. The Hugoniot locus of state \mathbf{w}^- is the projection of the zero set:

$$\{ (\mathbf{w}^+, u^+, \sigma) \in \Omega \times \mathbb{R}^+ \times \mathbb{R} \mid \mathcal{H}_{\mathbf{w}^-}(\mathbf{w}^+, u^+, \sigma) = 0 \}, \quad (2.28)$$

into $\Omega \times \mathbb{R}^+$ and we will write it as $\mathcal{H}(\mathbf{w}^-)$, recall that $u^- = 1$ (nevertheless, there will be a couple of occasions where we will write $\mathcal{H}(\mathbf{w}^-, u^-)$ to select the exact Hugoniot locus passing through u^-). Very often it will be convenient to use the projection into state space Ω , which we will still call Hugoniot locus. In fact, it can be shown that both sets are in correspondence.

Away from the base point \mathbf{w}^- , the Hugoniot locus is typically a smooth curve. If the base point is a point of strict hyperbolicity the Hugoniot locus bifurcates into n branches (where we recall that n is the dimension of the state space Ω), see Dafermos [13] and Lambert [28]. If strict hyperbolicity fails this may not hold.

When verifying wave admissibility, it is necessary to calculate both the shock speed and the Darcy speed u^+ explicitly. Using Equation (2.10) this can be done by any two of the following equations:

$$\begin{cases} u^+ (F_k^+[G_j] - F_j^+[G_k]) &= u^- (F_k^-[G_j] - F_j^-[G_k]), \\ \sigma ([G_k]F_j^+ - [G_j]F_k^+) &= u^- (F_j^-F_k^+ - F_k^-F_j^+), \\ \sigma ([G_k]F_j^- - [G_j]F_k^-) &= u^+ (F_j^-F_k^+ - F_k^-F_j^+), \end{cases} \quad (2.29)$$

where $1 \leq j, k \leq n$, $j \neq k$, $G = (G_1, \dots, G_k, \dots, G_{n+1})$, $[G_k] = G_k^+ - G_k^-$ and \mathbf{w}^+ is given. According to the situation, it may be more useful to make the shock speed an explicit function of u^- or u^+ . To shorten the notation, we will write sometimes $P^- = (\mathbf{w}^-, u^-)$, $P^+ = (\mathbf{w}^+, u^+)$ and define:

$$\sigma(P^-; P^+) \equiv \sigma(\mathbf{w}^-, u^-; \mathbf{w}^+, u^+). \quad (2.30)$$

Wherever an Equation such as (2.30) is written it is implicit that the pairs (\mathbf{w}^-, u^-) and (\mathbf{w}^+, u^+) satisfy the Rankine-Hugoniot relationship (2.10).

Remark 2.9 Equation (2.29) shows explicitly that when calculating the shock speed the Darcy speed can only be given at one side of the discontinuity. Also, if we only need to draw the Hugoniot locus in Ω we may ignore u^- and u^+ .

2.2.2 Rarefaction waves

We now focus on smooth self-similar solutions.

Definition 2.10 A centered rarefaction curve of the i^{th} family emanating from (\mathbf{w}_0, u_0) is the maximal subset in the image of the solution of the Ordinary Differential Equation (2.20):

$$\begin{cases} (\dot{\mathbf{w}}(\xi), \dot{u}(\xi))^T &= \vec{r}_i(\mathbf{w}(\xi), u(\xi)), \\ (\mathbf{w}(\xi_0), u(\xi_0)) &= (\mathbf{w}_0, u_0), \end{cases}$$

such that the parametrization:

$$\xi \mapsto \lambda_i(\mathbf{w}(\xi), u(\xi)), \quad \xi \geq \xi_0,$$

is monotonically increasing.

In the previous Section we constructed this parametrization in the classical case of genuine non-linearity. A more general approach where genuine nonlinearity may fail in a special co-dimension one manifold can be found in Azevedo et al. [1]¹ and more references in book Dafermos [13].

Equation (2.19) allows us to compute u explicitly in terms of \mathbf{w} in a rarefaction as:

$$u(\xi) = u_0 \exp \left\{ \int_{\xi_0}^{\xi} r_{n+1}(\mathbf{w}(s)) ds \right\}, \quad (2.31)$$

so that, as was seen for shocks, rarefactions can also be completely described in terms of a reference velocity $u_0 = 1$.

2.2.3 Admissibility criteria

The most basic principle when constructing a Riemann solution is that the wave speeds increase from left to right so that all wave interaction are resolved at the initial time, a fact we will call the *monotonicity principle*. However, discontinuous solutions pose

¹On reference [1], the sentence below Equation (10): [Upon replacing η by $x/t...$] should read [Upon replacing η by $\eta(x/t)...$].

an extra difficulty since they can give rise to multiple Riemann solutions. The problem of admissibility ultimately imposes that the solution candidates satisfy a more accurate physical relation than the one described by first order hyperbolic equations of conservation laws themselves.

One early criterion is the Lax criterion. It was introduced to deal with weak shocks in genuinely nonlinear, strictly hyperbolic systems – particularly Euler equations for gas dynamics, from which much of the common nomenclature in use in mathematics today was borrowed. The Lax criterion states that from the point of view of the shock (traveling with a certain speed), the characteristics ahead of it are slower while the characteristics behind it are faster. In our case, it states that there is an index i , $1 \leq i \leq n$ such that the speed of a shock from point $P^- = (\mathbf{w}^-, u^-)$ to point $P^+ = (\mathbf{w}^+, u^+)$ (both in $\Omega \times \mathbb{R}^+$) satisfies:

$$\lambda_i(P^-) > \sigma(P^-; P^+) > \lambda_i(P^+), \quad (2.32)$$

as well as other inequalities. The Lax criterion was later extended allowing one of the inequalities in Equation (2.32) to be an equality.

Lax criterion lets us use the characteristic speeds to name some socks. We are led to the very useful concept of wave family.

Definition 2.11 (Wave family). *Let $P^-, P^+ \in \Omega \times \mathbb{R}^+$ be such that there exists an elementary wave, i.e., a centered rarefaction wave or a centered shock wave, joining them.*

Rarefaction: *This elementary wave is said to be a rarefaction of the i^{th} family if there exists i , $1 \leq i \leq n$ such that Definition 2.10 is satisfied.*

Shock: *This elementary wave is said to be a shock of the i^{th} family if Definition 2.7 is satisfied together with the relation:*

$$\lambda_i(P^-) \geq \sigma(P^-; P^+) \geq \lambda_i(P^+),$$

where only one of the inequalities is allowed to become an equality.

Remark 2.12 *We will often refer to a wave of the i^{th} characteristic family as an i -wave.*

Usually families are defined by placing their characteristic speeds in increasing order, so that when constructing the Riemann solution that involve only Lax shocks, the monotonicity principle is trivially satisfied. In our class of problems this is not possible: the relative order of the characteristic speeds may change when \mathbf{w} wanders around in state space Ω . Nevertheless, the concept of fast and slow wave still makes sense and is still needed to satisfy the monotonicity principle.

In this work we will have $n \leq 2$ so that we can follow the particular nomenclature:

Definition 2.13 Let $P^-, P^+ \in \Omega \times \mathbb{R}^+$, $\dim(\Omega) = 2$, be a pair of points joined by a centered shock wave of the i^{th} family. Call the other family “ k ”. It is a:

- Slow Lax shock, if:

$$\lambda_k(P^-) \geq \sigma(P^-; P^+), \quad \text{and} \quad \lambda_k(P^+) \geq \sigma(P^-; P^+).$$

- Fast Lax shock, if:

$$\lambda_k(P^-) \leq \sigma(P^-; P^+), \quad \text{and} \quad \lambda_k(P^+) \leq \sigma(P^-; P^+).$$

In each case only one of the inequalities is allowed to become an equality.

This is still not sufficient to ensure uniqueness in the Riemann solution: sometimes the Lax criterion becomes so stringent that it disallows any solution, other times it becomes insufficient. A way to extend the Lax criterion is to observe that Equation (2.1) is a first order approximation and often a better approximation to a model would look like:

$$\partial_t G(\mathbf{w}) + \partial_x u F(\mathbf{w}) = \epsilon \partial_x (D \partial_x \mathbf{w}), \quad (2.33)$$

where the matrix D is typically positive definite and ϵ is small. A traveling wave solution, with speed σ , is a bounded solution $(\mathbf{w}(\eta), u(\eta))$, $\eta = x - \sigma t$, of System (2.33). When we let ϵ go to zero we should recover an admissible shock for system (2.1), so that the problem of finding if the shock between a pair of points $P^-, P^+ \in \Omega \times \mathbb{R}^+$ is admissible can be transformed into the problem of finding a traveling wave satisfying:

$$\begin{cases} \epsilon D \frac{d}{d\eta} \mathbf{w} = u F(\mathbf{w}) - \sigma G(\mathbf{w}) - (u^- F(\mathbf{w}^-) - \sigma G(\mathbf{w}^-)), \\ (\mathbf{w}(-\infty), u(-\infty)) = P^- \quad \text{and} \quad (\mathbf{w}(+\infty), u(+\infty)) = P^+. \end{cases} \quad (2.34)$$

An admissible shock found in this way is said to possess a *viscous profile*, see Gelfand [20], and the processes of finding the admissible shocks by looking for traveling wave solutions of Equation (2.33) is called the *viscous profile criterion*. One can see that the original Lax slow and fast shocks lead to repeller to saddle and saddle to attractor solutions, when the hypotheses of the Lax criterion hold.

Unfortunately the viscous profile criterion is very difficult to be applied thoroughly. In the scalar case Oleřnik [39] showed that the viscous profile criterion is equivalent to a

simpler criterion, which bears her name. Later, Liu [34] extended the Oleřnik criterion to certain systems. To properly state the Liu criterion we recall that for a pair $P^-, P^+ \in \Omega \times \mathbb{R}^+$, $P^+ \in \mathcal{H}(P^-)$ the Hugoniot locus is typically a smooth curve. It is well known that we can find a neighborhood of P^- such that the i^{th} branch of the Hugoniot locus can be parametrized:

$$\zeta \mapsto P^\zeta = (\mathbf{w}(\zeta), u(\zeta)) \in \mathcal{H}(P^-), \quad \zeta \in [0, \zeta_0], \quad (2.35)$$

in a way that $\sigma(P^-; P^\zeta)$ is monotone decreasing.

Definition 2.14 (Liu criterion). *Let $P^-, P^+ \in \Omega \times \mathbb{R}^+$ be such that $P^+ \in \mathcal{H}(P^-)$ and the parametrization (2.35) satisfies $P^0 = P^-$ and $P^{\zeta_0} = P^+$. The centered shock wave from P^- to P^+ satisfies the Liu criterion if:*

$$\sigma(P^-; P^+) \leq \sigma(P^-; P^\zeta), \quad \forall \zeta \in [0, \zeta_0]. \quad (2.36)$$

Remark 2.15 *By its very design, the Liu criterion makes sense only in the context of shocks joining states in the same connected component of the Hugoniot locus. In this work this is always the case.*

The Liu and the viscous profile admissibility criteria are strongly interrelated but not quite equivalent and a comprehensive discussion can be found in Dafermos [13]. However, if we confine ourselves to shocks of moderate strength in systems where any pair of points satisfying (2.10) can be connected by a local branch of the Hugoniot locus we may use Liu's criterion. For certain cases, equivalence of the Liu and the viscous profile criteria is discussed in Conlon [10]. See also the work of Majda and Pego [35]. For strong shocks or general non strictly hyperbolic systems of conservation laws each case must be treated individually. In our class, the Liu criterion turns out to be an excellent compromise.

2.2.4 Wave groups and nomenclature

Throughout this section we will assume that there are exactly two distinct families. We introduce the notation $(\mathbf{w}^l, u^l) \xrightarrow{w} (\mathbf{w}^r, u^r)$ to express the fact that (\mathbf{w}^l, u^l) is connected to (\mathbf{w}^r, u^r) (on the right) by an elementary wave of type w . The elementary wave types, are denoted as follows:

- R_i^p : p rarefaction of the i -family;
- S_i^p : p shock of the i -family.

In this work, “ p ” will typically refer to fast (S_i^f, R_i^f) and slow (S_i^s, R_i^s) i -waves. Concrete examples are the Buckley-Leverett or Evaporation family waves, to be defined in the two-phase region, see Chapter 4. However, there will be times when both inequalities in Definition 2.13 will become equalities: this shock will be called a double-contact of the i -family and the elementary wave will be denoted as S_i^d . Elementary Riemann solutions for which the i -characteristic field satisfies:

$$\nabla \lambda_i(\mathbf{w}, u) \cdot \vec{r}_i(\mathbf{w}, u) = 0, \quad (2.37)$$

identically, are usually called genuine contact discontinuities of the i -family and will be denoted as C_i .

Remark 2.16 *Of course, the purpose of the nomenclature “fast and a slow rarefaction” is to remind that the relative size of characteristic speeds change.*

Elementary waves can get away from each other creating constant states or move together as a single entity.

Definition 2.17 (Wave group). *A wave group is a self-similar solution of the Riemann problem 2.5, with no embedded sectors of constant states. The number, type and arrangement of the elementary waves in the wave group determine the wave group type.*

Since in our class of systems strict hyperbolicity typically does not hold, it is not possible to associate to all wave groups a well defined characteristic family. However, most wave groups can still be distinguished by their relative speed, for example as a fast wave group or as a slow wave group.

Definition 2.18 (p -wave group). *We define the succession of elementary waves:*

$$(\mathbf{w}^l, u^l) \rightarrow \cdots \rightarrow (\mathbf{w}^r, u^r), \quad (2.38)$$

to be a p -wave group if it is a wave group and all waves satisfy the same property “ p ”: they are fast, slow or belong to the i -family.

Definition 2.19 *Denote by (\mathbf{w}, u) a p -wave group. We define, for $\xi = x/t$:*

- *Its initial state as:*

$$(\mathbf{w}^l, u^l) = \lim_{\xi \downarrow -\infty} (\mathbf{w}(\xi), u(\xi)).$$

- Its final state as:

$$(\mathbf{w}^r, u^r) = \lim_{\xi \uparrow +\infty} (\mathbf{w}(\xi), u(\xi)).$$

Definition 2.20 (Forward p-wave curve). *We define the forward p-wave curve based on $(\mathbf{w}^l, u^l) \in \Omega \times \mathbb{R}^+$, denoted $\mathcal{W}_+^p(\mathbf{w}^l, u^l)$, to be the projection into state space of the p-wave group that has a fixed initial state (\mathbf{w}^l, u^l) .*

Definition 2.21 (Backward p-wave curve). *We define the backward p-wave curve based on $(\mathbf{w}^r, u^r) \in \Omega \times \mathbb{R}^+$, denoted $\mathcal{W}_-^p(\mathbf{w}^r, u^r)$, to be the projection into state space of the p-wave group that has a fixed final state (\mathbf{w}^r, u^r) .*

Genuine constant states will be denoted by capital, bold, roman letters, like \mathbf{M} . Intermediate states in wave groups, which do not appear as regions in the wave profile, will additionally possess a hat, like $\widehat{\mathbf{M}}$.

2.3 Bifurcation manifolds

In the general situation there are sets in state space that play a fundamental role in the construction of Riemann solutions. We will describe them briefly, just to motivate their definitions. More details can be found in Furtado [19]. Many of them can be written as the zero sets of certain functions so that it is commonplace to call them manifolds.

Remark 2.22 *The boundary of the state space is a potential source of trouble: the main tool to characterize the bifurcation loci is the inverse function theorem, the usefulness of which may diminish if we only have a lateral derivative defined. We write:*

$$\Omega = \mathring{\Omega} \cup \partial\Omega, \tag{2.39}$$

where $\mathring{\Omega}$ is the interior and $\partial\Omega$ is the boundary of the state space. When needed, the boundary will be treated individually.

2.3.1 Coincidence locus

The coincidence locus is the set where strict hyperbolicity is lost. It is, typically, responsible for bifurcations in the behavior of both shock and rarefaction curves.

We recall Definition 2.1 before writing:

Definition 2.23 *The coincidence locus between two families is the set:*

$$\mathcal{C}_{i,j} = \{ \mathbf{w} \in \mathring{\Omega} \mid \tilde{\lambda}_i(\mathbf{w}) = \tilde{\lambda}_j(\mathbf{w}), 1 \leq i, j \leq n \text{ and } i \neq j \}.$$

Remark 2.24 *In this work there will be only one coincidence locus (which possesses two connected components in our case).*

2.3.2 Inflection locus

Points in the inflection locus are those where genuine nonlinearity is lost. Generically, the eigenvalue does not vary monotonically along a corresponding integral curve near an inflection point. Thus rarefaction curves stop at this locus.

From Definition 2.3 and recalling Equations (2.15) and (2.19) we find:

Definition 2.25 *The inflection locus of the i^{th} family is the set:*

$$\mathcal{I}_i = \left\{ \mathbf{w} \in \overset{\circ}{\Omega} \mid \sum_{1 \leq k \leq n} \partial_k \tilde{\lambda}_i(\mathbf{w}) r_i^k(\mathbf{w}) + \tilde{\lambda}_i(\mathbf{w}) r_i^{n+1}(\mathbf{w}) = 0 \right\}.$$

Here we used r_i^k , $1 \leq k \leq n+1$, for the k^{th} component of the i^{th} family eigenvector \vec{r}_i .

2.3.3 Self-intersection and secondary bifurcation loci

The Hugoniot locus based in $\mathbf{w}^- \in \Omega$ is generically a smooth curve, away from \mathbf{w}^- . If we can find a state $\mathbf{w}^+ \neq \mathbf{w}^-$, such that $\mathbf{w}^+ \in \mathcal{H}(\mathbf{w}^-)$ and the Hugoniot locus is not a smooth curve in any neighborhood of \mathbf{w}^+ then the Jacobian of the Hugoniot function (2.27) cannot have maximal rank at this point. We write its differential:

$$\begin{aligned} d\mathcal{H}_{\mathbf{w}^-}(\mathbf{w}^+, u^+, \sigma) &= (u^+ DF(\mathbf{w}^+) - \sigma DG(\mathbf{w}^+)) d\mathbf{w}^+ + F(\mathbf{w}^+) du^+ \\ &\quad - (G(\mathbf{w}^+) - G(\mathbf{w}^-)) d\sigma, \end{aligned} \quad (2.40)$$

and, by recalling Equations (2.13) and (2.18), we can see that $d\mathcal{H}_{\mathbf{w}^-}(\mathbf{w}^+, u^+, \sigma)$ will not have maximal rank if the following identities hold:

$$\sigma = \lambda_i(\mathbf{w}^+, u^+) \quad \text{and} \quad \vec{l}_i(\mathbf{w}^+)(G(\mathbf{w}^+) - G(\mathbf{w}^-)) = 0, \quad 1 \leq i \leq n. \quad (2.41)$$

Commonly, the Hugoniot locus fails to be a smooth curve at points where it self-intersects, which is our case. Before defining the self-intersection locus we need some preparation. First we will rewrite the Hugoniot function to make explicit its dependence on the state \mathbf{w}^- :

$$\mathcal{H}(\mathbf{w}^-, \mathbf{w}^+, u^+, \sigma) = u^+ F(\mathbf{w}^+) - F(\mathbf{w}^-) - \sigma (G(\mathbf{w}^+) - G(\mathbf{w}^-)). \quad (2.42)$$

We define the set:

$$\Delta = \{(\mathbf{w}^-, \mathbf{w}^+, u^+) \in \mathring{\Omega} \times \mathring{\Omega} \times \mathbb{R}^+ \mid \mathbf{w}^- = \mathbf{w}^+\}, \quad (2.43)$$

and write:

$$\mathcal{D} = \mathring{\Omega} \times \mathring{\Omega} \times \mathbb{R} \setminus \Delta. \quad (2.44)$$

We want to define the self-intersection locus as the zero set of a smooth function; to this end we fix a family $1 \leq i \leq n$ and motivated by (2.41) we write:

$$\mathcal{F}_{(i)} : \mathcal{D} \rightarrow \mathbb{R}^{n+2}, \quad (\mathbf{w}^-, \mathbf{w}^+, u^+) \mapsto \left(\mathcal{H}(\mathbf{w}^-, \mathbf{w}^+, u^+, \lambda_i(\mathbf{w}^+, u^+)), \vec{l}_i(\mathbf{w}^+)[G] \right), \quad (2.45)$$

where $[G] = G(\mathbf{w}^+) - G(\mathbf{w}^-)$.

Definition 2.26 *The self-intersection locus of the i^{th} family is the set:*

$$\mathcal{A}_i = \{ (\mathbf{w}^-, \mathbf{w}^+, u^+) \in \mathcal{D} \mid \mathcal{F}_{(i)}(\mathbf{w}^-, \mathbf{w}^+, u^+) = 0 \}.$$

A related and very important locus is the one that encodes the change in the topology of the shock curves. It is called the *secondary bifurcation locus*, since in the three-phase flow models where it was observed first (see Isaacson et al. [26]), it happens to be exactly the same as the set where the Hugoniot locus has a second self-intersection (the primary self-intersection always occur at the base state \mathbf{w}^-). We call it the secondary bifurcation of the i^{th} family as \mathcal{B}_i . In our class it satisfies:

$$\mathcal{B}_i \subsetneq \overline{\mathcal{A}_i}, \quad (2.46)$$

where the symbol \subsetneq means proper inclusion and $\overline{\mathcal{A}_i}$ is the closure of the self-intersection locus of the i^{th} family.

Remark 2.27 *We will see that in the particular case of the secondary bifurcation we need to consider the boundary of Ω , because otherwise, it would be empty.*

2.3.4 Double contact locus

We define a two-sided (or double) contact discontinuity to be a solution $(\mathbf{w}^-, u^-; \mathbf{w}^+, u^+)$ of the Rankine-Hugoniot relation (2.10) such that a characteristic speed for (\mathbf{w}^-, u^-) coincides with the shock speed $\sigma(\mathbf{w}^-, u^-; \mathbf{w}^+, u^+)$, as well as with the another characteristic speed for (\mathbf{w}^+, u^+) . By Remark 2.8 we only need to consider the reference speed $u^- = 1$.

Definition 2.28 *The double contact locus between the j^{th} and k^{th} families is the set:*

$$\mathcal{D}_{j,k} = \left\{ (\mathbf{w}^-, \mathbf{w}^+, u^+) \in \mathcal{D} \mid (\mathbf{w}^+, u^+) \in \mathcal{H}(\mathbf{w}^-) \quad \text{and} \quad \lambda_k^+ = \sigma = \lambda_j^- \right\},$$

where

$$\lambda_k^+ = \lambda_k(\mathbf{w}^+, u^+), \quad \sigma = \sigma(\mathbf{w}^-, u^-; \mathbf{w}^+, u^+) \quad \text{and} \quad \lambda_j^- = \lambda_j(\mathbf{w}^-, 1).$$

2.3.5 Extension locus

We can concatenate elementary waves together wherever the shock speed equals a characteristic speed of the base state. This is particularly useful and, after fixing the notation:

$$\lambda_i^+ = \lambda_i(\mathbf{w}^+, u^+), \quad \sigma = \sigma(\mathbf{w}^-, u^-; \mathbf{w}^+, u^+), \quad \text{and} \quad \lambda_i^- = \lambda_i(\mathbf{w}^-, u^-), \quad (2.47)$$

leads to the definition:

Definition 2.29 (Extension locus of a point.) *We write the right extension locus of the point (\mathbf{w}^-, u^-) in the i^{th} family as:*

$$\mathcal{E}_i^+(\mathbf{w}^-, u^-) = \left\{ (\mathbf{w}^+, u^+) \in \mathring{\Omega} \times \mathbb{R}^+ \mid (\mathbf{w}^+, u^+) \in \mathcal{H}(\mathbf{w}^-, u^-) \quad \text{and} \quad \sigma = \lambda_i^+ \right\},$$

and the left extension locus of the point (\mathbf{w}^-, u^-) in the i^{th} family as:

$$\mathcal{E}_i^-(\mathbf{w}^-, u^-) = \left\{ (\mathbf{w}^+, u^+) \in \mathring{\Omega} \times \mathbb{R}^+ \mid (\mathbf{w}^+, u^+) \in \mathcal{H}(\mathbf{w}^-, u^-) \quad \text{and} \quad \sigma = \lambda_i^- \right\}.$$

Remark 2.30 *Often the extension of a point consists of several points.*

A natural “extension” of the previous definition is:

Definition 2.31 (Extension locus of a curve.) *Let γ be a curve in $\mathring{\Omega} \times \mathbb{R}^+$. Its right extension locus in the i^{th} family is:*

$$\mathcal{E}_i^+(\gamma) = \left\{ (\mathbf{w}^+, u^+) \in \mathring{\Omega} \times \mathbb{R}^+ \mid \exists (\mathbf{w}^-, u^-) \in \gamma; (\mathbf{w}^+, u^+) \in \mathcal{H}(\mathbf{w}^-, u^-) \quad \text{and} \quad \sigma = \lambda_i^+ \right\},$$

and its left extension locus in the i^{th} family is:

$$\mathcal{E}_i^-(\gamma) = \left\{ (\mathbf{w}^+, u^+) \in \mathring{\Omega} \times \mathbb{R}^+ \mid \exists (\mathbf{w}^-, u^-) \in \gamma; (\mathbf{w}^+, u^+) \in \mathcal{H}(\mathbf{w}^-, u^-) \quad \text{and} \quad \sigma = \lambda_i^- \right\}.$$

2.4 On notation

Following Smoller [46] we will use four derivative notations along this work: D , ∇ , $'$ and a superimposed dot ($\dot{}$). In what follows the respective functions are smooth and U is an open set.

If we have a function $F : U \subset \mathbb{R}^n \rightarrow \mathbb{R}^m$ where $n, m > 1$ then we will write its derivative (Jacobian) as:

$$\mathbf{w} \mapsto DF(\mathbf{w}) \in \mathbb{R}^{nm}, \quad n, m > 1.$$

If we have a real valued function $f : U \subset \mathbb{R}^n \rightarrow \mathbb{R}$ with $n > 1$ then we will write its derivative (gradient) as:

$$\mathbf{w} \mapsto \nabla f(\mathbf{w}) \in \mathbb{R}^n, \quad n > 1.$$

If we have a real valued function of the real line $f : U \subset \mathbb{R} \rightarrow \mathbb{R}$ then we will write its derivative as:

$$\xi \mapsto f'(\xi) \in \mathbb{R}.$$

Finally, if the derivative is with respect to “time” or if we have a parametrization (function) from the real line to some \mathbb{R}^m with $m > 1$, $\mathbf{x} : U \subset \mathbb{R} \rightarrow \mathbb{R}^m$, then we will write the derivative of this parametrization as:

$$\xi \mapsto \dot{\mathbf{x}}(\xi) \in \mathbb{R}^m, \quad m > 1.$$

Chapter 3

Physical model

In this chapter we motivate the equations of our model following broadly the work of Bruining and Marchesin [4].

3.1 Flow of fluids and qualitative behavior

We consider the injection of gaseous volatile oil into a cylindrical horizontal core with constant porosity and absolute permeability. The core is originally filled with oil. The oil consists of a mixture of dead oil and volatile oil.

Physical quantities are evaluated at a representative pressure throughout the core; we assume that pressure variations are negligible compared to the prevailing pressure. Thermal expansion of the liquid will be disregarded. All fluids are considered incompressible. We assume Darcy's law for two-phase flow. The tube diameter is considered sufficiently small so that gravity segregation does not occur and temperature is homogeneous radially.

3.2 Thermodynamic fundamentals

Let us describe the phase behavior. We always assume that there is local thermodynamic equilibrium. Our interest is confined to situations where we have: (1) two phases, i.e. oleic (or liquid) (o) and gaseous (g) and (2) one phase, i.e. oleic or gaseous. There are two components viz. volatile oil (v) and dead oil (d). We define dead oil as an oil with zero vapor pressure, which can only exist in liquid form, and volatile oil as an oil with nonzero vapor pressure.

We use the following convention for subscripts: the first subscript (o, g) refers to the phase, the second subscript (v, d) refers to the component. With these conventions the

concentration [kg/m^3] of (dead) volatile oil in the oleic phase is denoted as $(\rho_{od}) \rho_{ov}$. The pure phase densities of liquid volatile oil and liquid dead oil are denoted as ρ_V and ρ_D respectively. The pure phase densities of volatile oil vapor is denoted by ρ_{gV} .

Gibbs' phase rule

$$f = c - p + 2, \quad (3.1)$$

dictates the number of degrees of freedom (f) for the thermodynamic variables given the number of phases (p) and the number of components (c). In the two phase zone we have two phases ($p = 2$) and two components ($c = 2$), which gives $f = 2$, so we have the two concentrations as functions of the temperature and the pressure. As in this model the pressure at which the displacement is conducted is fixed, we have that all concentrations are functions of the temperature only.

In the single phase liquid zone we have one phase and two components, which gives three degrees of freedom: the temperature, the pressure (fixed) and the concentration of dead oil in the liquid. By assumption, the single phase gas zone has only one chemical component: again the main variable is the temperature.

We disregard any heat of mixing between volatile oil and dead oil. Moreover we disregard any volume contraction effects resulting from mixing. For ideal fluids we can write

$$\frac{\rho_{ov}}{\rho_V} + \frac{\rho_{od}}{\rho_D} = 1. \quad (3.2)$$

The pure liquid densities ρ_V, ρ_D [kg/m^3] are considered to be independent of temperature, and the pure vapor density is considered to obey the ideal gas law, i.e., $\rho_{gV} = M_V P / RT$, where M_V denote the molar weight of volatile oil. P is (the fixed) pressure and the gas constant is $R = 8.31 [J/mol/K]$.

3.2.1 Two-phase behavior

Since the concentrations are functions of the temperature in the two-phase region we need to equate this dependence. We will use a simple model derived from basic principles (in opposition to a model which fits experimental data). From the engineering point of view, the model is sufficiently accurate in the regimes for which we propose its use.

We assume that the volatile oil vapor pressure P_v is determined by the Clausius-Clapeyron law together with Raoult's law (see Moore [37]), which states that the vapor pressure of volatile oil is equal to its pure vapor pressure times the equilibrium mole

fraction x_{ov}^{eq} of volatile oil in the liquid oleic phase. Therefore we obtain:

$$P_v(T) = x_{ov}^{eq} P^{ref} \exp\left(\frac{-M_V \Lambda_V(T_b^V)}{R} \left(\frac{1}{T} - \frac{1}{T_b^V}\right)\right), \quad (3.3)$$

where T_b^V is the normal boiling temperature of volatile oil at P^{ref} , a reference pressure; $\Lambda_V(T_b^V)$ is the evaporation heat of pure volatile oil at the normal boiling temperature T_b^V of volatile oil and M_V is the molar weight of volatile oil. Furthermore we assume that the total pressure is the volatile oil vapor pressure, i.e. $P^{tot} = P_v$. All these thermodynamical constants are given in Table A.1.

Finally we need to derive an equation that relates the oleic phase densities to the mole fractions. From the definition of the mole fraction (moles volatile oil / total moles):

$$x_{ov} = \frac{\rho_{ov}/M_V}{\rho_{ov}/M_V + \rho_{od}/M_D}, \quad (3.4)$$

where M_D is the molar weight of the dead oil. The light oil mole fraction and the dead oil mole fraction, in the oil, must add to one:

$$x_{ov} + x_{od} = 1, \quad (3.5)$$

so combining equation (3.4) with the first ideal mixing rule (3.2) we find after some algebraic manipulations:

$$\rho_{ov} = \frac{x_{ov} \rho_D \rho_V M_V}{x_{ov} \rho_D M_V + x_{od} \rho_V M_D}, \quad \rho_{od} = \frac{x_{od} \rho_D \rho_V M_D}{x_{ov} \rho_D M_V + x_{od} \rho_V M_D}. \quad (3.6)$$

The pure phase densities (ρ_V, ρ_D) and molar weights (M_V, M_D) are given in Table A.1. Temperature dependent quantities such as the evaporation heat of volatile oil ($\Lambda_V(T_b^V)$) are given in Appendix A.1.

Remark 3.1 Equations (3.6) express that the set of molar fractions are mapped in a one to one way onto the set of concentrations, i.e., $x_{o\alpha} \mapsto \rho_{o\alpha}(x_{o\alpha})$, $\alpha \in \{v, d\}$ is a diffeomorphism. Since the concentrations (ρ_{ov}, ρ_{od}) are the quantities that appear naturally in the conservation laws, they are best suited to be used as variables to solve the Riemann problem. However, to represent the state space and draw pictures it is more convenient to use the molar concentrations (x_{ov}, x_{od}) as they always take values between 0 and 1.

3.3 Darcy's law for two-phase flow

When dealing with multi-phase flow in porous media it is common place to use the concept of *saturation*: the fraction of one of the fluids in the pores averaged over a representative elementary volume. We write s_g for the gas saturation and s_o for the oil saturation. The rock is filled with a mixture of oil and gas, i.e.:

$$s_g + s_o = 1. \quad (3.7)$$

Following the Corey model [11], we take very particular gas and oil relative permeabilities (which we denote by k_{rg} and k_{ro} respectively), which are quadratic functions of the saturations alone:

$$k_{rg} = s_g^2, \quad \text{and} \quad k_{ro} = s_o^2. \quad (3.8)$$

The capillary pressure between the phases is also a function of the saturations: it is assumed (see Aziz [2]) that the gas-oil capillary pressure $p_g - p_o = p_{c,go}(s_g)$ depends on the gas saturation.

In the absence of gravity terms Darcy's law for multiphase flow reads:

$$\begin{cases} u_o = \frac{kk_{ro}}{\mu_o} \frac{\partial p_o}{\partial x} = \lambda_o \frac{\partial p_o}{\partial x}, \\ u_g = \frac{kk_{rg}}{\mu_g} \frac{\partial p_g}{\partial x} = \lambda_g \frac{\partial p_g}{\partial x}, \end{cases} \quad (3.9)$$

where the viscosities μ_α , $\alpha \in \{o, g\}$ are functions of the temperature and the composition, see Appendix A.1, the porous rock permeability is given in Table A.1 and λ_α , $\alpha \in \{o, g\}$ stands for mobilities. It is possible to express all phase velocities u_α in terms of the total velocity u :

$$u = u_g + u_o, \quad (3.10)$$

and the capillary pressure:

$$\begin{cases} u_o = uf_o + \lambda_g f_o \frac{\partial p_{c,go}}{\partial x}, \\ u_g = uf_g - \lambda_o f_g \frac{\partial p_{c,go}}{\partial x}, \end{cases} \quad (3.11)$$

where the fractional flow functions f_α are defined as:

$$f_\alpha = \frac{\lambda_\alpha}{\lambda_o + \lambda_g}, \quad \text{for } \alpha \in \{g, o\}, \quad (3.12)$$

and, of course, $\lambda_g f_o = \lambda_o f_g$.

Remark 3.2 *The fractional flow function is smooth (in all variables), non-negative, monotonically increasing function of the saturations with range in the $[0, 1]$ interval. Its derivative vanishes for states at pure oil saturation or at pure gas saturation and has a single, non-degenerate, global maximum.*

The expression for $p_{c,go}$ will not be used (directly) in this work, but we remark that after using the chain rule, we can write:

$$\mathcal{D}_{go} = \lambda_o f_g \frac{dp_{c,go}}{ds_g}, \quad (3.13)$$

where \mathcal{D}_{go} is non-negative (the subscript stands as a reminder of its functional dependence). The final form of equations (3.11) is:

$$\begin{cases} u_o &= u f_o - \mathcal{D}_{go} \frac{\partial s_o}{\partial x}, \\ u_g &= u f_g - \mathcal{D}_{go} \frac{\partial s_g}{\partial x}. \end{cases} \quad (3.14)$$

Notice the change of sign in equation (3.14a) relative to (3.11a), which is due to the use of equation (3.7).

3.4 Balance equations

Systems of form (2.1) are a prototype for multiphase flow in porous media with mass transfer between different phases. In this thesis we are only concerned with *physical mechanisms* of mass transfer: evaporation and condensation, both “reversible” in nature (in opposition to *chemical mechanisms* like combustion).

Our main interest is not the balance laws themselves but the conservation laws which we can derive from them when we allow the source terms to relax towards their equilibria. In the approach we follow we do not need the precise form of the source terms: only its qualitative behavior in the thermodynamical equilibrium.

Typically, conservation laws arise as first order approximations to more complicated dynamics. Very often they do not suffice to select a *physically meaningful* solution, indeed. The mathematical selection criterion is called *entropy condition* and a very sensible one is to consider a better approximation (of the complicated dynamics), which here is a convection-diffusion equation – and finally look for the solutions of the conservation laws that can be realized as traveling waves of the convection-diffusion system. This reasoning is part of the motivation of our adoption of the Liu entropy criterion, see discussion in Subsection 2.2.3. In what follows we will derive the convection-diffusion model for the sake of completeness, however they will not be used in the current work.

3.4.1 Mass balance equations

The balance of mass of each component in each phase is given by the following equations, which express volatile oil mass balance in the gaseous phase, volatile oil mass balance in the liquid phase and the dead oil mass conservation in the liquid phase (remember that by assumption there is no dead oil in the vapor phase):

$$\left\{ \begin{array}{l} \frac{\partial}{\partial t}(\varphi \rho_{ov} s_o) + \frac{\partial}{\partial x}(\rho_{ov} u_o) = +q_{g \rightarrow o, v}, \\ \frac{\partial}{\partial t}(\varphi \rho_{gV} s_g) + \frac{\partial}{\partial x}(\rho_{gV} u_g) = -q_{g \rightarrow o, v}, \\ \frac{\partial}{\partial t}(\varphi \rho_{od} s_o) + \frac{\partial}{\partial x}(\rho_{od} u_o) = 0. \end{array} \right. \quad (3.15)$$

The concentrations of dead and volatile oil in the liquid are related by equation (3.2), which states the ideal mixing rule. The gaseous phase is pure volatile alkane vapor, thus the gas density is ρ_{gV} in equation (3.15b). The source term $q_{g \rightarrow o, v}$ is the volatile vapor condensation rate: it denotes the mass transfer of volatile oil from the gaseous to the liquid phase. Of course the rock porosity is denoted by φ and is assumed constant.

Combining equations (3.11) with the system (3.15) we can write the mass balance equations in terms of the total Darcy speed and the fractional flow functions:

$$\left\{ \begin{array}{l} \varphi \frac{\partial}{\partial t} (\rho_{ov} s_o) + \frac{\partial}{\partial x} (\rho_{ov} u f_o) = +q_{g \rightarrow o,v} + \frac{\partial}{\partial x} \left(\rho_{ov} \mathcal{D}_{go} \frac{\partial s_o}{\partial x} \right), \\ \varphi \frac{\partial}{\partial t} (\rho_{gV} s_g) + \frac{\partial}{\partial x} (\rho_{gV} u f_g) = -q_{g \rightarrow o,v} + \frac{\partial}{\partial x} \left(\rho_{gV} \mathcal{D}_{go} \frac{\partial s_g}{\partial x} \right), \\ \varphi \frac{\partial}{\partial t} (\rho_{od} s_o) + \frac{\partial}{\partial x} (\rho_{od} u f_o) = \frac{\partial}{\partial x} \left(\rho_{od} \mathcal{D}_{go} \frac{\partial s_o}{\partial x} \right). \end{array} \right. \quad (3.16)$$

3.4.2 Energy balance equations

The conservation of energy in terms of enthalpy is given as:

$$\frac{\partial}{\partial t} (H_r + \varphi (s_o H_o + s_g H_g)) + \frac{\partial}{\partial x} (u_o H_o + u_g H_g) = \frac{\partial}{\partial x} \left(\kappa \frac{\partial T}{\partial x} \right), \quad (3.17)$$

where capital H is used as a nomenclature for enthalpies per unit volume, κ is the effective coefficient of the heat conductivity term and T is temperature. Mixing effects are disregarded. The oleic and gaseous enthalpies are given as:

$$H_o = \rho_{ov} h_{oV} + \rho_{od} h_{oD}, \quad H_g = \rho_{gV} h_{gV}. \quad (3.18)$$

The enthalpies h are all per unit mass and depend on temperature (see Appendix A.1). The enthalpy of volatile oil in the gaseous phase is h_{gV} . Furthermore h_{oV} and h_{oD} are the enthalpies of liquid volatile oil and dead oil. Rock enthalpy H_r is a function of temperature only. Following Bruining and Marchesin [4] we make the simplifying assumption that the heat capacities with respect to volume of volatile and dead oil are equal so that H_o is independent of composition. This simplification is very useful and more than adequate for our purposes. Plugging equation (3.14) into equation (3.17) we get, with $\widehat{H}_r = H_r/\varphi$:

$$\begin{aligned} \varphi \frac{\partial}{\partial t} (\widehat{H}_r + s_o H_o + s_g H_g) + \frac{\partial}{\partial x} \left[u (f_o H_o + f_g H_g) \right] &= \frac{\partial}{\partial x} \left(\kappa \frac{\partial T}{\partial x} \right) \\ &+ \frac{\partial}{\partial x} \left[\mathcal{D}_{go} \left(H_o \frac{\partial s_o}{\partial x} + H_g \frac{\partial s_g}{\partial x} \right) \right]. \end{aligned} \quad (3.19)$$

3.4.3 The main state space and state variables

Systems (3.16) and (3.19) together describe the two-phase flow of a two component mixture in which only one of the components is allowed to exist in the gas. Once we use

equations (3.2) and (3.6) to write $\rho_{ov} = \rho_{ov}(x_{od})$, we can define the main state space as:

$$\Omega = \{(s_o, T, \rho_{od}) \mid 0 \leq s_o \leq 1, T > T_0 \text{ and } 0 \leq x_{od} \leq 1\}, \quad (3.20)$$

and, here, we remind the reader of Remark 3.1.

Any solution of this model can be fully described by a quartet:

$$(s_o, T, \rho_{od}, u) \in \Omega \times \mathbb{R}^+, \quad (3.21)$$

which from now on will be called the *state variables*. Of course, the set $\Omega \times \mathbb{R}^+$ will be called the *state space*. Since we have four unknowns and four equations we hope that the problem is well determined and we may proceed.

On the right-hand side of Equations (3.15) we can see the source term, the volatile vapor condensation rate. In our class of problems the main feature of this type of source term is to select an *equilibrium* set in state space and to force the solution to converge towards this set, or *relax* to this set. Relaxation is a very active topic of research (see the 1999 survey by Natalini [38]) and a crucial question is to measure the effective time the solution of balance laws needs to approach the equilibrium set.

This is a difficult topic that will not be pursued here, but motivates the following: it is commonly accepted, for our class of models, that the effective time of relaxation is far smaller than the effective time of the displacement (the ratio of a characteristic length in the porous rock by the maximum speed of the displacement), so we will assume local thermodynamical equilibrium. This makes the problem tractable and, as far as we know, it is a good approximation.

3.5 Configurations in thermodynamical equilibrium

In this section we describe the configurations in thermodynamical equilibrium that are relevant to our work.

3.5.1 Single phase gaseous region (SPG)

In the SPG there is only light alkane gas ($s_o = 0$ and $x_{od} = 0$) thus the light alkane vapor pressure must equal the total pressure. A simple observation is that these constraints

together with equation (3.3) give:

$$1 = \exp \left(\frac{-M_V \Lambda_V (T_b^V)}{R} \left(\frac{1}{T} - \frac{1}{T_b^V} \right) \right), \quad (3.22)$$

so $T = T_{bV}$ is the minimum temperature where pure light alkane gas can exist in thermodynamical equilibrium.

We have one component and one phase so by Gibbs' phase rule, equation (3.1), there is only one thermodynamical degree of freedom. We can write the state space as:

$$\Omega_{\mathbf{SPG}} = \{ (s_o, T, x_{od}) \mid s_o = 0, T \geq T_{bV} \text{ and } x_{od} = 0 \}. \quad (3.23)$$

The single phase gas state space is a one dimensional manifold in main state space parametrized by the temperature. In these conditions the model equations (3.16) and (3.19) reduce to:

$$\begin{cases} \varphi \frac{\partial}{\partial t} \rho_{gV} + \frac{\partial}{\partial x} (u \rho_{gV}) = 0, \\ \varphi \frac{\partial}{\partial t} (\widehat{H}_r + H_g) + \frac{\partial}{\partial x} (u H_g) = \frac{\partial}{\partial x} \left(\kappa \frac{\partial}{\partial x} T \right), \end{cases} \quad (3.24)$$

where we recall Remark 3.2.

The natural parametrization of the single phase gas state space (3.23) will be called **SPG** and, with a small abuse of notation, write this as the set:

$$\mathbf{SPG} = \{ T \mid T \geq T_{bV} \}, \quad (3.25)$$

with the topology induced from the real line. Solutions of system (3.24) can be completely determined in terms of the variables

$$(T, u) \in \mathbf{SPG} \times \mathbb{R}^+. \quad (3.26)$$

Remark 3.3 *Lambert [28], [29] used the name primary variables to represent the variables that parametrize the state space, in this case they are the temperature. The other state variables, the values of which were inferred from the equilibrium equations were called trivial variables, in this case the oil saturation and the dead oil mole fraction. The name secondary variable was reserved to the variable u .*

3.5.2 Single phase liquid region (SPL)

The single phase liquid region has two components in liquid form ($s_o = 1$). Combining equation (3.3) with equation (3.5) we can calculate, for each temperature, the maximum amount of dead oil which can exist in a single phase liquid in thermodynamical equilibrium with light alkane and we call this quantity $x_{od}^{eq}(T)$. So, a single phase liquid can only exist if:

$$x_{od}^{eq}(T) \leq x_{od}. \quad (3.27)$$

We can write the state space for the single phase liquid region as:

$$\Omega_{\mathbf{SPL}} = \{ (s_o, T, \rho_{od}) \mid s_o = 1, T > T_{bV} \text{ and } x_{od}^{eq}(T) \leq x_{od} \leq 1 \}, \quad (3.28)$$

see Remark 3.1.

Gibbs' phase rule gives three degrees of freedom, see Section 3.2, and since the oleic saturation is fixed, the one phase liquid state space is a two dimensional manifold in the main state space parametrized by the temperature and by the dead oil concentration. In these conditions the model equations (3.16) and (3.19) reduce to:

$$\left\{ \begin{array}{l} \varphi \frac{\partial}{\partial t} \rho_{ov} + \frac{\partial}{\partial x} (u \rho_{ov}) = 0, \\ \varphi \frac{\partial}{\partial t} \rho_{od} + \frac{\partial}{\partial x} (u \rho_{od}) = 0, \\ \varphi \frac{\partial}{\partial t} (\widehat{H}_r + H_o) + \frac{\partial}{\partial x} u H_o = \frac{\partial}{\partial x} \left(\kappa \frac{\partial}{\partial x} T \right), \end{array} \right. \quad (3.29)$$

see Remark 3.2 for the fractional flow functions properties.

Multiplying equation (3.29a) by $1/\rho_V$, equation (3.29b) by $1/\rho_D$, adding the results and using the ideal mixture law (3.2) we get $\partial_x u = 0$, so u is constant in space. Since we are interested in conservation laws we ignore heat conduction, so that system (3.29) simplifies further to:

$$\left\{ \begin{array}{l} \varphi \frac{\partial}{\partial t} \rho_{od} + u \frac{\partial}{\partial x} \rho_{od} = 0, \\ \varphi \frac{\partial}{\partial t} (\widehat{H}_r + H_o) + u \frac{\partial}{\partial x} H_o = 0, \\ \partial_x u = 0. \end{array} \right. \quad (3.30)$$

The parametrization of the single phase liquid state space (3.28) will be called **SPL**

and, with a small abuse of notation, we write the set:

$$\mathbf{SPL} = \{ (T, \rho_{od}) \mid T \geq T_{bV} \text{ and } x_{od}^{eq}(T) \leq x_{od} \leq 1 \}. \quad (3.31)$$

Solutions of system (3.30) can be completely determined in terms of the variables:

$$(T, \rho_{od}, u) \in \mathbf{SPL} \times \mathbb{R}^+. \quad (3.32)$$

3.5.3 Two-phase region (TP)

In the two-phase region the two components can coexist in liquid form (consisting of light and dead alkanes) and gas form (with only light alkane vapor), with concentrations derived by equation (3.3) as functions of the temperature (for any temperature greater than the boiling temperature of the light alkane). Of course this model is unreliable for very high temperatures.

As in the previous cases, we can combine equation (3.3) with equation (3.5) to calculate, for each temperature, the amount of dead oil in thermodynamical equilibrium with light alkane vapor and we call this quantity $x_{od}^{eq}(T)$. To sum up, a two-phase mixture exists if:

$$x_{od} = x_{od}^{eq}(T). \quad (3.33)$$

We can write the state space for the single phase liquid region as:

$$\Omega_{\mathbf{TP}} = \{ (s_o, T, \rho_{od}(T)) \mid 0 \leq s_o \leq 1, T > T_{bV} \text{ and } x_{od} = x_{od}^{eq}(T) \}, \quad (3.34)$$

Gibbs' phase rule gives two degrees of freedom, and since the pressure is fixed (see Section 3.2), we have the temperature as a free thermodynamical degree of freedom. However in the two-phase region the oleic saturation must be another degree of freedom in the model so the two-phase state space is a two dimensional manifold in the main state space parametrized by the temperature and by the oleic saturation. In these conditions the model equations (3.16) and (3.19) reduces to:

3.5.4 On notation

For brevity we will typically use bold, roman, lower-case characters to denote points in some state space. For example, points in the **TP** will be written as:

$$\mathbf{w} \in \mathbf{TP},$$

and similarly for the **SPL**. The reason for this is that both sets have dimension greater than one. We will make only one exception: we will write all variables explicitly if one of them needs to be identified. For example, if we need to identify a saturation for a point in **TP** we will write:

$$(s_o^*, T) \in \mathbf{TP},$$

and say something about s_o^* .

The **SPG** is one dimensional so we will just write the name of the physical variable it parametrizes, namely the temperature:

$$T \in \mathbf{SPG}.$$

Chapter 4

Basic facts on the two phase region

Riemann solutions in the two phase region (**TP**) are fundamental. The **TP** is a source of genuine nonlinearity in our model, and is directly responsible for all of the bifurcations in the solution. In this chapter we will focus on the elementary waves and bifurcation structures inside **TP**.

4.1 Characteristic speeds and eigenvectors

We will recall some basic facts. In Section 3.5.3 we derived the system of conservation laws:

$$\left\{ \begin{array}{l} \varphi \frac{\partial}{\partial t} (\rho_{gV} s_g + \rho_V s_o) + \frac{\partial}{\partial x} u (\rho_{gV} f_g + \rho_V f_o) = 0, \\ \varphi \frac{\partial}{\partial t} (\rho_{od} s_o) + \frac{\partial}{\partial x} u (\rho_{od} f_o) = 0, \\ \varphi \frac{\partial}{\partial t} (\widehat{H}_r + s_o H_o + s_g H_g) + \frac{\partial}{\partial x} u (f_o H_o + f_g H_g) = 0, \end{array} \right. \quad (4.1)$$

and introduced a natural parametrization of the two phase state space:

$$\mathbf{TP} = \{ (s_o, T) \mid 0 \leq s_o \leq 1, T > T_{bV} \}. \quad (4.2)$$

A solution of the Riemann problem for system (4.1) is a convenient parametrization of the real line onto $\mathbf{TP} \times \mathbb{R}^+$, which we will write as $\xi \mapsto (s_o(\xi), T(\xi), u(\xi))$, where $\xi = x/t$. In this chapter we will reserve the bold, lower-case, roman characters to denote arbitrary points in the two phase region. Quite often we will write $(s_o, T) \equiv \mathbf{w} \in \mathbf{TP}$, for a given point.

System (4.1) can be written in compact form as:

$$\partial_t G(\mathbf{w}) + \partial_x u F(\mathbf{w}) = 0, \quad (4.3)$$

where:

$$G(s_o, T) = \varphi \begin{pmatrix} \rho_{gV} s_g + \rho_V s_o \\ \rho_{od} s_o \\ \widehat{H}_r + s_o H_o + s_g H_g \end{pmatrix} \quad \text{and} \quad F(s_o, T) = \begin{pmatrix} \rho_{gV} f_g + \rho_V f_o \\ \rho_{od} f_o \\ f_o H_o + f_g H_g \end{pmatrix}. \quad (4.4)$$

As it was discussed in Chapter 2, smooth solutions of the conservation laws are related to a generalized eigenvalue problem, which we call the characteristic equation of the system. Recalling Section 2.1, the matrix of this equation is written as:

$$J(\mathbf{w}, u; \lambda) = (uDF(\mathbf{w}) - \lambda DG(\mathbf{w}), F(\mathbf{w})), \quad (4.5)$$

where the D denotes differentiation relative to \mathbf{w} .

Let $(\mathbf{w}(\xi), u(\xi))$ be a smooth self-similar solution of (4.1) conveniently parametrized by ξ and \vec{r}_i a right eigenvector of matrix (4.5). They must satisfy together the ordinary differential equation:

$$(\dot{\mathbf{w}}(\xi), \dot{u}(\xi)) = \vec{r}_i(\mathbf{w}(\xi), u(\xi)), \quad (4.6)$$

for all points in the domain of the parametrization and a suitable initial datum. The eigenvector $\vec{r}_i(\mathbf{w}, u)$ solves the equation:

$$J(\mathbf{w}, u; \lambda_i) \vec{r}_i(\mathbf{w}, u) = 0, \quad (4.7)$$

for some family i , since \mathbf{TP} is a two dimensional manifold – see Equation (4.2). Further details in the derivation of the model can be found in Chapter 3, particularly in Section 3.5.3 where we derive the system of conservation laws in two phase equilibrium, together with its state space. A review of the basic theory of conservation laws can be found in Chapter 2.

4.1.1 Calculations

To calculate the characteristic equation for system (4.1), we define the temperature-dependent quantities:

$$\alpha = \rho_V - \rho_{gV}, \quad \beta = \rho_{od} \quad \text{and} \quad \gamma = H_o - H_g, \quad (4.8)$$

to get from Equations (4.4) and (4.5):

$$J = \begin{pmatrix} \alpha(u\partial_{s_o}f_o - \varphi\lambda) & u\partial_T(\alpha f_o + \rho_{gV}) - \varphi\lambda\partial_T(\alpha s_o + \rho_{gV}) & \alpha f_o + \rho_{gV} \\ \beta(u\partial_{s_o}f_o - \varphi\lambda) & u\partial_T(\beta f_o) - \varphi\lambda\partial_T(\beta s_o) & \beta f_o \\ \gamma(u\partial_{s_o}f_o - \varphi\lambda) & u\partial_T(\gamma f_o + H_g) - \varphi\lambda\partial_T(\gamma s_o H_o + H_g + \widehat{H}_r) & \gamma f_o + H_g \end{pmatrix}. \quad (4.9)$$

Gaussian elimination in (4.9) on the second and third elements of the first column yields:

$$\tilde{J} = \begin{pmatrix} \alpha(u\partial_{s_o}f_o - \varphi\lambda) & u\partial_T(\alpha f_o + \rho_{gV}) - \varphi\lambda\partial_T(\alpha s_o + \rho_{gV}) & \alpha f_o + \rho_{gV} \\ 0 & u(a_1 f_o + b_1) - \varphi\lambda(a_1 s_o + b_1) & -\beta\rho_{gV} \\ 0 & u(a_2 f_o + b_2) - \varphi\lambda(a_2 s_o + b_2 + \alpha\widehat{H}'_r) & -\gamma\rho_{gV} + H_g \end{pmatrix}, \quad (4.10)$$

where a_1, a_2, b_1, b_2 are functions of the temperature given by:

$$\begin{cases} a_1 = \alpha\partial_T\beta - \beta\partial_T\alpha, \\ b_1 = -\beta\partial_T\rho_{gV}, \\ a_2 = \alpha\partial_T\gamma - \gamma\partial_T\alpha, \\ b_2 = \alpha\partial_T H_g - \gamma\partial_T\rho_{gV}. \end{cases} \quad (4.11)$$

The Buckley-Leverett characteristic speed appears very clearly from (4.10) as:

$$\lambda_b = \frac{u}{\varphi}\partial_{s_o}f_o. \quad (4.12)$$

The (right) eigenvector associated to the Buckley-Leverett eigenvalue is also very easily obtained as (a multiple of):

$$\vec{r}_b = (1, 0, 0)^T. \quad (4.13)$$

It will become clear that the Buckley-Leverett waves, which will often be indicated by the subscript b , represent solely fluid transport with no temperature changes. This can be readily seen for the rarefactions. To complete the description of b waves let us focus on left eigenvectors. Notice that the left eigenvector associated to λ_b spans the annihilator of the second and third columns of J , Equation (4.9). Wherever strict hyperbolicity holds, the annihilator is a one dimensional space and $\vec{l}_b(\mathbf{w})$ is a scalar multiple of the cross product

of the second and third columns of J , Equation (4.9).

Remark 4.1 Notice that the left b -eigenvector is independent of the Darcy speed u . This is a typical property in this class of models, satisfied by all wave families, see section 2.1.

The other eigenvalue is associated to temperature variations and mass transfer between the two phases, for example, evaporation. Due to this fact we write its characteristic speed as λ_e . Regarding the latter eigenvalue we can state the very useful:

Proposition 4.2 As long as $\lambda_e(\mathbf{w}) \neq \lambda_b(\mathbf{w})$ for a state $\mathbf{w} = (s_o, T)$ in **TP** the left e -eigenvector can be written as a function of the temperature alone: $\vec{l}_e = \vec{l}_e(T)$.

Proof. Since we are examining states where the system is strictly hyperbolic, the first column of (4.9) does not vanish. We write the cross product of the first and the third columns and cancel out the vanishing terms to obtain (the cross product is indicated by \times):

$$\vec{l}_e = (\alpha, \beta, \gamma) \times (\rho_{gV}, 0, H_g). \quad (4.14)$$

This vector is clearly a function of temperature only and is orthogonal to the first and the third columns of J . We proceed to show that this vector is non zero. Writing it explicitly we get:

$$\begin{aligned} \vec{l}_e &= (\beta H_g, \gamma \rho_{gV} - \alpha H_g, -\beta \rho_{gV}) \\ &= (\rho_{od} H_g, (H_o - H_g) \rho_{gV} - (\rho_V - \rho_{gV}) H_g, -\rho_{od} \rho_{gV}) \\ &= (\rho_{od} H_g, \rho_V \rho_{gV} (h_o - h_g), -\rho_{od} \rho_{gV}). \end{aligned}$$

By Equations (3.3), (3.5) and (3.6) the dead oil concentration can only vanish at T_{bV} , where the gas and liquid alkane enthalpies cannot cancel out because of their very definitions (see Appendix A.1). The proof is complete. \square

We proceed to calculate the e -characteristic speed. To calculate the eigenvalue λ_e we only need to compute the determinant of the 2×2 right lower block of equation (4.10). This yields:

$$\lambda_e(\mathbf{w}, u) = \frac{u A f_o + B_1}{\varphi A s_o + B_2}. \quad (4.15)$$

where:

$$\begin{cases} A(T) &= \rho_V (h_g - h_o) \partial_T \rho_{od} + \rho_{od} (\partial_T H_o - \rho_{gV} \partial_T h_g), \\ B_1(T) &= \rho_{od} \rho_{gV} h'_g, \\ B_2(T) &= \rho_{od} (\rho_{gV} h'_g + H'_r), \end{cases} \quad (4.16)$$

and the reader should keep in mind that $'$ stands for differentiation.

Remark 4.3 *The quantities A , B_1 and B_2 are positive for any $T \geq T_{bV}$. This can be readily seen for B_1 and B_2 since they are the product of densities by heat capacities. To see that A is positive, first notice that ρ_{od} is a strictly increasing function of the temperature in **TP** so its derivative must be positive. The gas enthalpy is strictly greater than the oil enthalpy at the boiling temperature due to the vaporization latent heat (see A.4) so that $\rho_V(h_g - h_o)\partial_T\rho_{od}$ is positive near T_{bV} . As the heat capacity of the oil is greater than the heat capacity of the gas one can see that the term $\rho_{od}(\partial_T H_o - \rho_{gV}\partial_T h_g)$ is always positive, at least for our specific values of oil and vapor parameters. This is sufficient for our purposes. The reader may verify that these quantities remains positive for high temperatures, by noticing that the first term of (4.16a) is $O(T^{-1})$ while the second one is $O(1)$ so that a computation shows that $A(T)$ remains positive.*

Remark 4.4 *Notice that the eigenvalues have the form: $\lambda_i(\mathbf{w}, u) = u\tilde{\lambda}_i(\mathbf{w})$, the reader should recall Section 2.1.*

To calculate the right e -eigenvector we rewrite (4.10) replacing λ by $u\tilde{\lambda}_e$ as:

$$\tilde{J} = \begin{pmatrix} u l_{11}(\tilde{\lambda}_e; \mathbf{w}) & u l_{12}(\tilde{\lambda}_e; \mathbf{w}) & l_{13}(\mathbf{w}) \\ 0 & u d_{11}(\tilde{\lambda}_e; \mathbf{w}) & d_{12}(\mathbf{w}) \\ 0 & u d_{21}(\tilde{\lambda}_e; \mathbf{w}) & d_{22}(\mathbf{w}) \end{pmatrix}. \quad (4.17)$$

Notice that we have just changed the nomenclature. For example, the element in the first row and first column in Equation (4.10) is written in Equation (4.17) as:

$$l_{11}(\tilde{\lambda}_e, \mathbf{w}) = \alpha(\partial_{s_o} f_o - \varphi\tilde{\lambda}_e). \quad (4.18)$$

Returning to the calculation of the eigenvector we have:

$$l_{13} = \rho_V f_o + \rho_{gV} f_g, \quad (4.19)$$

which never vanishes. Using the notation $\vec{r}_e \equiv (r_1, r_2, r_3)^T$, we can solve the first equation of the system $\tilde{J}\vec{r}_e = 0$ as:

$$r_3 = -\frac{u}{l_{13}}(l_{11}r_1 + l_{12}r_2); \quad (4.20)$$

substituting r_3 into the second equation in $\tilde{J}\vec{r}_e = 0$, see (4.17), we obtain:

$$m(\mathbf{w})r_2 = l_{11}d_{12}r_1, \quad (4.21)$$

where we have introduced the notation

$$m(\mathbf{w}) = l_{13}d_{11} - l_{12}d_{12}, \quad (4.22)$$

Now we can write down the eigenvector associated with λ_e :

$$\vec{r}_e(\mathbf{w}, u) = \left(m, l_{11}d_{12}, -u \frac{l_{11}}{l_{13}}(m + l_{12}) \right). \quad (4.23)$$

This choice can only vanish at points \mathbf{w} for which $m(\mathbf{w}) = 0$ and $l_{11}(\mathbf{w}) = 0$ simultaneously. Noticing that $l_{11}(\mathbf{w}) = 0$ implies $(\partial_{s_o} f_o - \varphi \hat{\lambda}_e) = 0$, we are led to the following:

Definition 4.5 *The singular set in the \mathbf{TP} region is the set:*

$$\mathbb{S} = \{\mathbf{w} \in \mathbf{TP} \mid m(\mathbf{w}) = 0 \text{ and } \tilde{\lambda}_b(\mathbf{w}) = \tilde{\lambda}_e(\mathbf{w})\}.$$

We will study a range of temperatures in which \mathbb{S} consists of the single point shown in Figure 4.1. The singular point will play a crucial role in the Riemann solution. Of course, an eigenvector is defined up to a multiplicative factor and we may ask, for example, if the singular point is a removable zero of this formula for \vec{r}_e . This is not the case and in the Subsection 4.5.1 we will tackle this issue and, in particular, show that the singular set corresponds to the place where the geometric multiplicity of the Jacobian (4.5) changes. In our case the eigenvectors form a vector field. Figure 4.1 shows an orbit of the flow induced in \mathbf{TP} by the smooth function on the right hand side of Equation (4.23).

4.2 Elementary wave curves

A Riemann solution is a concatenation of constant states and elementary waves, *i.e.*, rarefaction waves and shock waves (discontinuous solutions). Elementary wave curves are the projection of certain parametrizations of admissible elementary waves into state space. In our case, rarefaction wave curves are determined by the integral curves of the vector fields given by the right eigenvectors given in (4.13) and (4.23). Shock wave curves are determined by the Hugoniot locus, see Equations (4.28), (2.28).

4.2.1 Rarefaction curves

A rarefaction curve of the i^{th} family emanating from (\mathbf{w}^*, u^*) is the maximal subset in the image of the solution of the Ordinary Differential Equation:

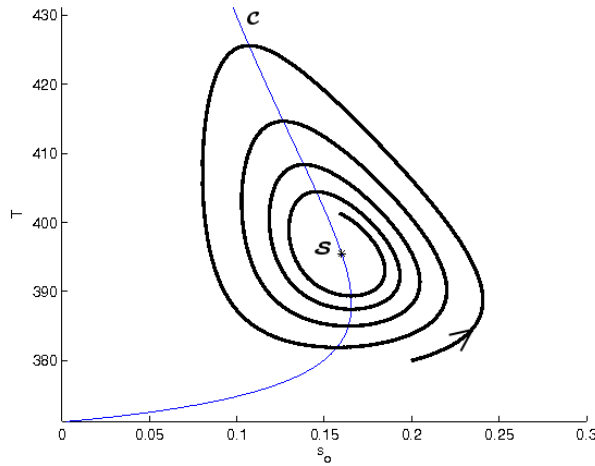


Figure 4.1: A spiraling orbit of the flux induced in \mathbf{TP} by the vector field (4.23) near the singular point \mathcal{S} ; in our case the eigenvectors form a vector field. The singular point \mathcal{S} lies on the coincidence curve \mathcal{C} .

$$\begin{cases} (\dot{\mathbf{w}}(\xi), \dot{u}(\xi))^T = \vec{r}_i(\mathbf{w}(\xi), u(\xi)), \\ (\mathbf{w}(\xi^*), u(\xi^*)) = (\mathbf{w}^*, u^*), \end{cases} \quad (4.24)$$

such that the parametrization:

$$\xi \mapsto \lambda_i(\mathbf{w}(\xi), u(\xi)), \quad \xi \geq \xi^*, \quad (4.25)$$

is monotonically increasing and the right eigenvector (\vec{r}_i) is given by (4.13) or (4.23). Since we can compute u explicitly in terms of \mathbf{w} , we will only show their projections into the state space \mathbf{TP} . More information can be found in Chapter 2.

The Buckley-Leverett rarefaction curves are horizontal lines, as can be seen from Equation (4.13).

The e -rarefaction curves possess a more sophisticated behavior. Beginning from a singular point, see Definition 4.5, there is no preferential direction to leave (or reach) it with a rarefaction curve. We will return to this issue in Proposition 4.18. Singular points that arise in this work are the zeros of the smooth function on the right hand side of Equation (4.23). The image of this function is a vector field. In our case, generically the singular points are attractors or repellers, according to the orientation given to $\vec{r}_e(\mathbf{w}, u)$. In a sufficiently small neighborhood of a singular point, the orbits of:

$$(\dot{\mathbf{w}}(\xi), \dot{u}(\xi))^T = \vec{r}_e(\mathbf{w}(\xi), u(\xi)), \quad (4.26)$$

must cross the inflection locus \mathcal{I}_e (see Subsection 4.5.2): it is not difficult to see that the rarefaction curves go around the singular point. This is illustrated in Figure 4.2.

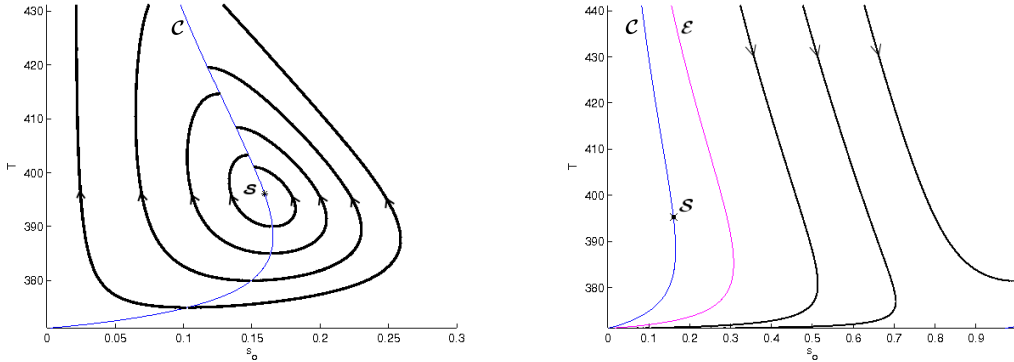


Figure 4.2: Some e -rarefaction curves in **TP**. Left: rarefaction curves begin at the inflection curve $\mathcal{C} \subset \mathcal{I}_e$, below the singular point \mathcal{S} , and end at the same inflection curve, above the singular point. Right: e -rarefaction curves far away from the singular point.

4.2.2 Shock curves

A shock wave of speed σ connecting the pairs (\mathbf{w}^+, u^+) , (\mathbf{w}^-, u^-) is a jump discontinuity that satisfies the Rankine-Hugoniot Equation (2.10), which we repeat:

$$u^+ F(\mathbf{w}^+) - u^- F(\mathbf{w}^-) - \sigma (G(\mathbf{w}^+) - G(\mathbf{w}^-)) = 0. \quad (4.27)$$

Typically, our interest is to fix an initial state (w^-, u^-) and ask which is the locus of states (w^+, u^+) that satisfy Equation (4.27). To this end we define the Hugoniot function, $\mathcal{H}_{\mathbf{w}^-} : \Omega \times \mathbb{R}^+ \times \mathbb{R} \rightarrow \mathbb{R}^3$, as:

$$\mathcal{H}_{\mathbf{w}^-}(\mathbf{w}^+, u^+, \sigma) = u^+ F(\mathbf{w}^+) - F(\mathbf{w}^-) - \sigma (G(\mathbf{w}^+) - G(\mathbf{w}^-)), \quad (4.28)$$

and by Remark 2.8 it is sufficient to consider the case $u^- = 1$. The Hugoniot locus, or shock curve, of state \mathbf{w}^- is the projection of the zero set:

$$\{ (\mathbf{w}^+, u^+, \sigma) \in \Omega \times \mathbb{R}^+ \times \mathbb{R} \mid \mathcal{H}_{\mathbf{w}^-}(\mathbf{w}^+, u^+, \sigma) = 0 \}, \quad (4.29)$$

into $\Omega \times \mathbb{R}^+$ and we will write it as $\mathcal{H}(\mathbf{w}^-)$, recall that $u^- = 1$ (nevertheless, there will be a couple of occasions where we will write $\mathcal{H}(\mathbf{w}^-, u^-)$ to select exactly the Hugoniot locus passing through (\mathbf{w}^-, u^-)). Very often it will be convenient to use the projection

into state space Ω , which we will still call Hugoniot locus. In fact, it can be shown that both sets are in one to one correspondence.

Away from the base point \mathbf{w}^- , typically the Hugoniot locus is a smooth curve. Locally, if the base point is a point of strict hyperbolicity the Hugoniot locus bifurcates into 2 branches (the dimension of the state space \mathbf{TP}), see Lax [32] or the more recent reference Dafermos [13]. If strict hyperbolicity fails this may not hold, *e.g.*, at the umbilic point in [26].

Now we will give a global description for the \mathbf{TP} branches of the Hugoniot locus. To this end, we rewrite the Rankine-Hugoniot Equation (4.27) in matrix form:

$$(F(\mathbf{w}^+); F(\mathbf{w}^-); [G]) \cdot (u^+, -u^-, -\sigma)^T = 0, \quad (4.30)$$

where $[G] = (G(\mathbf{w}^+) - G(\mathbf{w}^-))$ and point out that if Equation (4.30) holds then:

$$\mathcal{H}(\mathbf{w}^-) = \{\mathbf{w}^+ \in \mathbf{TP} \mid \det(F(\mathbf{w}^+); F(\mathbf{w}^-); [G]) = 0\}. \quad (4.31)$$

Proposition 4.6 (Buckley-Leverett branch of the Hugoniot locus). *The locus $\mathcal{H}(\mathbf{w}^-)$ always contains an isothermal branch in \mathbf{TP} . In this branch, the following equalities hold:*

$$u^+ = u^- \quad \text{and} \quad \sigma = u^+ \frac{f_o^+ - f_o^-}{s_o^+ - s_o^-}. \quad (4.32)$$

Proof. Choose (\mathbf{w}^-, u^-) , (\mathbf{w}^+, u^+) , with $\mathbf{w} = (s_o, T)$, such that $T^- = T^+ = T$. From Equations (4.4) and (4.8) we have:

$$[G] = \begin{pmatrix} \alpha \\ \beta \\ \gamma \end{pmatrix} (s_o^+ - s_o^-) \quad \text{and} \quad F^\pm = \begin{pmatrix} \alpha \\ \beta \\ \gamma \end{pmatrix} f_o^\pm + \begin{pmatrix} \rho_{gV} \\ 0 \\ H_g \end{pmatrix}, \quad (4.33)$$

where $\alpha = \alpha(T)$, $\beta = \beta(T)$, $\gamma = \gamma(T)$ and $f_o^\pm = f_o(s_o^\pm, T)$. From Equation (4.33) we can readily see that Equation (4.31) is satisfied.

Clearly, Equations (4.32) and (4.33) satisfy Equation (4.30). To see that these are the sole solutions for u^- fixed, notice that the matrix $(F(\mathbf{w}^+); F(\mathbf{w}^-); [G])$ has a one dimensional kernel (see the proof of Proposition 4.2). \square

Remark 4.7 *Of course, admissible shocks in the Buckley-Leverett branch are b-shocks.*

Proposition 4.6 motivates calling this isothermal branch as \mathcal{H}_b , where the subscript

stands for Buckley-Leverett. We therefore have for a state $\mathbf{w}^- = (s_o^-, T^-)$:

$$\mathcal{H}_b(\mathbf{w}^-) = \{ \mathbf{w}^+ = (s_o^+, T^+) \in \mathbf{TP} \mid T^+ - T^- = 0 \}. \quad (4.34)$$

Motivated by Proposition 4.6 we write the function:

$$h_e(\mathbf{w}^-; \mathbf{w}^+) = \begin{cases} \frac{\det(F(\mathbf{w}^+); F(\mathbf{w}^-); [G])}{T^+ - T^-}, & \text{when } T^+ \neq T^-, \\ \lim_{T^+ \rightarrow T^-} \frac{\det(F(\mathbf{w}^+); F(\mathbf{w}^-); [G])}{T^+ - T^-}, & \text{otherwise.} \end{cases} \quad (4.35)$$

It is a simple but long computation to show that the limit in Equation (4.35b) is well defined and h_e a smooth function. We define:

$$\mathcal{H}_e(\mathbf{w}^-) = \{ \mathbf{w}^+ \in \mathbf{TP} \mid h_e(\mathbf{w}^-; \mathbf{w}^+) = 0 \}, \quad (4.36)$$

which we call the evaporation branch of the Hugoniot locus with base state \mathbf{w}^- .

Remark 4.8 *Admissible shock waves in the \mathcal{H}_e branches are e -shocks.*

Remark 4.9 *Of course: $\mathcal{H}(\mathbf{w}^-) = \mathcal{H}_b(\mathbf{w}^-) \cup \mathcal{H}_e(\mathbf{w}^-)$.*

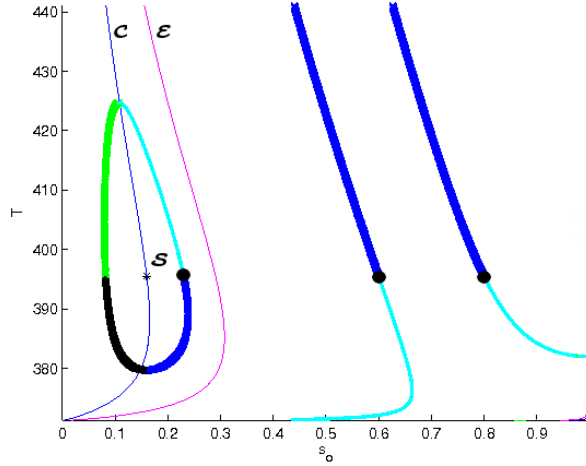


Figure 4.3: Some e -branches in \mathbf{TP} . The black dot identifies the base state. Horizontal saturation b -branches are omitted.

In our case, away from the singular points the topology of the e -branch changes, but it is always a smooth curve. Beginning from a singular point, see Definition 4.5, we have

that if $\mathbf{w}_0 \in \mathbb{S}$ then $\mathcal{H}_e(\mathbf{w}_0) = \{\mathbf{w}_0\}$. In the neighborhood of a singular point the e branch of the Hugoniot locus is diffeomorphic to a circle, resembling an oval. A proof of this fact could be given through Morse Lemma, however, we will not do this: we will just rely on numerical evidence. Away from the singular points the \mathcal{H}_e is a closed unbounded curve. We will return to this change of topology issue in Section 4.5.3. Some branches are shown in Figure 4.3.

To conclude this section we recall that when verifying wave admissibility, it is necessary to calculate both the shock speed and the Darcy speed u^+ explicitly. Since the e -branch does not have simple formulas, as those in Equation (4.32), we need to fall back to the full set of Equations (4.27). The calculation can be done by any two of the three equations:

$$\left\{ \begin{array}{l} u^+ (F_k^+[G_j] - F_j^+[G_k]) = u^- (F_k^-[G_j] - F_j^-[G_k]), \\ \sigma ([G_k]F_j^+ - [G_j]F_k^+) = u^- (F_j^- F_k^+ - F_k^- F_j^+), \\ \sigma ([G_k]F_j^- - [G_j]F_k^-) = u^+ (F_j^- F_k^+ - F_k^- F_j^+), \end{array} \right. \quad (4.37)$$

where $1 \leq j, k \leq 3$, $j \neq k$, $[G_k] = G_k^+ - G_k^-$ and $\mathbf{w}^-, \mathbf{w}^+$ are given. According to the situation, it could be more useful to make the shock speed an explicit function of u^- or u^+ .

4.3 Triple Shock Rule and properties of the Darcy speed

The Triple Shock Rule is among the simplest and most useful results in hyperbolic conservation laws. It allows one to characterize shocks that differ in state space but give rise to the same physical profile. In our particular problem, it will be a very useful tool to characterize the bifurcations in the Riemann solution.

Theorem 4.10 (Triple Shock Rule). *Let three points $P^a = (\mathbf{w}^a, u^a)$, $P^b = (\mathbf{w}^b, u^b)$ and $P^c = (\mathbf{w}^c, u^c)$ be such that all pairs among them satisfy the Rankine-Hugoniot relation (4.27). Denote the corresponding shock speeds by $\sigma_1 = \sigma(a; b)$, $\sigma_2 = \sigma(b; c)$ and $\sigma_3 = \sigma(c; a)$.*

If $G^a = G(\mathbf{w}^a)$, $G^b = G(\mathbf{w}^b)$ and $G^c = G(\mathbf{w}^c)$ are linearly independent then:

$$\sigma_1 = \sigma_2 = \sigma_3.$$

Proof. After writing the Rankine-Hugoniot relation (4.27) for points $P^a = (\mathbf{w}^a, u^a)$, $P^b = (\mathbf{w}^b, u^b)$ and $P^c = (\mathbf{w}^c, u^c)$:

$$\begin{cases} \sigma_1 (G^b - G^a) = u^b F^b - u^a F^a, \\ \sigma_2 (G^c - G^b) = u^c F^c - u^b F^b, \\ \sigma_3 (G^a - G^c) = u^a F^a - u^c F^c; \end{cases}$$

by adding the equations above we find:

$$(\sigma_3 - \sigma_1)G^a + (\sigma_1 - \sigma_2)G^b + (\sigma_2 - \sigma_3)G^c = 0, \quad (4.38)$$

and the Theorem is proved. \square

A small peculiarity emerges in this class of problems: we need to deal with the Darcy speed u . In Theorem 4.10, using Equation (4.37a) and assuming that the denominators are nonzero we see that the Darcy speed u^c is given by two different expressions:

$$u^c = u^a \frac{F_k^a [G_j^c - G_j^a] - F_j^a [G_k^c - G_k^a]}{F_k^c [G_j^c - G_j^a] - F_j^c [G_k^c - G_k^a]}, \quad (4.39)$$

and

$$u^c = u^a \frac{F_k^b [G_j^c - G_j^b] - F_j^b [G_k^c - G_k^b]}{F_k^c [G_j^c - G_j^b] - F_j^c [G_k^c - G_k^b]} \frac{F_k^a [G_j^b - G_j^a] - F_j^a [G_k^b - G_k^a]}{F_k^b [G_j^b - G_j^a] - F_j^b [G_k^b - G_k^a]}, \quad (4.40)$$

for a fixed pair of indices $1 \leq j \neq k \leq 3$. To make the computations clearer, for a pair of states \mathbf{w}^+ , \mathbf{w}^- let us introduce the rescaled speed:

$$\mathbf{U}(\mathbf{w}^-, \mathbf{w}^+) = \frac{F_k^- [G_j^+ - G_j^-] - F_j^- [G_k^+ - G_k^-]}{F_k^+ [G_j^+ - G_j^-] - F_j^+ [G_k^+ - G_k^-]}, \quad 1 \leq j \neq k \leq 3, \quad (4.41)$$

which makes sense wherever the denominator is nonzero and is smooth. In the limit $\mathbf{w}^+ \rightarrow \mathbf{w}^-$, $\mathbf{U}(\mathbf{w}^-, \mathbf{w}^+) \rightarrow 1$ (see the characterization of the Hugoniot locus in a neighborhood where strict hyperbolicity holds, [28]). Proposition 4.6 yields that if $\mathbf{w}^- = (s_o^-, T^-)$, $\mathbf{w}^+ = (s_o^+, T^+)$ satisfy $T^- = T^+$ then $\mathbf{U}(\mathbf{w}^-, \mathbf{w}^+) = 1$ for $s_o^- \neq s_o^+$. Equations (4.39) and (4.40) express the property for the Darcy speed summarized as:

$$\mathbf{U}(\mathbf{w}^a, \mathbf{w}^c) = \mathbf{U}(\mathbf{w}^a, \mathbf{w}^b) \cdot \mathbf{U}(\mathbf{w}^b, \mathbf{w}^c). \quad (4.42)$$

For \mathbf{w}^- fixed, an important property of the rescaled speed (4.41) is that it is only a function of the temperature T^+ . To see this, let us write the Rankine-Hugoniot Equation (4.27) for system (4.1):

$$\left\{ \begin{array}{l} \sigma [\alpha^+ s_o^+ + \rho_{gV}^+ - F_1^-] - u^+ (\alpha^+ f_o^+ + \rho_{gV}^+) + u^- F_1^- = 0, \\ \sigma [\beta^+ s_o^+ - F_2^-] - u^+ \beta^+ f_o^+ + u^- F_2^- = 0, \\ \sigma [\gamma^+ s_o^+ + H_g^+ + H_r^+ - F_3^-] - u^+ (\gamma^+ f_o^+ + H_g^+) + u^- F_3^- = 0, \end{array} \right. \quad (4.43)$$

where we used the nomenclature defined in Equations (4.4) and (4.8). In our case $\beta = \rho_{od}$ never vanishes: see Equations (3.3), (3.5), (3.6) and recall the definition of the two phase state space (4.2). Thus, we can recast Equations (4.43b) and (4.43c) without the dependence in s_o^+ :

$$\left\{ \begin{array}{l} \sigma (\alpha^+ F_2^- - \beta^+ F_1^- + \beta^+ \rho_{gV}^+) - u^+ \beta^+ \rho_{gV}^+ + u^- (\beta^+ F_1^- - \alpha^+ F_2^-) = 0, \\ \sigma [\gamma^+ F_2^- - \beta^+ F_3^- + \beta^+ (H_g^+ + H_r^+)] - u^+ \beta^+ H_g^+ + u^- (\beta^+ F_3^- - \gamma^+ F_2^-) = 0. \end{array} \right. \quad (4.44)$$

Eliminating σ in Equations (4.44) we obtain u^+ as a function of u^- , \mathbf{w}^- and T^+ . If we require that for any $\mathbf{w}^+ \in \mathcal{H}(\mathbf{w}^-)$ the Hugoniot matrix (4.30) has a one dimensional kernel, then the value u^+ obtained from Equation (4.44) with the choice $u^- = 1$ must agree with $\mathbf{U}(\mathbf{w}^-, \mathbf{w}^+)$ given in Equation (4.41). We have proved:

Proposition 4.11 *Let $(s_o^+, T^+) = \mathbf{w}^+ \in \mathcal{H}(\mathbf{w}^-)$ be such that the rows of the matrix in the Rankine-Hugoniot relation (4.30) for \mathbf{w}^- , \mathbf{w}^+ are not parallel. Then the rescaled speed $\mathbf{U}(\mathbf{w}^-, \mathbf{w}^+)$ is a function of \mathbf{w}^- and T^+ .*

Despite Proposition 4.11, Equation (4.41) is very useful in applications, since it is simpler than the formula obtained from Equations (4.44). A similar result holds for the shock speed.

Proposition 4.12 *Assume that $\mathbf{w}^b = (s_o^b, T^b)$, $\mathbf{w}^c = (s_o^c, T^c)$ satisfy $\mathbf{w}^b, \mathbf{w}^c \in \mathcal{H}(\mathbf{w}^a)$ and $T^b = T^c = T$. We use the notation $u^b = \mathbf{U}(\mathbf{w}^a, \mathbf{w}^b)$ and $u^c = \mathbf{U}(\mathbf{w}^a, \mathbf{w}^c)$ for Darcy speeds and $P^a = (\mathbf{w}^a, u^a)$, $P^b = (\mathbf{w}^b, u^b)$ and $P^c = (\mathbf{w}^c, u^c)$ for points. If the conditions of Proposition 4.11 and Theorem 4.10 are satisfied then:*

1. $\mathbf{U}(\mathbf{w}^a, \mathbf{w}^b) = \mathbf{U}(\mathbf{w}^a, \mathbf{w}^c)$,

$$2. (\mathbf{w}^c, u^c) \in \mathcal{H}(\mathbf{w}^b, u^b),$$

$$3. \sigma(P^a; P^b) = \sigma(P^b; P^c) = \sigma(P^c; P^a).$$

Proof. The equality in (1) follows from Proposition 4.11. Proposition 4.6 together with (1) implies (2). By (1) and (2) the points P^a , P^b and P^c satisfy the hypotheses of the Triple Shock Rules 4.10, which yields (3). \square

4.4 The Bethe-Wendroff Theorem

In our case, away from the singular points, the Hugoniot branches are smooth curves and can be parametrized by a single variable. Let a superimposed dot denote differentiation with respect to this variable. Fix a branch $\mathcal{H}_i(\mathbf{w}^-)$, $i \in \{b, e\}$, and consider the parametrization:

$$\zeta \mapsto P^\zeta = (\mathbf{w}(\zeta), u(\zeta)) \in \mathcal{H}_i(\mathbf{w}^-), \quad \zeta \in [0, \zeta_0), \quad (4.45)$$

such that $P^0 = (\mathbf{w}^-, 1)$. The shock speed between P^0 and P^ζ , given by Equation (4.37b), will be written as $\sigma(\zeta) = \sigma(P^0; P^\zeta)$.

Theorem 4.13 (Bethe-Wendroff). *Consider the Hugoniot locus through a state \mathbf{w}^- . Assume that for $\mathbf{w}(\zeta) \in \mathcal{H}(\mathbf{w}^-)$:*

$$\vec{l}_i(\mathbf{w}(\zeta)) (G(\mathbf{w}(\zeta)) - G(\mathbf{w}^-)) \neq 0.$$

Then the following are equivalent: (a) $\dot{\sigma}(\zeta) = 0$, (b) $\lambda_i(\mathbf{w}(\zeta), u(\zeta)) = \sigma(\zeta)$, for a family $i \in \{b, e\}$. In this case, $\lambda_i(\mathbf{w}(\zeta), u(\zeta)) - \sigma(\zeta)$ and $\dot{\sigma}(\zeta)$ vanish to the same order and the locus is tangent to an integral curve of the i^{th} -family, with the same order of tangency.

A proof of this theorem, adapted to our class of problems, can be found in Lambert [28]. A stronger version for classical systems can be found in Furtado [19]. Roughly, the Bethe-Wendroff Theorem relates the monotonicity of the shock speed along the Hugoniot locus with the admissibility of shock waves, see the Liu criterion 2.14. Moreover, by giving a geometric characterization of admissibility it is fundamental tool in the construction of the Riemann solution.

4.5 Bifurcation manifolds in TP

These are sets in state space that play a fundamental role in the construction of Riemann solutions. More details can be found in Section 2.3, in the monograph by Furtado [19] and in the monograph by Lambert [28].

4.5.1 Coincidence locus

Among the loci that are relevant for the behavior of the solution, the coincidence locus is perhaps the most easily defined one. As it is known, even a single, isolated point of coincidence of characteristic speeds can greatly complicate the solution, see Isaacson, Marchesin, Plohr, and Temple [26].

In this work the coincidence locus is the set of points where strict hyperbolicity fails, see Definition 2.1.

Definition 4.14 *The coincidence locus in TP is the set:*

$$\mathcal{C} = \{\mathbf{w} \in \mathbf{TP} \mid \tilde{\lambda}_b(\mathbf{w}) = \tilde{\lambda}_e(\mathbf{w})\},$$

see Equations (4.12), (4.15) and Remark 4.4.

The coincidence locus is well behaved in our class of problems. It is the union of two smooth curves in the TP region. It also has an elegant graphical interpretation, see Figure 4.4.

Fix $T \geq T_{bV}$. Notice that from Equation (4.15), $\tilde{\lambda}_e(\cdot, T)$ can be visualized as the slope of a secant to the graph of $f_o(\cdot, T)$ from the point $(-B_2/A, -B_1/A)$. Since $\tilde{\lambda}_b(s_o^*, T)$ is the slope of the line tangent to the graph of $f_o(s_o^*, T)$ for any $0 \leq s_o^* \leq 1$, as can be seen by equation (4.12), it is not difficult to see that the slope of this secant must equal the tangent of f_o at two points: the first one at a minimum and the second one at a maximum of $\tilde{\lambda}_e$.

This reasoning can easily be made analytical. First notice that:

Proposition 4.15 *Fix $T \geq T_{bV}$. If s^* is maximizer for $\tilde{\lambda}_b(\cdot, T)$ then $\tilde{\lambda}_b(s^*, T) > \tilde{\lambda}_e(s^*, T)$.*

Proof. The Buckley-Leverett speed is smooth, non-negative, it vanishes for states at pure oil saturation or at pure gas saturation and it has a single global maximum (which is therefore a critical point), see Section 3.3 and, particularly, Remark 3.2. Since $f_o(0, T) = 0$, $f_o(1, T) = 1$ and $f_o(\cdot, T)$ is quadratic near 0 then its slope must be greater than 1 at its maximum, *i.e.*, $\tilde{\lambda}_b(s^*, T) > 1$.

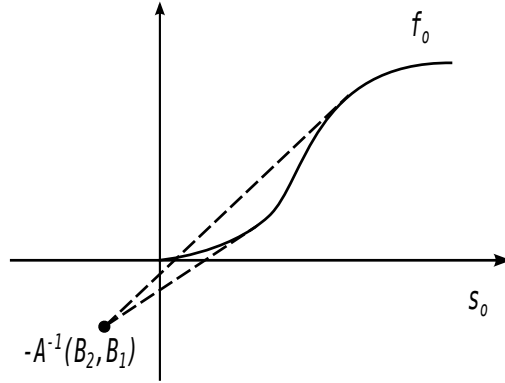


Figure 4.4: Fix some $T \geq T_{bV}$. Notice that $\tilde{\lambda}_e(\cdot, T)$, Equation (4.15), can be visualized as a secant to the graph of $f_o(\cdot, T)$ from the point $(-B_2/A, -B_1/A)$. Since $\tilde{\lambda}_b(s_o^*, T)$ is the slope of the line tangent to the graph of $f_o(s_o^*, T)$ for any $0 \leq s_o^* \leq 1$, as can be seen by equation (4.12), it is not difficult to see that the slope of this secant must equal the tangent of f_o at two points: first at a minimum and then at a maximum of $\tilde{\lambda}_e$.

Assume that we have $\tilde{\lambda}_b(s^*, T) \leq \tilde{\lambda}_e(s^*, T)$. The line through $(s^*, f_o(s^*, T))$ with slope $\tilde{\lambda}_b(s^*, T)$ is:

$$s \mapsto \tilde{\lambda}_b(s^*, T)s + f_o(s^*, T) - \tilde{\lambda}_b(s^*, T)s^*,$$

and the pair $(-B_2/A, -B_1/A)$ in the hatched region in Figure 4.5 must satisfy :

$$-\frac{B_1}{A} \leq -\tilde{\lambda}_b(s^*, T)\frac{B_2}{A} + f_o(s^*, T) - \tilde{\lambda}_b(s^*, T)s^*.$$

Since $A > 0$, this gives:

$$B_1 \geq \tilde{\lambda}_b(s^*, T)B_2 + A \left(\tilde{\lambda}_b(s^*, T)s^* - f_o(s^*, T) \right) \geq B_2.$$

Since $B_2 > B_1$, see Remark 4.3, we have a contradiction. The proof is complete. \square

This simple observation yields at once:

Proposition 4.16 *The coincidence locus is the union of two smooth disconnected curves in the **TP** region.*

Proof. Let us define $g : \mathbf{w} \mapsto g(\mathbf{w}) = \tilde{\lambda}_b(\mathbf{w}) - \tilde{\lambda}_e(\mathbf{w})$, see Equations (4.12) and (4.15). The coincidence locus is clearly the zero set of g . The derivative of g with respect to the

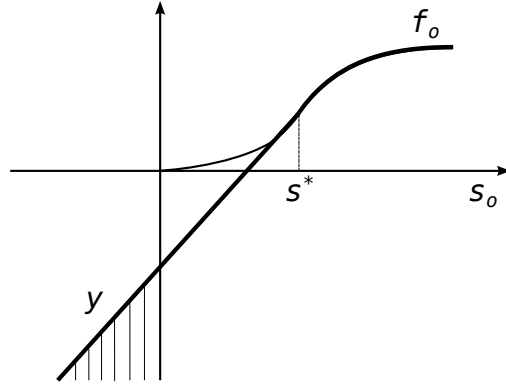


Figure 4.5: Bold curve: begin with the Buckley-Leverett flux function and it is drawn at left of its inflection s^* a straight line with slope $\partial_{s_o} f_o(s^*, T)$.

oil saturation s_o in $\mathbf{w} = (s_o, T)$ is:

$$\partial_{s_o} g(\mathbf{w}) = \partial_{s_o} \tilde{\lambda}_b(\mathbf{w}) - \frac{\tilde{\lambda}_b(\mathbf{w}) - \tilde{\lambda}_e(\mathbf{w})}{As_o + B_2}.$$

Proposition 4.15 says that for any $\mathbf{w}^* = (s_o^*, T^*)$, $T > T_{bV}$ on the coincidence locus we have:

$$\partial_{s_o} g(\mathbf{w}^*) = \partial_{s_o} \tilde{\lambda}_b(\mathbf{w}^*) \neq 0,$$

so C is locally a curve parametrized by the temperature in **TP**.

Now we will count the number of connected components that form the coincidence locus. Fix $T \geq T_{bV}$. Since $\tilde{\lambda}_b = \partial_{s_o} f_o$ vanishes at pure oil saturation and pure gas saturation (see Remark 3.2) and $\tilde{\lambda}_e$ is positive (see Remark 4.3), we have that $\tilde{\lambda}_b(0, T) - \tilde{\lambda}_e(0, T) < 0$ and $\tilde{\lambda}_b(1, T) - \tilde{\lambda}_e(1, T) < 0$ and by Proposition 4.15 there is a s^* between 0 and 1 where $\tilde{\lambda}_b(s^*, T) - \tilde{\lambda}_e(s^*, T) > 0$ so that $f(\cdot, T)$ has at least two roots, say (s_1, s_2) .

One can see that it has at most two roots by noticing that $\tilde{\lambda}_e(\cdot, T)$ is monotone increasing at (s_1, s_2) . Clearly s_1 must be minimum and s_2 a maximum of $\tilde{\lambda}_e(\cdot, T)$. \square

Remark 4.17 Notice that any point $\mathbf{w} = (s_o^*, T) \in C$ must be an isolated global maximum or minimum point for $\tilde{\lambda}_e$ as a function of s_o and fixed T .

Besides the identification of points in state space for which the algebraic multiplicity of the Jacobian (4.5) is greater than one, it is also very important to know when the geometric multiplicity of J is greater than one. Points in state space that are isolated coincidence points and for which the characteristic matrix of the system vanishes are

called *umbilic points*. A great deal is already known about them: they are the primary source of difficulty in the study of three-phase flow and a constant headache for anyone interested in understanding the properties of solutions of conservation laws. Proposition 4.16 says that such umbilic points do not occur in this model but singular points do occur.

Definition 4.5 says that the singular points are the intersection of the zero sets of two smooth maps. We point out that it asserts change in the geometric multiplicity of the Jacobian (4.5).

Proposition 4.18 *The singular set \mathbb{S} is exactly the subset of the coincidence locus where the geometric multiplicity equals the algebraic multiplicity.*

Proof. In fact, let \mathbf{w} be a point on the coincidence. As long as the quantity (4.22) satisfies $m(\mathbf{w}) \neq 0$ we have that $\vec{r}_e \parallel \vec{r}_b$: while the algebraic multiplicity is two, the geometric multiplicity is only one. If we set $m(\mathbf{w}) = 0$ we are saying that the second and third columns of J are indeed linearly dependent. Since the first column vanishes under such conditions and the third column never vanishes, J has a two dimensional kernel. \square

Remark 4.19 *Recall that we have a generalized eigenvalue problem: the standard Jordan normal form is not available for it.*

This is the closest the Jacobian of this system can become to a multiple of the identity matrix. Of course, such loci cannot be isolated as points on the coincidence locus but the singular points form a discrete set. Notice that the zero set of m is a smooth one dimensional manifold, transverse to the coincidence locus, see Figure 4.6.

This let us state:

Proposition 4.20 *The singular set \mathbb{S} is discrete in \mathbf{TP} : if $\mathbf{w}_0 \in \mathbb{S}$ then there is an open neighborhood W of \mathbf{w}_0 in \mathbf{TP} such that $W \cap \mathbb{S} = \mathbf{w}_0$.*

4.5.2 Inflection locus

Points on the inflection locus are those where genuine nonlinearity is lost, see the discussion in Chapter 2. Generically, the characteristic speed does not vary monotonically along a corresponding integral curve near an inflection point. Thus rarefaction curves stop at this locus.

We recall Definition 2.25 and Equation (4.13) to write the b inflection locus as:

$$\mathcal{I}_b = \left\{ \mathbf{w} \in \mathbf{TP} \mid \partial_{s_o} \tilde{\lambda}_b(\mathbf{w}) = 0 \right\}. \quad (4.46)$$

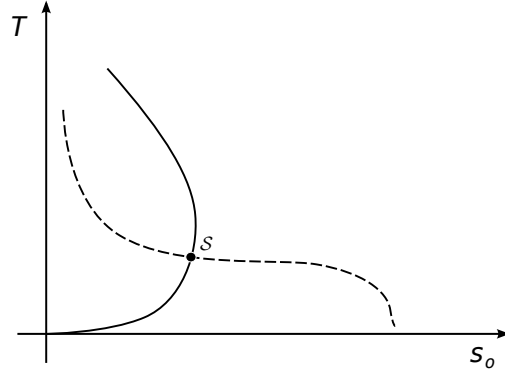


Figure 4.6: Singular point as the intersection of the coincidence locus (solid) and the zero set of m (dashed).

Remark 4.21 Notice that from Equation (4.12) and Remark 3.2 we can readily see that the b inflection locus is a smooth curve.

We now focus on the e -inflection locus. Definition 2.25 gives:

$$\mathcal{I}_e = \left\{ \mathbf{w} \in \mathbf{TP} \mid \partial_{s_o} \tilde{\lambda}_2(\mathbf{w}) r_e^1(\mathbf{w}) + \partial_T \tilde{\lambda}_e(\mathbf{w}) r_e^2(\mathbf{w}) + \tilde{\lambda}_e(\mathbf{w}) r_e^3(\mathbf{w}) = 0 \right\}. \quad (4.47)$$

where $\vec{r}_e(\mathbf{w}, u) = (r_e^1(\mathbf{w}), r_e^2(\mathbf{w}), u r_e^3(\mathbf{w}))^T$. Using Equations (4.15), (4.16), (4.18), (4.19), (4.22) and (4.23) we can rewrite the inflection locus (4.47) as:

$$\mathcal{I}_e = \left\{ \mathbf{w} \in \mathbf{TP} \mid \left(\tilde{\lambda}_b - \tilde{\lambda}_e \right) (\mathbf{w}) = 0 \quad \text{or} \quad \mathcal{G}(\mathbf{w}) = 0 \right\}, \quad (4.48)$$

where:

$$\mathcal{G} = \frac{m}{A s_o + B_2} + \alpha d_{12} - \frac{\alpha}{l_{13}} (m + l_{12}). \quad (4.49)$$

The reader should recall Equation (4.22) and the nomenclature (4.17), relative to Equation (4.10). Let us define the exceptional locus:

$$\mathcal{E} = \mathcal{G}^{-1}(0). \quad (4.50)$$

Proposition 4.22 The exceptional locus \mathcal{E} is a smooth curve that satisfies:

$$\mathcal{E} = \left\{ (s_o, T) \in \mathbf{TP} \mid \tilde{\lambda}_e(s_o, T) = \tilde{\lambda}_e(0, T) \right\}. \quad (4.51)$$

The proof of equality (4.51) is long and will be omitted. However, since Equation

(4.51) is established, it is very easy to see that \mathcal{E} is a smooth curve: one just need to explore the properties of the critical points of $\partial_{s_o} \tilde{\lambda}_e(s_o, T)$ as in the proof of Proposition 4.16. Figure 4.4 provides a good illustration of what is happening.

Remark 4.23 *Later we will show that the curve \mathcal{E} is a genuine e-contact: the e-integral curve emanating from any of its points coincides with the e-branch of the shock curve emanating from the same point. This behavior is an example of the result established in Temple [50].*

Remark 4.24 *For convenience we will list, in advance, the main properties of the curve \mathcal{E} : it is a genuine contact, a secondary bifurcation and both right and left extension of the boundary line $\{(s_o, T) \in \mathbf{TP} \mid s_o = 0\}$. The reader should keep in mind the curve \mathcal{E} as meaning exceptional. A part of its influence on Riemann solutions will be clarified in Chapter 6.*

4.5.3 The self-intersection set

These are points $\mathbf{w}^+ \neq \mathbf{w}^-$, $\mathbf{w}^+ \in \mathcal{H}(\mathbf{w}^-)$, where the Hugoniot locus self-intersects. Following the discussion on Section 2.3.3 such behavior can only occur at points where the Jacobian $D\mathcal{H}_{\mathbf{w}^-}(\mathbf{w}^+, u^+, \sigma)$ does not have maximal rank. In this situation the following identities must hold:

$$\sigma = \lambda_i(\mathbf{w}^+, u^+) \quad \text{and} \quad \vec{l}_i(\mathbf{w}^+)(G(\mathbf{w}^+) - G(\mathbf{w}^-)) = 0, \quad 1 \leq i \leq n, \quad (4.52)$$

for the family i . We will present the notation used throughout this section. We define the diagonal:

$$\Delta = \{(\mathbf{w}^-, \mathbf{w}^+, u^+) \in \mathring{\Omega} \times \mathring{\Omega} \times \mathbb{R}^+ \mid \mathbf{w}^- = \mathbf{w}^+\}, \quad (4.53)$$

and write:

$$\mathcal{D} = \left\{ \mathring{\Omega} \times \mathring{\Omega} \times \mathbb{R} \right\} \setminus \Delta. \quad (4.54)$$

We want to define the self-intersection locus as the zero set of a smooth function; to this end we fix a family $1 \leq i \leq n$ and motivated by (4.52) we write:

$$\mathcal{F}_{(i)} : \mathcal{D} \rightarrow \mathbb{R}^4, \quad (\mathbf{w}^-, \mathbf{w}^+, u^+) \mapsto \left(\mathcal{H}(\mathbf{w}^-, \mathbf{w}^+, u^+, \lambda_i(\mathbf{w}^+, u^+)), \vec{l}_i(\mathbf{w}^+)[G] \right), \quad (4.55)$$

where $[G] = G(\mathbf{w}^+) - G(\mathbf{w}^-)$ and the function \mathcal{H} is given in Equation (2.42). Finally we can write the self-intersection set of the i^{th} family as:

$$\mathcal{A}_i = \left\{ (\mathbf{w}^-, \mathbf{w}^+, u^+) \in \mathcal{D} \mid \mathcal{F}_{(i)}(\mathbf{w}^-, \mathbf{w}^+, u^+) = 0 \right\}. \quad (4.56)$$

Since our interest is the *locus*, it is sufficient to only consider the reference value $u^- = 1$ for the Darcy speed, see Remark 2.8. However, some results of this Section will be needed later, in a context where the admissibility of waves will be important. For this reason, we will write explicitly the dependence on the Darcy speed u^- in a few Lemmas. Most of the time we will work with points of type $P^- = (\mathbf{w}^-, u^-)$, $P^+ = (\mathbf{w}^+, u^+)$ in $\mathbf{TP} \times \mathbb{R}^+$. We will often write:

$$\sigma(P^-; P^+) = \sigma(\mathbf{w}^-, u^-; \mathbf{w}^+, u^+), \quad (4.57)$$

with the implicit assumption that $(\mathbf{w}^+, u^+) \in \mathcal{H}(\mathbf{w}^-, u^-)$.

We only need to consider the self-intersection locus \mathcal{A}_e . In what follows it will be shown that the projection map of \mathcal{A}_e into \mathbf{TP} is an open map. The first step is:

Lemma 4.25 *Let $(\mathbf{w}^-, u^-) \neq (\mathbf{w}^+, u^+)$ be points at the same temperature. If $\sigma(P^-; P^+) = \lambda_e(\mathbf{w}^+, u^+)$ holds then $\sigma(P^-; P^+) = \lambda_e(\mathbf{w}^-, u^-)$.*

Proof. Here $\mathbf{w} = (s_o, T)$ and we set $\sigma \equiv \sigma(P^-; P^+)$. Notice that the isothermal shocks are the Buckley-Leverett shocks such that $u^+ = u^- = u$. These shocks have speed:

$$\sigma = \frac{u f_o^+ - f_o^-}{\varphi s_o^+ - s_o^-}.$$

The eigenvalue from Equation (4.15) is written as:

$$\lambda_e(\mathbf{w}^+, u^+) = \frac{u A(T) f_o^+ + B_1(T)}{\varphi A(T) s_o^+ + B_2(T)}.$$

These equalities can be read as:

$$u(f_o^+ - f_o^-) = \varphi \sigma (s_o^+ - s_o^-), \text{ and } u[A(T) f_o^+ + B_1(T)] = \varphi \sigma [A(T) s_o^+ + B_2(T)]. \quad (4.58)$$

Multiplying (4.58a) by $-A(T)$ and adding to (4.58b) we get:

$$u[A(T) f_o^- + B_1(T)] = \varphi \sigma [A(T) s_o^- + B_2(T)].$$

Since $[A(T) s_o^- + B_2(T)]$ never vanishes the result follows. \square

Remark 4.26 *Of course the lemma remains true switching the role of the minus and the plus superscripts.*

Next we show that, among other facts, the previous lemma is not vacuous.

Lemma 4.27 *There are pairs \mathbf{w}^- , \mathbf{w}^+ (at the same temperature) in a neighborhood of the coincidence locus \mathcal{C} in **TP** such that:*

$$\tilde{\lambda}_e(\mathbf{w}^-) = \tilde{\lambda}_e(\mathbf{w}^+) \quad \text{and} \quad \vec{l}_e(\mathbf{w}^+)(G^+ - G^-) = 0. \quad (4.59)$$

Proof. First we choose some state (s_o^-, T) , $T > T_{bV}$ sufficiently near the coincidence locus, in a sense that will be clear *a posteriori*. Let's say it is at left of the leftmost coincidence. Since the point (s^*, T) on the coincidence locus is a global minimum for

$$\tilde{\lambda}_e(s_o, T) = \frac{A(T)f_o + B_1(T)}{A(T)s_o + B_2(T)},$$

as a function of s_o , we can choose s^- sufficiently near s^* so that the level set for the value $\tilde{\lambda}_e(s_o^-, T)$ has (at least) two points, say $\{s_o^-, s_o^+\}$. We have so far:

$$\tilde{\lambda}_e(s_o^-, T) = \tilde{\lambda}_e(s_o^+, T) = \frac{A(T)f_o^+ + B_1(T) - A(T)f_o^- - B_1(T)}{A(T)s_o^+ + B_2(T) - A(T)s_o^- - B_2(T)} = \sigma(s_o^+, T; s_o^-, T)/u^-,$$

where the last equality comes from the isothermal branch of the Hugoniot locus.

To finish the proof notice that:

$$\begin{aligned} \vec{l}_e(s_o^+, T)(G^+ - G^-) &= (l_e^1 (\rho_V - \rho_{gV}) + l_e^2 \rho_{od} + l_e^3 (H_o - H_g)) (s_o^+ - s_o^-) \\ &= (l_e^1 \alpha + l_e^2 \beta + l_e^3 \gamma) (s_o^+ - s_o^-) \\ &= 0, \end{aligned}$$

by the very definition of \vec{l}_e , in Equation (4.14). □

Corollary 4.28 (Of the proof) *No point on the coincidence locus can lie in \mathcal{A}_e .*

Proof. By Equations (4.55) and (4.56) any pair \mathbf{w}^- , \mathbf{w}^+ in \mathcal{A}_e satisfies Equation (4.59). Fix a $T^* > T_{bV}$. If $\mathbf{w}^* = (s_o^*, T^*)$ is a point on the coincidence locus then it must be a global maximum or a global minimum of $\lambda_e(\cdot, T^*)$, therefore, its corresponding pair does not exist. □

Remark 4.29 *Corollary 4.28 says that \mathcal{A}_e cannot contain points where strictly hyperbolicity fails.*

We now have the basic tools needed to characterize the Hugoniot self-intersection locus. We will restrict our attention to self-intersections due to crossing: the two different branches of the Hugoniot locus intersect. In our particular problem, one can use the

regularity of the two branches of the Hugoniot locus to show that this is the sole source of self-intersection, if the two base points belong to the **TP**. Of course, such behavior is not general.

Theorem 4.30 *Assume that the Hugoniot locus in **TP** only ceases to be a curve at intersections of the b-branch, Equation (4.34), with the e-branch, Equation (4.36). Then \mathcal{A}_e is a two dimensional manifold.*

Proof. The map $\mathcal{F}_{(e)}$, Equation (4.55), is smooth and we have $\mathcal{A}_e = \mathcal{F}_{(e)}^{-1}(0)$, which is not empty because of Lemma 4.27. We now examine the Jacobian of $\mathcal{F}_{(e)}$. The differential of

$$\mathcal{H}(\mathbf{w}^-, \mathbf{w}^+, u^+, \lambda_e(\mathbf{w}^+, u^+))$$

is written (recall: $\lambda_e(\mathbf{w}^+, u^+) = u^+ \tilde{\lambda}_e(\mathbf{w}^+)$):

$$d\mathcal{H} = (DF(\mathbf{w}^-) - \lambda_e(\mathbf{w}^+, u^+)DG(\mathbf{w}^-)) d\mathbf{w}^- + \left(\tilde{\lambda}_e(\mathbf{w}^+)[G] - F(\mathbf{w}^+) \right) du^+ + \partial_{\mathbf{w}^+} \mathcal{H} d\mathbf{w}^+, \quad (4.60)$$

where the term $\partial_{\mathbf{w}^+} \mathcal{H}$ is:

$$\partial_{\mathbf{w}^+} \mathcal{H} = - (DF(\mathbf{w}^+) - \lambda_e(\mathbf{w}^+, u^+)DG(\mathbf{w}^+)) + [G] \cdot u^+ \nabla \tilde{\lambda}_e(\mathbf{w}^+)^T, \quad (4.61)$$

and clearly satisfies $\vec{l}_e(\mathbf{w}^+) \partial_{\mathbf{w}^+} \mathcal{H} = 0$ by the definitions of \vec{l}_e (Equation (4.14)) and \mathcal{A}_e (see the discussion in the beginning of this subsection). This shows that the columns of $\partial_{\mathbf{w}^+} \mathcal{H}$ lie in the orthogonal space to $\vec{l}_e(\mathbf{w}^+)$, which has dimension two. Next we will show that all columns of $D\mathcal{H}$ are spanned by a basis of the orthogonal space to $\vec{l}_e(\mathbf{w}^+)$.

Since \mathbf{w}^+ , \mathbf{w}^- lie on an isotherm, using Proposition 4.6, we see that $\tilde{\lambda}_e(\mathbf{w}^+)[G] - F(\mathbf{w}^+) = -F(\mathbf{w}^-)$. Plugging this into (4.60) we see that the first 4×3 block $D\mathcal{F}_{(e)}$ (containing derivatives with respect to \mathbf{w}^- and u^+) evaluated at a point in \mathcal{A}_e reads (set $\lambda_e^+ \equiv \lambda_e(\mathbf{w}^+, u^+)$):

$$\begin{pmatrix} \partial_{s_o} F_1(\mathbf{w}^-) - \lambda_e^+ \partial_{s_o} G_1(\mathbf{w}^-) & \partial_T F_1(\mathbf{w}^-) - \lambda_e^+ \partial_T G_1(\mathbf{w}^-) & -F_1(\mathbf{w}^-) \\ \partial_{s_o} F_2(\mathbf{w}^-) - \lambda_e^+ \partial_{s_o} G_2(\mathbf{w}^-) & \partial_T F_1(\mathbf{w}^-) - \lambda_e^+ \partial_T G_2(\mathbf{w}^-) & -F_2(\mathbf{w}^-) \\ \partial_{s_o} F_3(\mathbf{w}^-) - \lambda_e^+ \partial_{s_o} G_3(\mathbf{w}^-) & \partial_T F_1(\mathbf{w}^-) - \lambda_e^+ \partial_T G_3(\mathbf{w}^-) & -F_3(\mathbf{w}^-) \\ -\vec{l}_e(\mathbf{w}^+) \partial_{s_o} G(\mathbf{w}^-) & -\vec{l}_e(\mathbf{w}^+) \partial_T G(\mathbf{w}^-) & 0 \end{pmatrix}, \quad (4.62)$$

and then by Lemma 4.25 the upper 3×3 matrix has rank at most two. From Corollary 4.28 the algebraic multiplicity of the eigenvalue is one and so the rank must equal two.

Proposition 4.2 implies that the column space of $D\mathcal{F}_{(e)}$ is spanned by the column space of (4.62) and that the rank of $D\mathcal{F}_{(e)}$ is three, so that by the Rank Theorem (see Rudin [43]), we have that \mathcal{A}_e is a smooth manifold of dimension $\dim(\mathcal{D}) - 3 = 2$. \square

Corollary 4.31 *The projection:*

$$\pi : \mathcal{A}_e \rightarrow \mathbf{TP}, \quad \pi(\mathbf{w}^-, \mathbf{w}^+, u^+) = \mathbf{w}^+; \quad (4.63)$$

is an open mapping.

Proof. Since the matrix $(\partial_{\mathbf{w}^-}\mathcal{F}_{(e)}, \partial_{u^+}\mathcal{F}_{(e)})$, given in Equation (4.62), is injective, \mathcal{A}_e is locally the graph of a smooth function defined in \mathbf{TP} . \square

Remark 4.32 *Notice that by Lemma 4.25 and Propositions 4.6 and 4.2, the self-intersection locus \mathcal{A}_e is invariant under interchange of \mathbf{w}^- and \mathbf{w}^+ , in our case.*

Let us write the projection of the self-intersection locus \mathcal{A}_e into state space as:

$$\mathcal{O}_e = \pi(\mathcal{A}_e). \quad (4.64)$$

By Corollary 4.31, \mathcal{O}_e is an open set and by the proof of Lemma 4.27, it is the union of four disjoint open sets that contain a neighborhood of the coincidence locus \mathcal{C} . Its boundary is:

$$\partial\mathcal{O}_e = \mathcal{C} \cup \{s_o = 0\} \cup \mathcal{E}^-(\{s_o = 0\}) \cup \{s_o = 1\} \cup \mathcal{E}^-(\{s_o = 1\}), \quad (4.65)$$

where $\mathcal{E}^-(\{s_o = 0\})$ is the left extension of the boundary line $\{(s_o, T) \in \mathbf{TP} \mid s_o = 0\}$ and $\mathcal{E}^-(\{s_o = 1\})$ is the left extension of the boundary line $\{(s_o, T) \in \mathbf{TP} \mid s_o = 1\}$, see Subsection 2.3.5. Recall that by Corollary 4.28 the intersection of \mathcal{O}_e with the coincidence locus \mathcal{C} is empty. The open set \mathcal{O}_e is shown as the gray regions in Figure 4.7.

We will characterize the extension of the line $s_o = 0$, which is special.

Proposition 4.33 *Let $\mathbf{w}^- = (0, T^-)$, for any $T^- > T_{bV}$. Both the exceptional locus, Equation (4.50), and the boundary line $\{(s_o, T) \in \mathbf{TP} \mid s_o = 0\}$ are contained in $\mathcal{H}(\mathbf{w}^-)$. The shock speed between \mathbf{w}^- and any \mathbf{w}^+ lying either on the exceptional locus \mathcal{E} or on the boundary $\{(s_o, T) \in \mathbf{TP} \mid s_o = 0\}$ is both left-characteristic and right-characteristic with respect to the e -speed.*

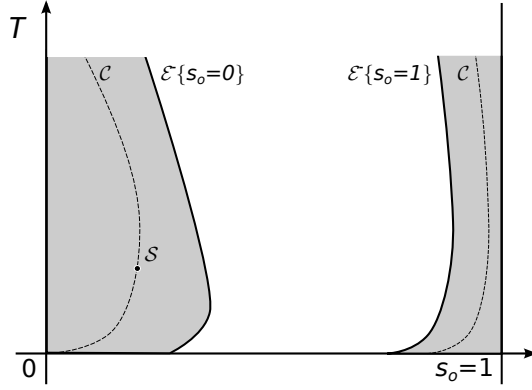


Figure 4.7: The gray regions are the projection of the self-intersection set \mathcal{A}_e into \mathbf{TP} . Both the rightmost part of the coincidence locus and the extension $\mathcal{E}^-(\{s_o = 1\})$ are drawn out of scale.

Proof. Let $\mathbf{w}^+ = (s_o^+, T^+)$. First assume that $s_o^+ \neq 0$. Writing the Rankine-Hugoniot relation (4.27) for Equation (4.1b) we have:

$$\sigma \rho_{od}^+ s_o^+ = u^+ \rho_{od}^+ f_o^+, \quad (4.66)$$

since $s_o^- = 0$. Using that $\rho_{od}(T^+) > 0$, see Equations (3.3), (3.5) and (3.6), we substitute Equation (4.66) into the Rankine-Hugoniot relation for Equations (4.1a) and (4.1c) to obtain, after a computation:

$$\begin{cases} \sigma (\rho_{gV}^+ - \rho_{gV}^-) = u^+ \rho_{gV}^+ - u^- \rho_{gV}^-, \\ \sigma (H_r^+ - H_r^- + H_g^+ - H_g^-) = u^+ H_g^+ - u^- H_g^-. \end{cases} \quad (4.67)$$

Eliminating u^- in Equation (4.67) we obtain:

$$\sigma = u^+ \frac{\rho_{gV}^- H_g^+ - \rho_{gV}^+ H_g^-}{\rho_{gV}^- H_g^+ - \rho_{gV}^+ H_g^- + \rho_{gV}^- (H_r^+ - H_r^-)} = \lambda_e((0, T^+), u^+), \quad (4.68)$$

where the last equality arises from Equations (3.18), (4.15) and (4.16). Using Equations (4.66) and (4.68), the same argument used in the proof of Lemma 4.25 yields:

$$\sigma = \lambda_e(\mathbf{w}^+, u^+), \quad (4.69)$$

and using Proposition 4.22 we obtain $\mathbf{w}^+ \in \mathcal{E}$. Eliminating u^+ in Equation (4.67) we

write, similarly:

$$\sigma = \lambda_e(\mathbf{w}^-, u^-), \quad (4.70)$$

so that the shock is left-characteristic and right-characteristic with respect to the e -speed.

If $s_o^+ = 0$, Equation (4.67) still holds while Equation (4.66) vanishes identically, leading to the following result: \square

Corollary 4.34 *The exceptional locus is an e -branch of the Hugoniot locus which lies on an e -integral curve, thus it is a genuine contact, see Temple [50].*

Proof. The preceding proposition together with the symmetry of the Rankine-Hugoniot Equation (4.27) implies that if $\mathbf{w}^- \in \mathcal{E}$ then $\mathcal{E} \subset \mathcal{H}(\mathbf{w}^-)$. Since the exceptional locus is contained in the set \mathcal{I}_e , Equation (4.47), the result follows. \square

Remark 4.35 *The exceptional locus is an example of an unbounded Hugoniot e -branch. See discussion in Subsection 4.2.2.*

4.5.4 Double contact locus

We define a two-sided (or double) contact discontinuity to be a solution $(\mathbf{w}^-, u^-; \mathbf{w}^+, u^+)$ of the Rankine-Hugoniot relation (4.27) such that a characteristic speed for (\mathbf{w}^-, u^-) coincides with the shock speed $\sigma(\mathbf{w}^-, u^-; \mathbf{w}^+, u^+)$, as well as with the another characteristic speed for (\mathbf{w}^+, u^+) , see discussion in Chapter 2. As a consequence of Theorem 4.30 and Lemma 4.25 we have that the double contact locus $\mathcal{D}_e \equiv \mathcal{D}_{e,e}$ contains \mathcal{A}_e .

The double contact locus $\mathcal{D}_b \equiv \mathcal{D}_{b,b}$ is a smooth curve. Its projection into state space is shown in Figure 4.8.

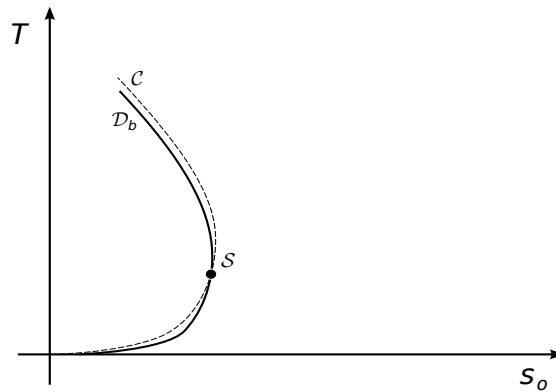


Figure 4.8: Projection on **TP** of \mathcal{D}_b (solid) and of the coincidence locus (dashed).

Chapter 5

Riemann problem I in TP

Here we solve the Riemann problem in a neighborhood of the singular point in the two phase region.

We point out that the material in this Chapter depends on definitions and results of Chapter 4. Familiarity with the basic concepts of Riemann solutions is assumed, see Section 2.2. The Triple Shock Rule 4.10 and the Bethe-Wendroff Theorem 4.13 are fundamental tools that the reader must bear in mind.

5.1 Bifurcations in the Riemann solution

As discussed on Chapter 2, the Riemann solution can be constructed by concatenating constant regions and fundamental waves: shocks and rarefactions. The projection of these elementary waves into state space are sufficient to construct the solution, as the Darcy speed u can be computed from its “initial” value and these projections. Taking advantage of this fact we will illustrate in figures the projection of the Riemann solutions in state space **TP** only.

Riemann solutions bifurcate when an elementary wave ceases to be admissible. The construction of the Riemann solution must proceed with another admissible elementary wave, respecting the monotonicity principle. We recall our choice of the Liu criterion to select admissible shocks, see Subsection 2.2.3. First, we will focus on the bifurcations in backward Riemann solutions that appears when the \mathbf{w}^L is allowed to change but the \mathbf{w}^R is fixed.

Definition 5.1 (Backward **L**-region). *Fix a pair $\mathbf{w}^L, \mathbf{w}^R$ in state space. The backward **L**-region $\mathcal{L}^-(\mathbf{w}^R)$ corresponding to the selected pair $\mathbf{w}^L, \mathbf{w}^R$ is the maximal subset of state space such that $\mathbf{w}^L \in \mathcal{L}^-(\mathbf{w}^R)$ and the Riemann solutions for any initial data*

$\mathbf{w}^* \in \mathcal{L}^-(\mathbf{w}^R)$, $u^* > 0$,

$$\mathbf{w}(x, 0) = \begin{cases} \mathbf{w}^*, & \text{if } x < 0, \\ \mathbf{w}^R, & \text{if } x > 0, \end{cases}$$

and

$$u(x, 0) = u^*, \quad \text{if } x < 0,$$

are constructed through wave fans consisting of the same type of concatenations of constant states and of the same fundamental wave types and families as in the solution for the pair \mathbf{w}^L , \mathbf{w}^R .

Remark 5.2 Typically there is a finite number of backward **L**-regions for a given \mathbf{w}^R . We will follow the usual habit and number them.

When the right state \mathbf{w}^R wanders in state space, the solutions may change topology, *i.e.*, the backward **L**-region diagram changes qualitatively. When such a change happens the Riemann solution bifurcates. Bifurcations often happens when \mathbf{w}^R crosses certain codimension one manifolds in state space.

Definition 5.3 (Backward **R**-region). Fix a \mathbf{w}^R in state space. The backward **R**-Region $\mathcal{R}^-(\mathbf{w}^R)$, containing \mathbf{w}^R , is the maximal subset of state space such that for any $\mathbf{w}^* \in \mathcal{R}^-(\mathbf{w}^R)$ the subdivision of state space into backward **L**-regions $\mathcal{L}^-(\mathbf{w}^*)$ is the same as the subdivision in $\mathcal{L}^-(\mathbf{w}^R)$.

Remark 5.4 We will use the lexicographic order of the plane to state the relative position of objects. For example, $\mathbf{w}^1 = (s_o^1, T^1)$ and $\mathbf{w}^2 = (s_o^2, T^2)$: state \mathbf{w}^2 is above \mathbf{w}^1 if $T^2 > T^1$. Accordingly, state \mathbf{w}^2 is at the right of \mathbf{w}^1 if $s_o^2 > s_o^1$.

The backward **R**-regions for **R** and **L** in a neighborhood of the singular point $\mathcal{S} = (s_o^S, T^S)$ are as follows, see Figure 5.1. The *region A* is bounded by the horizontal straight line that begins at \mathcal{S} and lies on the right side of the coincidence curve \mathcal{C} . It extends clockwise down to the portion of the double contact locus \mathcal{D}_b below the singular point \mathcal{S} . Still in the clockwise sense, the *region A'* lies between the double contact locus \mathcal{D}_b and the coincidence locus \mathcal{C} below the singular point \mathcal{S} . The *region B* lies above *region A*, at the right of the coincidence locus \mathcal{C} , above the horizontal straight line that begins at \mathcal{S} . The *region C* lies at the left of the coincidence locus.

To describe the Riemann solution in this chapter we will use the **R**-construction: we will exhibit the Riemann solution in each appropriate **L**-region when the right state \mathbf{w}^R

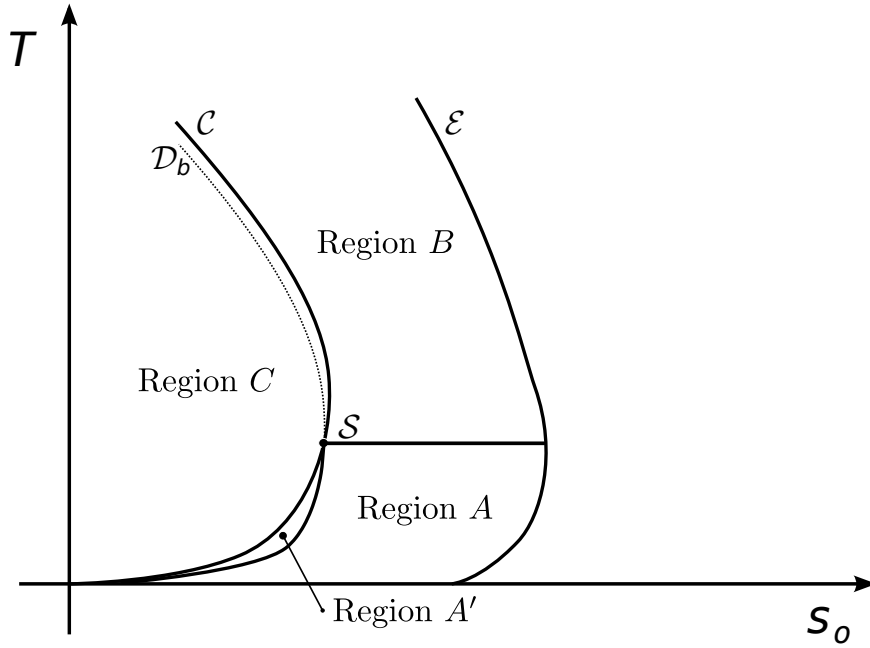


Figure 5.1: Backward \mathbf{R} -regions in a neighborhood of the singular point \mathcal{S} .

varies in the backward \mathbf{R} -region diagram. Of course, all regions lie above the isotherm $T = T_{bV}$ since they are in \mathbf{TP} .

Given the physical variables $(\mathbf{w}^M, u^M) \in \mathbf{TP} \times \mathbb{R}^+$ we will use the notation $\mathbf{M} = (\mathbf{w}^M, u^M)$ for brevity. To improve legibility in figures we display only the superscripts of the states. For example, we will write \mathbf{R} in place of \mathbf{w}^R .

5.2 Region A

Here the right state \mathbf{w}^R lies in Region A, in Figure 5.1. In the discussion that follows we will present the subdivision of a neighborhood of the singular point into backward \mathbf{L} -regions for \mathbf{w}^R , see Figure 5.2.

In a sufficiently small neighborhood of any \mathbf{w}^R state in Region A, e -waves are slow and b -waves are fast, see discussion in Subsection 4.5.1 and Proposition 4.16 (this behavior can change out of region A, producing bifurcations in the solution). Generically, a fast wave is needed to reach \mathbf{w}^R . In a sufficiently small neighborhood within this region the backward fast-wave curve that reaches \mathbf{w}^R must represent (fast) b -waves, which lie on an isotherm. Therefore the isotherm $T = T^R$ must be reached by slow waves in the construction of the Riemann solution, see Proposition 4.6. A slow wave that reaches the isotherm $T = T^R$ at the right of \mathbf{w}^R must be followed by a fast b -shock, since the \mathbf{w}^L and

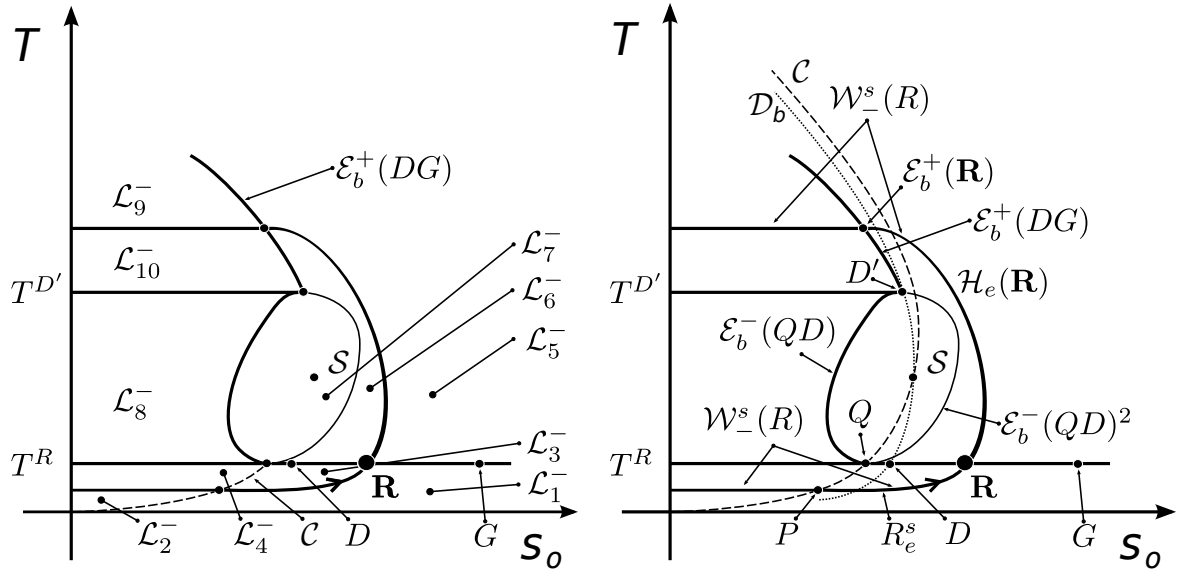


Figure 5.2: Left: backward L -regions for \mathbf{w}^R in region A. Right: boundaries.

\mathbf{w}^R states lie on the left side of the b inflection. We have exhausted slow waves; now we will focus on fast (characteristic) waves reaching this line.

The e -branch of the Hugoniot locus based on any point of this neighborhood of the singular point \mathcal{S} is a smooth, compact curve, with an oval shape, see Subsection 4.2.2. At a state \mathbf{w}^L at the left of the coincidence locus \mathcal{C} the e -waves are fast. For the time being we will focus on \mathbf{w}^L states above \mathbf{w}^R , below the singular point \mathcal{S} . Along the e -branch of the Hugoniot locus, the temperature decreases along Liu admissible shocks. The oval must have two points with horizontal tangents. Each shock reaching such points is a candidate to be characteristic with b -speed at the point of tangency due to the Bethe-Wendroff Theorem 4.13. In fact, the e -shocks are the main tool to “decrease the temperature” near the singular point.

Notice that the b double contact \mathcal{D}_b crosses the isotherm $T = T^R$ at one point, see Figure 4.8, which we will call \mathbf{w}^D . We write \mathbf{w}^Q for the state on the coincidence locus with the same temperature as \mathbf{w}^R . We denote by $\mathcal{E}_b^-(QD)$ the left extension locus of the rarefaction segment between points \mathbf{w}^Q and \mathbf{w}^D , *i.e.*, by construction from any point in $\mathcal{E}_b^-(QD)$ there is a shock reaching the segment \overline{QD} , which is characteristic with the b -speed at this segment. The connected branch of the locus $\mathcal{E}_b^-(QD)$ we are interested in is a curve, bounded by the points \mathbf{w}^Q and $\mathbf{w}^{D'} \in \mathcal{E}_b^-(D)$. Fast right characteristic shocks connect states at temperatures lying between T^R and $T^{D'}$ in this branch to the segment \overline{QD} . This construction is sufficient to guarantee the monotonicity principle if the wave preceding this fast right characteristic shock is a rarefaction. However, we need another

bifurcation curve to guarantee that this fast right characteristic shock and a preceding b -shock satisfy the monotonicity principle. To this end we will define a new left extension according to the conditions we will need.

Definition 5.5 (Double left extension locus.) *Let γ be a curve in $\mathbf{TP} \times \mathbb{R}^+$ and denote by $\mathcal{E}_i^-(\gamma)$ its left extension locus with respect to the i^{th} family. The double left extension locus of curve γ with respect to the i^{th} family is:*

$$\mathcal{E}_i^-(\gamma)^2 = \left\{ P^+ = (\mathbf{w}^+, u^+) \in \mathbf{TP} \times \mathbb{R}^+ \mid \exists P^0 \in \gamma \text{ and } P^1 \in \mathcal{E}_b^-(P^0); \right. \\ \left. P^+ \in \mathcal{H}_i(P^1) \text{ and } \sigma(P^1; P^+) = \sigma(P^0; P^1) = \lambda_i(P^0) \right\}.$$

The b -shocks joining states on the right side of locus $\mathcal{E}_b^-(QD)$ to the locus $\mathcal{E}_b^-(QD)$ satisfy the monotonicity principle if their base state is on the left side of $\mathcal{E}_b^-(QD)^2$. We still need to define the right extension locus of the segment between \mathbf{w}^D and generic states \mathbf{w}^G , which lie at the right of \mathbf{w}^R and satisfy $T^G = T^R$. The extension:

$$\mathcal{E}_b^+(DG), \tag{5.1}$$

has the property that from any of its points an e -shock emanates that reaches the segment \overline{DG} and is left characteristic with respect to b -waves, *i.e.* characteristic at $\mathcal{E}_b^+(DG)$.

Remark 5.6 *Notice that we have defined Region A such that any fast e -shock that reaches the isotherm $T = T^R$ can be followed by a fast b -rarefaction. The crucial fact is that the \mathbf{w}^R state is at the right of the intersection of the isotherm $T = T^R$ with the double contact locus \mathcal{D}_b .*

5.2.1 Riemann solutions with increasing temperatures

Here we describe the Riemann solutions in the backward \mathbf{L} -regions below the isotherm $T = T^R$, see Figure (5.2b). The relevant part of the backward slow wave curve $\mathcal{W}_-^s(\mathbf{R})$ from \mathbf{R} contains a slow b -rarefaction followed by a slow e -rarefaction:

$$R_b^s \longrightarrow R_e^s, \quad \text{for } T \leq T^R. \tag{5.2}$$

The wave curve $\mathcal{W}_-^s(\mathbf{R})$ and the coincidence locus are some of the bifurcation loci for the \mathbf{L} -regions in this Riemann solution, see Figure (5.2a).

Riemann solution for \mathcal{L}_1^-

The \mathbf{w}^L state lies below the isotherm $T = T^R$ on the right side of both the coincidence locus \mathcal{C} and the wave curve $\mathcal{W}_-^s(\mathbf{R})$, Equation (5.2). In \mathcal{L}_1^- the e -waves are slow and the b -waves are fast, see Subsection 4.5.1, which means that a slow rarefaction emanating from \mathbf{w}^L will reach the isotherm $T = T^R$ in the constant state \mathbf{M} at the right of \mathbf{w}^R . Thus, the admissible fast waves are b -shocks, and the solution is:

$$\mathbf{L} \xrightarrow{R_e^s} \mathbf{M} \xrightarrow{S_b^f} \mathbf{R}. \quad (5.3)$$

Remark 5.7 *This Riemann solution is just the Lax construction. Most of times we will suppress the description of the constant state for this type of construction.*

Riemann solution for \mathcal{L}_2^-

The \mathbf{L} -region \mathcal{L}_2^- is bounded by the wave curve $\mathcal{W}_-^s(\mathbf{R})$ and by the coincidence locus \mathcal{C} , see Figure 5.2a. In the transition from \mathcal{L}_1^- to \mathcal{L}_2^- we crossed the coincidence locus so that, now, in a neighborhood of state \mathbf{w}^L the b -waves are slow. The forward slow wave curve $\mathcal{W}_+^s(\mathbf{L})$ emanating from \mathbf{L} contains a slow b -rarefaction followed by a slow e -rarefaction, *i.e.*:

$$R_b^s \longrightarrow R_e^s. \quad (5.4)$$

The wave curve $\mathcal{W}_+^s(\mathbf{L})$ crosses the coincidence locus at an intermediate state $\widehat{\mathbf{M}}_1$ and reaches the isotherm $T = T^R$ at a (constant) state \mathbf{M}_2 . The solution is written as:

$$\mathbf{L} \xrightarrow{R_b^s} \widehat{\mathbf{M}}_1 \xrightarrow{R_e^s} \mathbf{M}_2 \xrightarrow{S_b^f} \mathbf{R}. \quad (5.5)$$

Riemann solution for \mathcal{L}_3^-

The \mathbf{L} -region \mathcal{L}_3^- lies at the left of the wave curve $\mathcal{W}_-^s(\mathbf{R})$, Equation (5.2), bounded by the isotherm $T = T^P$ and by the coincidence locus \mathcal{C} . Slow e -waves that reach the isotherm $T = T^R$ (in the constant state \mathbf{M}) must be followed by a b -rarefaction wave. The solution is:

$$\mathbf{L} \xrightarrow{R_e^s} \mathbf{M} \xrightarrow{R_b^f} \mathbf{R}. \quad (5.6)$$

Riemann solution for \mathcal{L}_4^-

Now \mathbf{w}^L is at the left of the coincidence locus and above the wave curve $\mathcal{W}_-^s(\mathbf{R})$. The b -waves are slow. The forward slow wave curve emanating from \mathbf{L} , $\mathcal{W}_+^s(\mathbf{L})$ is given in

Equation (5.4). It crosses the coincidence locus at an intermediate state $\widehat{\mathbf{M}}_1$ and reaches the isotherm $T = T^R$ at a constant state \mathbf{M}_2 . The Riemann solution is:

$$\mathbf{L} \xrightarrow{R_b^s} \widehat{\mathbf{M}}_1 \xrightarrow{R_e^s} \mathbf{M}_2 \xrightarrow{R_b^f} \mathbf{R}. \quad (5.7)$$

5.2.2 Riemann solutions with decreasing temperature

Now we focus on the backward **L**-regions above the isotherm $T = T^R$. In comparison to the previous subsection, the bifurcation structure will be complicated by the presence of the singular point.

The relevant part of $\mathcal{W}_-^s(\mathbf{R})$, backward slow wave curve from \mathbf{R} , contains a slow b -rarefaction followed by a left-characteristic e -shock:

$$R_b^s \longrightarrow S_e^s, \quad \text{for } T \geq T^R. \quad (5.8)$$

Wave curve $\mathcal{W}_-^s(\mathbf{R})$ originates the first remarkable bifurcation boundary for the backward **L**-regions. At its left side, the fast waves reaching relevant \mathbf{R} are b -rarefactions while at its right side the fast waves are b -shocks. As previously discussed at the beginning of this section, e -shocks are the temperature decreasing waves and must be used in Riemann solutions; the admissibility of these shocks will dictate other relevant bifurcations in the backward **L**-regions.

We mention for later use the portion of $\mathcal{W}_-^f(\mathbf{R})$, the backward fast wave curve from \mathbf{R} , that contains a right-characteristic fast e -shock, followed by a fast b -rarefaction:

$$S_e^f \longrightarrow R_b^f. \quad (5.9)$$

Remark 5.8 *A particularly interesting elementary wave is the e shock, which is responsible for decrease the temperature in the backward **L**-regions $\mathcal{L}_7^- - \mathcal{L}_{10}^-$. Physically it is a classical condensation shock, a fundamental wave in the Riemann solutions arising from oil recovery by gas injection.*

Riemann solution for \mathcal{L}_5^-

Here the \mathbf{w}^L state lies above the isotherm $T = T^R$, on the right side of $\mathcal{H}_e(\mathbf{w}^R) \cup \mathcal{E}_b^+(DG)$, see Figure 5.2 and the discussion preceding Equation (5.1). In this region e -waves are slow. The solution is given just by the Lax construction, the constant state \mathbf{M} lies in the isotherm $T = T^R$:

$$\mathbf{L} \xrightarrow{S_e^s} \mathbf{M} \xrightarrow{S_b^f} \mathbf{R}. \quad (5.10)$$

Riemann solution for \mathcal{L}_6^-

The \mathbf{L} -region \mathcal{L}_6^- is bounded by the e branch of the Hugoniot locus emanating from \mathbf{w}^R , by the extension $\mathcal{E}_b^+(DR)$, by the double extension $\mathcal{E}_b^-(QD)^2$ and by the isotherm $T = T^R$. Again, the e -waves are slow. This is the last case in the Region A to benefit from the Lax construction, again the constant state \mathbf{M} lies in the isotherm $T = T^r$:

$$\mathbf{L} \xrightarrow{S_e^s} \mathbf{M} \xrightarrow{R_b^f} \mathbf{R}. \quad (5.11)$$

Riemann solution for \mathcal{L}_7^-

This backward \mathbf{L} -region contains the coincidence locus \mathcal{C} so that the relative order between families is not fixed: on the left side of the coincidence locus, the b -waves are slow, while on its right side the e -waves are slow.

The boundary of this region consists of two branches in the loci $\mathcal{E}_b^-(QD)$ and $\mathcal{E}_b^-(QD)^2$, such that:

$$\mathcal{E}_b^-(QD) \cap \mathcal{E}_b^-(QD)^2 = \{Q, D'\}, \quad (5.12)$$

see Figure 5.2a. The e waves emanating from states $\mathbf{w}^R \in \mathcal{L}_7^-$ do not reach the segment \overline{QD} , so they cannot be used as a first wave in the Riemann solution. This is so because such a shock must be followed by a b wave, along which temperature is fixed. However, inside region \mathcal{L}_7^- we have that the b -shocks are slow.

Proposition 5.9 *The b -shock waves from $\mathbf{w}^L \in \mathcal{L}_7^-$ reaching curve $\mathcal{E}_b^-(QD)$ are slow.*

Proof. Fix a $\mathbf{w}^L = (s_o^L, T^L)$ in $\mathbf{w}^L \in \mathcal{L}_7^-$ and denote by $\mathbf{w}^* = (s_o^*, T^L)$ the point in $\mathcal{E}_b^-(QD)$ that intersects the isotherm $T = T^L$ and by \mathbf{w}^{**} the point in $\mathcal{E}_b^-(QD)^2$ that intersects the same isotherm. By Proposition 4.6, the Darcy speed u is constant in the \mathcal{H}_b branch, so it plays no role in wave admissibility here. We can thus make $u = 1$, see Remark 2.8.

The standard Buckley-Leverett theory implies that the speed of the b -shock based on \mathbf{w}^* is an increasing function in s_o^* , up to the right-characteristic extension of \mathbf{w}^* , $\mathcal{E}_b^+(\mathbf{w}^*)$. By choosing \mathbf{R} close enough to the singular point, we can make the whole region \mathcal{L}_7^- lie at the left of the b inflection. We have:

$$\sigma(\mathbf{w}^L; \mathbf{w}^*) < \sigma \equiv \sigma(\mathbf{w}^*; \mathbf{w}^{**}). \quad (5.13)$$

Notice that the fast e -shock from \mathbf{w}^* to the segment \overline{QD} has speed σ because of the definition of the double extension, see Definition 5.5, and:

$$\sigma(\mathbf{w}^L; \mathbf{w}^*) < \sigma < \tilde{\lambda}_e(\mathbf{w}^*), \quad (5.14)$$

because it is an e -shock.

Now we proceed to show that:

$$\sigma(\mathbf{w}^L; \mathbf{w}^*) < \tilde{\lambda}_e(\mathbf{w}^L). \quad (5.15)$$

If \mathbf{w}^L is at the left of the coincidence locus the e -shocks are fast, so that Equation (5.15) is trivially satisfied. Since we already discarded the existence of a b characteristic shock, Equation (5.15) must hold until \mathbf{w}^L reaches the self-intersection of $\mathcal{H}(\mathbf{w}^*)$. Using an argument to the one in the proof of Lemma 4.27, one can see that the self-intersection must lie at the right of $\mathcal{E}_b^-(\mathbf{w}^*)$ and, in particular, of \mathbf{w}^L . \square

Remark 5.10 *The proof in Proposition 5.9 implies that the shocks from $\mathcal{E}_b^-(QD)^2$ to the segment \overline{QD} have the property that all characteristics impinge in the shock, i.e., they are over-compressive.*

The Riemann solution is now clear: after the slow b -shock there is a constant state $\mathbf{M}_1 \in \mathcal{E}_b^-(QD)$, followed by the fast waves in $\mathcal{W}_-^f(\mathbf{w}^R)$. We denote by $\widehat{\mathbf{M}}_2 \in \{T = T^R\}$ the intermediate state between the fast waves. The solution is written:

$$\mathbf{L} \xrightarrow{S_b^s} \mathbf{M}_1 \xrightarrow{S_e^f} \widehat{\mathbf{M}}_2 \xrightarrow{R_b^f} \mathbf{R}. \quad (5.16)$$

Notice that we cannot use the slow b -rarefaction: it would not satisfy the monotonicity principle with the triple-shock that follows the b -rarefaction.

Remark 5.11 *The proof of Proposition 5.9 says that the region where a slow b -shock exists extends to \mathcal{L}_6^- . However, the type of construction shown for \mathcal{L}_7^- does not apply: this b -shock is faster than the right-characteristic e -shock which reaches the segment \overline{QD} .*

Riemann solution for \mathcal{L}_8^-

In the transition from \mathcal{L}_7^- to \mathcal{L}_8^- we crossed the extension $\mathcal{E}_b^-(QD)$. This backward \mathbf{L} -region is bounded above by the isotherm $T = T^{D'}$ and below by the isotherm $T = T^Q$ so that the Riemann solution must use a fast e -shock. Beginning with a slow b -rarefaction we reach a constant state that we denote by $\mathbf{M}_1 \in \mathcal{E}_b^-(QD)$. We denote the intermediate state between the fast waves in $\mathcal{W}_-^f(\mathbf{w}^R)$ by $\widehat{\mathbf{M}}_2$. Thus the solution reads.

$$\mathbf{L} \xrightarrow{R_b^s} \widehat{\mathbf{M}}_1 \xrightarrow{S_e^f} \widehat{\mathbf{M}}_2 \xrightarrow{R_b^f} \mathbf{R}. \quad (5.17)$$

Riemann solution for \mathcal{L}_9^-

In this backward \mathbf{L} -region, we are on the left side of the right extension of the isotherm $T = T^R$, Equation (5.1), and above the backward slow wave curve emanating from \mathbf{R} , see Equation (5.8) and the adjacent discussion. The b -waves are slow. The Riemann solution encompasses a slow b -rarefaction, joined to a slow left-characteristic e -shock at the intermediate state $\widehat{\mathbf{M}}_1 \in \mathcal{E}_b^+(DG)$. This slow shock reaches the isotherm $T = T^R$ at the constant state \mathbf{M}_2 , at the right of state \mathbf{w}^R (in the segment from \mathbf{w}^R to \mathbf{w}^G), and is followed by a fast b -shock.

$$\mathbf{L} \xrightarrow{R_b^s} \widehat{\mathbf{M}}_1 \xrightarrow{S_e^s} \mathbf{M}_2 \xrightarrow{S_b^f} \mathbf{R}. \quad (5.18)$$

Riemann solution for \mathcal{L}_{10}^-

In the transition from \mathcal{L}_9^- to \mathcal{L}_{10}^- we crossed the backward slow wave curve emanating from \mathbf{R} , Equation (5.8). Now the forward slow wave curve emanating from \mathbf{L} reaches the isotherm $T = T^R$ at the left of \mathbf{w}^R , and thus must be followed by a fast b -rarefaction. We write the intermediate state as $\widehat{\mathbf{M}}_1 \in \mathcal{E}_b^+(DG)$, and the constant state as \mathbf{M}_2 . The solution is written:

$$\mathbf{L} \xrightarrow{R_b^s} \widehat{\mathbf{M}}_1 \xrightarrow{S_e^s} \mathbf{M}_2 \xrightarrow{R_b^f} \mathbf{R}. \quad (5.19)$$

5.3 Region A'

Here the right state \mathbf{w}^R lies in Region A'. The subdivision of a neighborhood of the singular point in the backward \mathbf{L} -regions of \mathbf{w}^R , shown in Figure 5.3, is essentially the same as that of region A, see previous section. We will just highlight the difference.

In this region we set the \mathbf{w}^R state at the left of the intersection of the isotherm $T = T^R$ with the b double contact locus. We again, denote this intersection by \mathbf{w}^D . The intersection of the isotherm $T = T^R$ with the coincidence locus will be denoted by \mathbf{w}^Q as in the previous section. As can be expected, see Remark 5.6, we no longer can concatenate a fast b -wave after a temperature decreasing fast e -shock.

When state \mathbf{w}^R reaches \mathbf{w}^D , the e branch ($\mathcal{H}_e(\mathbf{w}^R)$) of the Hugoniot locus based on \mathbf{w}^R intersects the extension $\mathcal{E}_b^-(QD)$ in $\mathbf{w}^{D'}$. After letting state \mathbf{w}^R get at the right of

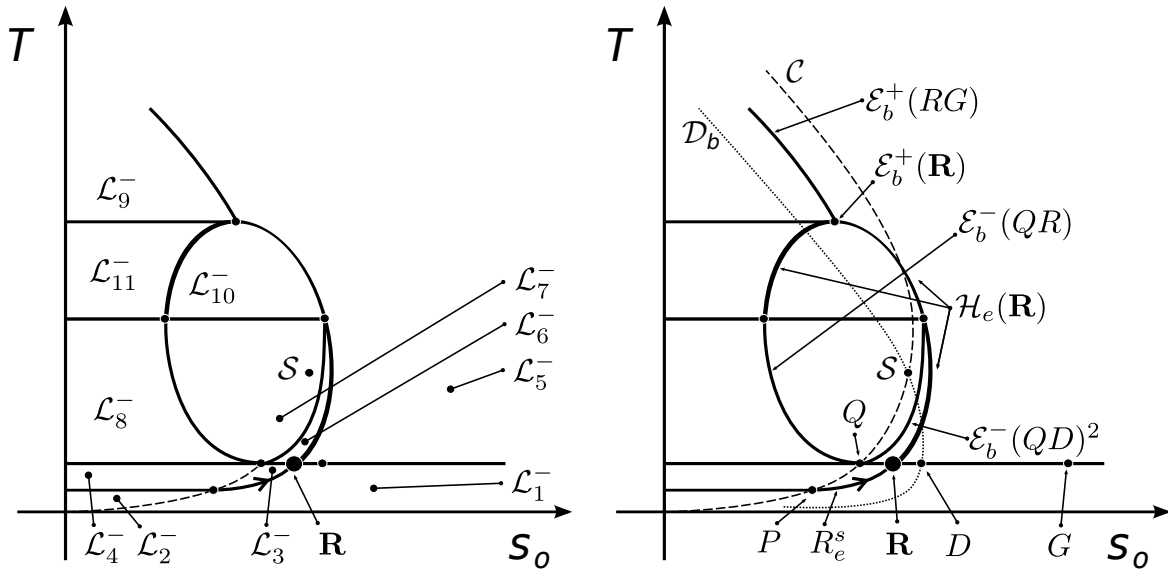


Figure 5.3: Left: backward \mathbf{L} -regions for \mathbf{w}^R in region A' . Right: boundaries.

\mathbf{w}^D , the fast e -shocks emanating from points in $\mathcal{E}_b^-(RD)$ can no longer be used in the Riemann solution: these shocks can only be followed by fast b -shocks which would violate the monotonicity principle. Therefore we can only use fast right-characteristic e -shocks to reach the segment \overline{QR} . To this end both loci: $\mathcal{E}_b^-(RD)$ and $\mathcal{E}_b^-(QR)^2$, see Definition 5.5. are useful as in Region A. For temperatures higher than the temperature of state $\mathcal{E}_b^-(R)$ we need to use the e -branch of the Hugoniot locus $\mathcal{H}_e(\mathbf{w}^R)$ emanating from \mathbf{w}^R . Since it is an oval, it must end with a left-characteristic b -shock at a state in $\mathcal{E}_b^+(R)$. From $\mathcal{E}_b^+(R)$ to higher temperatures, we use the left-characteristic b -shocks, as was done in Region A.

The temperature increasing Riemann solutions in regions \mathcal{L}_1^- through \mathcal{L}_4^- are the same as in Region A.

5.3.1 Riemann solutions with decreasing temperature

Here, the Riemann solutions for left states in regions $\mathcal{L}_5^-, \mathcal{L}_6^-, \dots, \mathcal{L}_9^-$ are the same as those for \mathbf{w}^R in Region A. In regions $\mathcal{L}_6^-, \mathcal{L}_7^-, \mathcal{L}_8^-$ the boundaries of the backward \mathbf{L} -regions differ from the case when \mathbf{w}^R lies in Region A. In the following we will describe these differences and give the Riemann solutions for \mathbf{w}^L states in regions \mathcal{L}_{10}^- and \mathcal{L}_{11}^- .

Riemann solution for \mathcal{L}_6^-

The backward \mathbf{L} -region \mathcal{L}_6^- is bounded on the left side by locus $\mathcal{E}_b^-(QR)^2$ and on the right side by locus $\mathcal{H}_e(\mathbf{w}^R)$. These loci intersect at $\mathcal{E}_b^-(R)^2$.

Riemann solution for \mathcal{L}_7^-

The backward **L**-region \mathcal{L}_7^- is bounded on its left side by locus $\mathcal{E}_b^-(QR)$ and on its right side by locus $\mathcal{E}_b^-(QR)^2$. It lies below the isotherm that contains $\mathcal{E}_b^-(R)$.

Riemann solution for \mathcal{L}_8^-

The backward **L**-region \mathcal{L}_8^- is bounded on its right side by locus $\mathcal{E}_b^-(QR)$. It is below the isotherm that contains $\mathcal{E}_b^-(R)$.

Riemann solution for \mathcal{L}_{10}^-

Region \mathcal{L}_{10}^- contains the coincidence locus so that in states at the right of the coincidence locus the e -waves are slow and in states at the left of the coincidence locus the b -waves are slow.

It can be shown that (with the help of the Triple Shock Rule the same argument given in Proposition 5.9 works) the b -shocks are slow. The Riemann solution is made with a slow b -shock to $\mathcal{H}_e(\mathbf{w}^R)$, where we write the constant state as $\mathbf{M} \in \mathcal{H}_e(\mathbf{w}^R)$. A fast e -shock follows. The Riemann solution is:

$$\mathbf{L} \xrightarrow{S_b^s} \mathbf{M} \xrightarrow{S_e^f} \mathbf{R}. \quad (5.20)$$

Riemann solution for \mathcal{L}_{11}^-

Region \mathcal{L}_{11}^- is at the left of the e -branch of the Hugoniot locus emanating from \mathbf{w}^R . In this backward **L**-region the b -waves are slow. The Riemann solution encompasses a slow b -rarefaction until the constant state \mathbf{M} in $\mathcal{H}_e(\mathbf{w}^R)$. It is followed by the fast e -shock. The Riemann solution is:

$$\mathbf{L} \xrightarrow{R_b^s} \mathbf{M} \xrightarrow{S_e^f} \mathbf{R}. \quad (5.21)$$

5.4 Region B

Here the right state \mathbf{w}^R lies in Region B. In the discussion that follows we will present the subdivision of a neighborhood of the singular point in the backward **L**-regions of \mathbf{w}^R , shown in Figure 5.4.

As in the case of the preceding regions, in a sufficiently small neighborhood of any \mathbf{w}^R state in Region B, e waves are slow and b waves are fast (this behavior can change

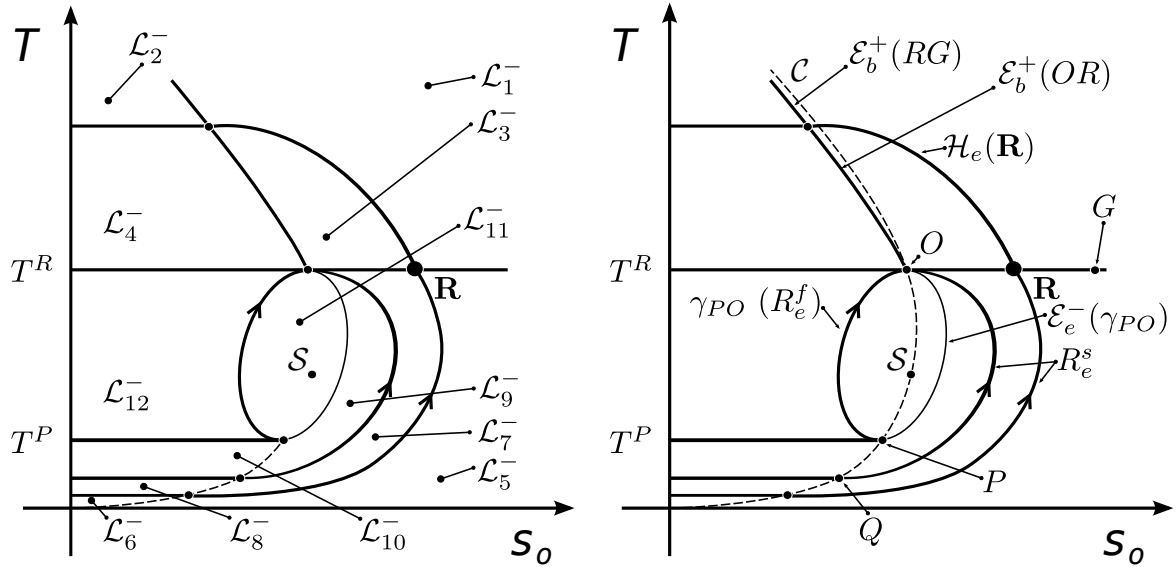


Figure 5.4: Left: backward **L**-regions for \mathbf{w}^R in region B. Right: boundaries.

out of region B, accounting for bifurcations in the solution). Generically, a fast wave is needed to reach \mathbf{w}^R . In a sufficiently small neighborhood of this region the backward fast-wave curve that reaches \mathbf{w}^R must represent (fast) b -waves, which lie on an isotherm. Therefore the isotherm $T = T^R$ must be reached through slow waves in order to construct the Riemann solution, see Proposition 4.6. A slow wave that reaches the isotherm $T = T^R$ at the right of \mathbf{w}^R must be followed by a fast b -shock. Of course, if the slow wave reaches the isotherm $T = T^R$ at the left of \mathbf{w}^R it must be followed by a fast b -rarefaction. We have exhausted slow waves; now we will focus on fast waves reaching this line.

Along an e -rarefaction temperature increases. On the left side of the coincidence they are fast and on the right side of the coincidence they are slow. Any slow e -rarefaction that reaches the isotherm $T = T^R$ can be followed by a fast b elementary wave.

Since the e -rarefactions are fast on the left side of the coincidence locus they must be chosen so that satisfies the monotonicity principle with respect to the b -rarefaction that follows. To this end we name the point \mathbf{w}^O which is the point of the coincidence locus with temperature $T = T^R$. The fast e -rarefaction wave that reaches \mathbf{w}^O is the sole one that satisfy the monotonicity requirement. We call \mathbf{w}^P the point where this rarefaction begins and denote this rarefaction curve as γ_{PO} .

To summarize we have that the fast backward wave curve that reaches \mathbf{w}^R has a fast e -rarefaction that remains entirely on the left side of the coincidence locus \mathcal{C} , begins at state \mathbf{w}^P and ends at state \mathbf{w}^O . This rarefaction is followed by a fast b -rarefaction beginning in \mathbf{w}^O . To further reference we write the relevant part of wave curve $\mathcal{W}_-^f(\mathbf{R})$

as:

$$R_e^f \longrightarrow R_b^f. \quad (5.22)$$

At the left of $\mathcal{W}_-^f(\mathbf{R})$ the slow waves are b -rarefactions. On the right side of $\mathcal{W}_-^f(\mathbf{R})$, the slow waves are b -shocks. These shocks cease to be slow when their base state crosses the left extension $\mathcal{E}_e^-(\gamma_{PO})$ of the e -rarefaction γ_{PO} . For states on the right side of $\mathcal{E}_e^-(\gamma_{PO})$, the b -shocks become fast, thus they cannot be used in this Riemann solution.

For states above the isotherm $T = T^R$, the temperature decreasing waves are the e -shocks. In order to satisfy the monotonicity principle we only allow the slow e -shocks based at the right extension of the line \overline{OG} with respect to the b family, which we denote as:

$$\mathcal{E}_b^+(OG). \quad (5.23)$$

5.4.1 Riemann solutions with decreasing temperatures

Here we will give the Riemann solutions for the backward \mathbf{L} -regions above the isotherm $T = T^R$. The segment of the slow backward wave curve $\mathcal{W}_-^s(\mathbf{R})$ from \mathbf{R} :

$$R_b^s \longrightarrow S_e^s, \quad (5.24)$$

and the right extension $\mathcal{E}_e^+(OG)$ are the bifurcation loci for the backward \mathbf{L} -regions in this Riemann solution, see Figure 5.4.

Riemann solution for \mathcal{L}_1^-

In the region \mathcal{L}_1^- the e family is slow and its admissible elementary waves are the shocks. Since we are on the right side of the slow backward wave curve $\mathcal{W}_-^s(\mathbf{R})$, a slow wave emanating from \mathbf{w}^L will reach the isotherm $T = T^R$ at the right of \mathbf{w}^R , in a constant state which we call by \mathbf{M} . The admissible fast waves are thus b -shocks. The solution is:

$$\mathbf{L} \xrightarrow{S_e^s} \mathbf{M} \xrightarrow{S_b^f} \mathbf{R}. \quad (5.25)$$

Riemann solution for \mathcal{L}_2^-

In the transition from \mathcal{L}_1^- to \mathcal{L}_2^- we crossed the extension $\mathcal{E}_b^+(RG)$ so that, now, in a neighborhood of state \mathbf{w}^L the b -waves are slow. A slow b -rarefaction emanating from \mathbf{w}^L crosses the extension $\mathcal{E}_b^+(RG)$ at an intermediate state $\widehat{\mathbf{M}}$; is followed by a left characteristic e -shock. This shock reaches the isotherm $T = T^R$ on the constant state \mathbf{M}_2 and is

followed by a fast b -shock. The solution is:

$$\mathbf{L} \xrightarrow{R_b^s} \widehat{\mathbf{M}}_1 \xrightarrow{S_e^s} \mathbf{M}_2 \xrightarrow{S_b^f} \mathbf{R}. \quad (5.26)$$

Riemann solution for \mathcal{L}_3^-

Here the slow waves are the e -shocks. Now the state \mathbf{w}^L is on the left side of the wave curve $\mathcal{W}_-^s(\mathbf{R})$, see Equation (5.24). We call \mathbf{M} the point where the slow shock wave emanating from \mathbf{w}^L reaches the isotherm $T = T^R$. It must be followed by a b -rarefaction wave. The solution is:

$$\mathbf{L} \xrightarrow{S_e^s} \mathbf{M} \xrightarrow{R_b^f} \mathbf{R}. \quad (5.27)$$

Riemann solution for \mathcal{L}_4^-

Again, we are at the left of the extension $\mathcal{E}_b^+(PO)$. Slow waves are the b -shocks and b -rarefactions. The forward slow wave curve $\mathcal{W}_+^s(\mathbf{L})$ emanating from \mathbf{w}^L :

$$R_b^s \longrightarrow R_e^s, \quad (5.28)$$

crosses the extension $\mathcal{E}_b^+(PO)$ at an intermediate state $\widehat{\mathbf{M}}_1$ and reaches the isotherm $T = T^R$ at a constant state \mathbf{M}_2 .

$$\mathbf{L} \xrightarrow{R_b^s} \widehat{\mathbf{M}}_1 \xrightarrow{S_e^s} \mathbf{M}_2 \xrightarrow{R_b^f} \mathbf{R}. \quad (5.29)$$

5.4.2 Riemann solutions with increasing temperatures

Now we focus on the backward \mathbf{L} -regions below the isotherm $T = T^R$. In comparison to the previous cases in Region B, the bifurcation structure will be complicated by the presence of the singular point.

The backward slow wave curve $\mathcal{W}_-^s(\mathbf{R})$ emanating from \mathbf{w}^R :

$$R_b^s \longrightarrow R_e^s, \quad (5.30)$$

is the first remarkable bifurcation in this backward \mathbf{L} -regions. At its left side, the fast waves reaching \mathbf{R} are the b -rarefactions while at its right side the fast waves are b -shocks. As was previously discussed, in the beginning of this section, temperature increases along e -waves.

We record for later use $\mathcal{W}_-^s(\mathbf{O})$, the backward slow wave curve emanating from \mathbf{w}^O :

$$R_b^s \longrightarrow R_e^s. \quad (5.31)$$

Riemann solution for \mathcal{L}_5^-

In this region the slow waves are e -waves. The Riemann solution is just the Lax construction, where the constant state \mathbf{M} lies on the isotherm $T = T^R$. The Riemann solution is written as:

$$\mathbf{L} \xrightarrow{R_e^s} \mathbf{M} \xrightarrow{S_b^f} \mathbf{R}. \quad (5.32)$$

Riemann solution for \mathcal{L}_6^-

In this region we are on the left side of the coincidence locus. A slow b -rarefaction wave emanating from \mathbf{L} reaches the coincidence locus in an intermediate state $\widehat{\mathbf{M}}_1$. It is followed by a slow e -rarefaction which reaches the isotherm $T = T^R$ in the constant state \mathbf{M}_2 . This wave is followed by a fast b -shock:

$$\mathbf{L} \xrightarrow{R_b^s} \widehat{\mathbf{M}}_1 \xrightarrow{R_e^s} \mathbf{M}_2 \xrightarrow{S_b^f} \mathbf{R}. \quad (5.33)$$

Riemann solution for \mathcal{L}_7^-

Again, the slow waves are e -shocks or e -rarefactions. This is the last case in the Region B to benefit from the Lax construction, where the constant state lies on the isotherm $T = T^R$. The solution is:

$$\mathbf{L} \xrightarrow{R_e^s} \mathbf{M} \xrightarrow{R_b^f} \mathbf{R}. \quad (5.34)$$

Riemann solution for \mathcal{L}_8^-

In the transition from \mathcal{L}_7^- to \mathcal{L}_8^- we crossed the coincidence locus. This backward \mathbf{L} -region is bounded above by wave curve $\mathcal{W}_-^s(\mathbf{O})$, Equation (5.31), and below by the wave curve $\mathcal{W}_-^s(\mathbf{w}^R)$, Equation (5.24). Beginning with a slow b -rarefaction we reach an intermediate state in the coincidence locus, which we denote by $\widehat{\mathbf{M}}_1$. This wave is followed by a slow e -rarefaction that reaches the isotherm $T = T^R$ at the constant state \mathbf{M}_2 . This wave is followed by a b -rarefaction.

$$\mathbf{L} \xrightarrow{R_b^s} \widehat{\mathbf{M}}_1 \xrightarrow{R_e^s} \mathbf{M}_2 \xrightarrow{R_b^f} \mathbf{R}. \quad (5.35)$$

Riemann solution for \mathcal{L}_9^-

In this region the state \mathbf{w}^L is on the left side of the wave curve $\mathcal{W}_-^s(PO)$ that reaches \mathbf{w}^O . The slow e -rarefaction emanating from the \mathbf{w}^L state reaches the extension $\mathcal{E}_e^-(PO)$ at an intermediate state, which we call $\widehat{\mathbf{M}}_1$. Lemma 4.25 shows that the b -shock emanating from $\widehat{\mathbf{M}}_1$ reaches the fast e -rarefaction curve γ_{PO} (see Figure 5.4) at the intermediate state $\widehat{\mathbf{M}}_2$. This b -shock is a double contact shock, thus it can be followed by the fast e -rarefaction emanating from $\widehat{\mathbf{M}}_2$. This rarefaction reaches the isotherm $T = T^R$ in $\widehat{\mathbf{O}}$, from where a fast b -rarefaction reaches \mathbf{R} . The Riemann solution reads:

$$\mathbf{L} \xrightarrow{R_e^s} \widehat{\mathbf{M}}_1 \xrightarrow{S_b^d} \widehat{\mathbf{M}}_2 \xrightarrow{R_e^f} \widehat{\mathbf{O}} \xrightarrow{R_b^f} \mathbf{R}. \quad (5.36)$$

Remark 5.12 *In this \mathbf{L} -region the Riemann solution is given by a single wave group, without embedded constant states. This is a direct consequence of the fact that slow e -rarefaction generically can be concatenated to fast e -rarefaction through b double contact (that joins a slow to a fast wave), near the coincidence locus \mathcal{C} . See Lemma 4.25 and Theorem 4.30. This type of behavior was theoretically predicted for double sonic transitional waves in Schechter et al. [44]. To the authors' knowledge, this is the first practical example.*

Riemann solution for \mathcal{L}_{10}^-

In the transition from \mathcal{L}_9^- to \mathcal{L}_{10}^- we crossed the coincidence locus. The slow waves in the previous region are preceded by a slow b -rarefaction from \mathbf{w}^L to $\widehat{\mathbf{M}}_0$ on the coincidence locus. The solution is:

$$\mathbf{L} \xrightarrow{R_b^s} \widehat{\mathbf{M}}_0 \xrightarrow{R_e^s} \widehat{\mathbf{M}}_1 \xrightarrow{S_b^d} \widehat{\mathbf{M}}_2 \xrightarrow{R_e^f} \widehat{\mathbf{O}} \xrightarrow{R_b^f} \mathbf{R}. \quad (5.37)$$

Riemann solution for \mathcal{L}_{11}^-

In this region we are on the right side of the $\mathcal{W}_-^f(\mathbf{R})$. The slow wave is a b -shock, which reaches the fast backward wave curve emanating from \mathbf{w}^R at a constant state $\mathbf{M}_1 \in \gamma_{PO}$. The solution is:

$$\mathbf{L} \xrightarrow{S_b^s} \mathbf{M}_1 \xrightarrow{R_e^f} \widehat{\mathbf{O}} \xrightarrow{R_b^f} \mathbf{R}. \quad (5.38)$$

Riemann solution for \mathcal{L}_{12}^-

Now we are on the left side of $\mathcal{W}_-^f(\mathbf{R})$. The slow b -rarefaction emanating from \mathbf{w}^L reaches the fast backward wave curve emanating from \mathbf{w}^R at a constant state \mathbf{M}_1 . The Riemann solution is:

$$\mathbf{L} \xrightarrow{R_b^s} \mathbf{M}_1 \xrightarrow{R_e^f} \widehat{\mathbf{O}} \xrightarrow{R_b^f} \mathbf{R}. \quad (5.39)$$

5.5 Region C

The last case occurs for states \mathbf{w}^R in Region C. In the discussion that follows we will present the subdivision of a neighborhood of the singular point into backward \mathbf{L} -regions of \mathbf{w}^R see Figure 5.5.

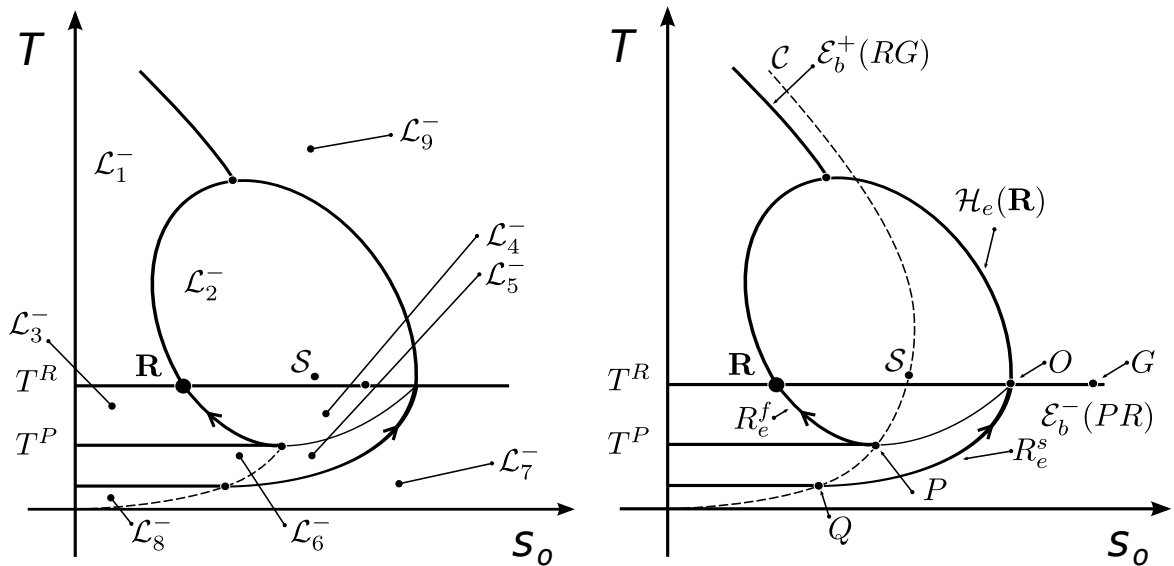


Figure 5.5: Left: backward \mathbf{L} -regions for \mathbf{w}^R in region C. Right: boundaries.

In a small neighborhood of the \mathbf{R} state the fast waves are the e elementary waves. The backward fast wave curve with decreasing temperature is the Hugoniot locus of \mathbf{R} . Away from \mathbf{R} , this curve intersects the isotherm $T = T^R$ at the state \mathbf{O} . The right extension $\mathcal{E}_b^+(OG)$ intersects the locus $\mathcal{H}_e(\mathbf{w}^R)$ at point \mathbf{w}^S , since \mathbf{w}^R , \mathbf{w}^O and \mathbf{w}^S form a triple shock, see Proposition 4.12. As in the case for Region B, the rarefactions that reach points \mathbf{w}^R and \mathbf{w}^O will play a fundamental role in the Riemann solution. The last relevant locus is $\mathcal{E}_e^-(\gamma_{PR})$, the left extension of the rarefaction orbit γ_{PR} .

5.5.1 Riemann solutions

Region C exhibits most of the bifurcation mechanisms appearing in the previously described backward **L**-regions.

Riemann solution for region \mathcal{L}_1^-

This **L**-region lies above the isotherm $T = T^R$ and on the left side of the Hugoniot locus $\mathcal{H}_e(\mathbf{w}^R)$. In the first four regions the classical Lax construction holds. The Riemann solution is:

$$\mathbf{L} \xrightarrow{R_b^s} \mathbf{M} \xrightarrow{S_e^f} \mathbf{R}. \quad (5.40)$$

In this **L**-region we have $\mathbf{M} \in T = T^R$, however we recall the reader that we will suppress the description of constant states given by the Lax construction in the spirit of Remark 5.7 .

Riemann solution for region \mathcal{L}_2^-

This region lies above the isotherm $T = T^R$ and inside the e branch $\mathcal{H}_e(\mathbf{w}^R)$ of the Hugoniot locus based on \mathbf{w}^R . The Riemann solution is:

$$\mathbf{L} \xrightarrow{S_b^s} \mathbf{M} \xrightarrow{S_e^f} \mathbf{R}. \quad (5.41)$$

Riemann solution for region \mathcal{L}_3^-

This region lies below the isotherm $T = T^R$ and on the left side of the rarefaction curve γ_{PR} . The Riemann solution is:

$$\mathbf{L} \xrightarrow{R_b^s} \mathbf{M} \xrightarrow{R_e^f} \mathbf{R}. \quad (5.42)$$

Riemann solution for region \mathcal{L}_4^-

This region lies below the isotherm $T = T^R$ and between the rarefaction curve γ_{PR} and its extension $\mathcal{E}_e^-(\gamma_{PR})$. The solution is:

$$\mathbf{L} \xrightarrow{S_b^s} \mathbf{M} \xrightarrow{R_e^f} \mathbf{R}. \quad (5.43)$$

Riemann solution for \mathcal{L}_5^-

This **L**-region lies below the isotherm $T = T^R$ and is bounded by the coincidence locus, the extension $\mathcal{E}_e^-(\gamma_{PR})$ and the rarefaction curve that emanates from \mathbf{w}^Q .

In this region the solution is similar to the case of \mathcal{L}_9^- in region B, in the sense that the b double contact joins a slow e -rarefaction with a fast e -rarefaction. The solution is:

$$\mathbf{L} \xrightarrow{R_e^s} \widehat{\mathbf{M}}_1 \xrightarrow{S_b^d} \widehat{\mathbf{M}}_2 \xrightarrow{R_e^f} \mathbf{R}, \quad (5.44)$$

where $\widehat{\mathbf{M}}_1 \in \mathcal{E}_e^-(\gamma_{PR})$ and $\widehat{\mathbf{M}}_2 \in \gamma_{PR}$.

Riemann solution for \mathcal{L}_6^-

This region is bounded by the isotherms T^P and T^Q and by the coincidence locus. In the transition from \mathcal{L}_5^- to \mathcal{L}_6^- the \mathbf{w}^L states crossed the coincidence locus. The Riemann solution is a b -rarefaction which ends at $\widehat{\mathbf{M}}_0 \in \mathcal{C}$, is followed by the a construction similar to the previous one:

$$\mathbf{L} \xrightarrow{R_b^s} \widehat{\mathbf{M}}_0 \xrightarrow{R_e^s} \widehat{\mathbf{M}}_1 \xrightarrow{S_b^d} \widehat{\mathbf{M}}_2 \xrightarrow{R_e^f} \mathbf{R}. \quad (5.45)$$

Riemann solution for \mathcal{L}_7^-

This region lies below the isotherm $T = T^R$, on the right side of the rarefaction curve emanating from \mathbf{w}^Q , on the right side of the coincidence locus, The Riemann solution is a slow e -rarefaction that ends at the constant state \mathbf{M} with $\{T = T^R\}$, followed by a fast b -shock:

$$\mathbf{L} \xrightarrow{R_e^s} \mathbf{M} \xrightarrow{S_b^f} \mathbf{R}. \quad (5.46)$$

Riemann solution for \mathcal{L}_8^-

This region lies on the left side of the coincidence locus \mathcal{C} , below the isotherm $T = T^Q$. Again, the solution is a slow b -rarefaction followed by a construction of the same type of the preceding Riemann solution:

$$\mathbf{L} \xrightarrow{R_b^s} \widehat{\mathbf{M}}_0 \xrightarrow{R_e^s} \mathbf{M} \xrightarrow{S_b^f} \mathbf{R}, \quad (5.47)$$

where $\widehat{\mathbf{M}}_0 \in \mathcal{C}$.

Riemann solution for \mathcal{L}_9^-

This region lies above the isotherm $T = T^R$, as well as and on the right side of the e branch of the Hugoniot locus based on \mathbf{w}^R , $\mathcal{H}_e(\mathbf{w}^R)$. The solution is a slow e -shock ending at the constant state $\mathbf{M} \in \{T = T^R\}$, followed by a fast b -shock:

$$\mathbf{L} \xrightarrow{S_e^s} \mathbf{M} \xrightarrow{S_b^f} \mathbf{R}. \quad (5.48)$$

Chapter 6

Intermezzo

In this chapter we state the basic results and definitions needed to find the complete solution of the Riemann problem with data in the two phase region or in the single phase liquid region, a representative set of which will be given in Chapter 7. Also, in this chapter we elaborate on the mechanisms that provide the transition between the Riemann solutions in Chapter 5 and in Chapter 7. This chapter will build on definitions and results of all previous chapters.

Our motivation originates from the observation that it is impossible to solve the Riemann problem for all pairs of left and right states in the two phase region using only waves defined within the two phase region. Nevertheless, it is still possible to find all Riemann solutions if one is allowed to use waves from other thermodynamical configurations, in addition to those defined inside the two phase region. Similar statements hold for the single phase liquid region: it is impossible to solve the Riemann problem for all pairs of left and right states in the single phase region using only waves defined within this region, one needs to use waves from other thermodynamical configurations.

6.1 Riemann solutions in TP

As was seen in Chapter 5, the Riemann solution possesses a very rich bifurcation structure in a neighborhood of the singular point. Nevertheless, there are other structures in the two phase region with great impact on the Riemann solutions.

As discussed on Chapter 2, the Riemann solution is constructed by concatenating constant regions and fundamental waves: shocks and rarefactions. As in Chapter 5, when making figures we take advantage of the fact that the projection of elementary waves onto state space is sufficient to construct the solutions.

Riemann solutions bifurcate when an elementary wave ceases to be admissible: the

construction of the Riemann solution must proceed with another admissible elementary wave. First, we will focus on the bifurcations in forward constructions of Riemann solutions that appear when \mathbf{w}^R is allowed to vary but \mathbf{w}^L is fixed.

Definition 6.1 (Forward **R**-region). *Fix a pair $\mathbf{w}^L, \mathbf{w}^R$ in state space. The forward **R**-region $\mathcal{R}^+(\mathbf{w}^L)$, corresponding to the selected pair $\mathbf{w}^L, \mathbf{w}^R$, is the maximal subset of state space such that $\mathbf{w}^R \in \mathcal{R}^+(\mathbf{w}^L)$ and the Riemann solutions for any initial data $\mathbf{w}^* \in \mathcal{R}^+(\mathbf{w}^L)$, $u^* > 0$,*

$$\mathbf{w}(x, 0) = \begin{cases} \mathbf{w}^L, & \text{if } x < 0, \\ \mathbf{w}^*, & \text{if } x > 0, \end{cases}$$

and

$$u(x, 0) = u^*, \quad \text{if } x < 0,$$

are constructed through a wave fan consisting of the same concatenations of constant states and the same fundamental wave types and families as for the solution associated to the pair $\mathbf{w}^L, \mathbf{w}^R$.

Remark 6.2 *Typically there is a finite number of forward **R**-regions for a given \mathbf{w}^L . We will follow the usual habit and number them.*

When the left state \mathbf{w}^L wanders in state space, the solutions may change topology, *i.e.*, the forward **R**-region diagram changes qualitatively. When such a change happens the Riemann solution bifurcates. Bifurcations generically happen when \mathbf{w}^L crosses certain codimension one manifolds in state space.

Definition 6.3 (Forward **L**-region). *Fix \mathbf{w}^L in state space. The forward **L**-Region $\mathcal{L}^+(\mathbf{w}^L)$, containing \mathbf{w}^L , is the maximal subset of state space such that for any $\mathbf{w}^* \in \mathcal{L}^+$ the subdivision of state space into forward **R**-regions $\mathcal{R}^+(\mathbf{w}^*)$ is the same as the subdivision in $\mathcal{R}^+(\mathbf{w}^L)$.*

Remark 6.4 *The reader should pay attention to the differences between the **R**-construction described by Definitions 5.1, 5.3 and the **L**-construction described by Definitions 6.1, 6.3.*

Remark 6.5 *Again we will use the lexicographic order of the plane to indicate relative position of objects. For example, $\mathbf{w}^1 = (s_o^1, T^1)$ and $\mathbf{w}^2 = (s_o^2, T^2)$: state \mathbf{w}^2 is above \mathbf{w}^1 if $T^2 > T^1$. Accordingly, state \mathbf{w}^2 is at the right of \mathbf{w}^1 if $s_o^2 > s_o^1$.*

6.1.1 The influence of the exceptional locus on Riemann solutions

The exceptional locus \mathcal{E} is a genuine contact of the e family, see Propositions 4.22 and 4.33. In a suitable neighborhood of the exceptional locus, elementary wave curves must be close to it. This is so because \mathcal{E} coincides with both an e -integral curve and with the Hugoniot e -branch of \mathbf{w}^- for any $\mathbf{w}^- \in \mathcal{E}$; this fact is illustrated in Figure 6.1.

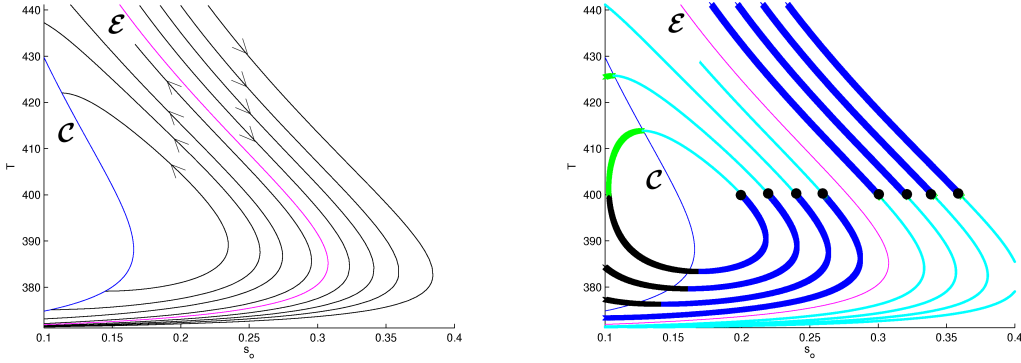


Figure 6.1: Elementary waves near the exceptional locus \mathcal{E} . Left: rarefaction curves. Right: shock curves, with the base state represented by a bold dot.

Since this neighborhood can be disjoint from the coincidence locus \mathcal{C} , the two families are transversal in such a neighborhood, b -waves are fast and Lax construction holds, *i.e.*, the Riemann solution is given by a slow e -wave, followed by a fast b -wave. Since b -waves lie along isotherms, see Proposition 4.6, Riemann solutions along isotherms can be obtained by the standard fractional flow theory, in other words, Oleřnik construction [39]. The bifurcations generated in the Riemann solutions by the b inflection, Equation (4.46), can also be described by the fractional flow theory, *i.e.*, Oleřnik construction. In our particular case, these bifurcations complicate the description of Riemann solutions without adding any essential novelty.

Remark 6.6 *We will disregard bifurcations in Riemann solutions that arise from the b inflection in order to focus on the organizing structures that characterize our particular case: the singular point and the boundary between the single phase liquid region and the two phase region.*

Let us return to the Riemann solution near the exceptional locus \mathcal{E} . On its left side, along an e -rarefaction wave the temperature increases. The Riemann solution in this neighborhood of the exceptional locus is given by cases \mathcal{L}_1^- and \mathcal{L}_5^- for \mathbf{w}^R in Regions A

and B, see Sections 5.2, 5.4. In our case, the Riemann solution given in Chapter 5 can be extended down to the exceptional locus \mathcal{E} without change.

Remark 6.7 *In fact, by Propositions 4.22 and 4.33 the boundary line $\{s_o = 0\}$ must also be a contact discontinuity, with the same properties as the exceptional locus \mathcal{E} . For Riemann data near any of the two loci, the same kind of influence is felt in the solutions.*

In the particular case when both $\mathbf{w}^L, \mathbf{w}^R$ belong to \mathcal{E} , the solution is a genuine contact discontinuity with speed $\sigma = \lambda_e(\mathbf{w}^L, u) = \lambda_e(\mathbf{w}^R, u)$.

Temperature decreases along an e -rarefaction wave with \mathbf{w}^L states on the right side of the exceptional locus. For pairs of states $\mathbf{w}^L = (s_o^L, T^L)$ and $\mathbf{w}^R = (s_o^R, T^R)$ in a neighborhood on the right side of the exceptional locus the Riemann solution is given by the Lax construction, written as:

$$\mathcal{R}_1^+ : \text{for } T^R > T^L \text{ and } s_o^R > s_o^L, \quad \mathbf{L} \xrightarrow{S_e^s} \mathbf{M} \xrightarrow{S_b^f} \mathbf{R}. \quad (6.1)$$

$$\mathcal{R}_2^+ : \text{for } T^R > T^L \text{ and } s_o^R < s_o^L, \quad \mathbf{L} \xrightarrow{S_e^s} \mathbf{M} \xrightarrow{R_b^f} \mathbf{R}. \quad (6.2)$$

$$\mathcal{R}_3^+ : \text{for } T^R < T^L \text{ and } s_o^R < s_o^L, \quad \mathbf{L} \xrightarrow{R_e^s} \mathbf{M} \xrightarrow{R_b^f} \mathbf{R}. \quad (6.3)$$

$$\mathcal{R}_4^+ : \text{for } T^R < T^L \text{ and } s_o^R > s_o^L, \quad \mathbf{L} \xrightarrow{R_e^s} \mathbf{M} \xrightarrow{S_b^f} \mathbf{R}. \quad (6.4)$$

This construction can be extended as follows: let us denote by γ the rarefaction curve that intersects the right-hand side branch of the coincidence locus in the boundary of the **TP**, $\{T = T_{bV}\}$. For any \mathbf{w}^L state in the region between the exceptional locus and γ , the two families are genuinely nonlinear and System (4.1) is strictly hyperbolic. The preceding Lax construction holds for any \mathbf{w}^R state in state space on the left side of the b inflection. For \mathbf{w}^R states on the right side of the b inflection the b waves change according to the fractional flow theory.

6.1.2 Riemann solutions near the pure oil boundary

We will focus on \mathbf{w}^L states on the right side of the exceptional locus \mathcal{E} between the b inflection locus (Equation (4.46)) and the extension of the boundary $\{s_o = 1\}$. The subdivision of state space into forward **R**-regions is shown in Figure 6.2.

Riemann solution for \mathcal{R}_1^+

The region \mathcal{R}_1^+ lies on the right side of $\mathcal{H}_e(\mathbf{w}^L)$, which is the e -branch of the Hugoniot locus emanating from \mathbf{w}^L , above $\{T = T^L\}$. The Lax construction gives the solution:

$$\mathbf{L} \xrightarrow{S_e^s} \mathbf{M} \xrightarrow{S_b^f} \mathbf{R}, \quad (6.7)$$

where $\mathbf{M} \in \mathcal{H}_e(\mathbf{w}^L) \cap \{T = T^R\}$. In what follows we will not write down the definition of constant states given by the Lax construction, as it is obvious.

Riemann solution for \mathcal{R}_2^+

The region \mathcal{R}_2^+ lies on the left side of $\mathcal{H}_e(\mathbf{w}^L)$, which is the e -branch of the Hugoniot locus emanating from \mathbf{w}^L , above $\{T = T^L\}$. The solution is:

$$\mathbf{L} \xrightarrow{S_e^s} \mathbf{M} \xrightarrow{R_b^f} \mathbf{R}. \quad (6.8)$$

Riemann solution for \mathcal{R}_3^+

The region \mathcal{R}_3^+ lies on the left side of the e -rarefaction emanating from \mathbf{w}^L , between the isotherms $\{T = T^L\}$ and $\{T = T^Q\}$. The solution is:

$$\mathbf{L} \xrightarrow{R_e^s} \mathbf{M} \xrightarrow{R_b^f} \mathbf{R}. \quad (6.9)$$

Riemann solution for \mathcal{R}_4^+

The region \mathcal{R}_4^+ lies on the right side of the e -rarefaction emanating from \mathbf{w}^L . It is bounded by the aforementioned rarefaction, by the extension $\mathcal{E}_e^-(\gamma_{PQ})$, by the boundary $\{(s_o, T) \in \mathbf{TP} \mid s_o = 1, T^O \leq T \leq T^L\}$ and by the isotherm $T = T^L$. This is the last region to benefit from the Lax construction:

$$\mathbf{L} \xrightarrow{R_e^s} \mathbf{M} \xrightarrow{S_b^f} \mathbf{R}. \quad (6.10)$$

Riemann solution for \mathcal{R}_5^+

The region \mathcal{R}_5^+ is bounded by extension $\mathcal{E}_e^-(\gamma_{PQ})$, by the coincidence locus \mathcal{C} and by γ_{PQ} , a segment of the rarefaction emanating from \mathbf{w}^L . The construction of extension $\mathcal{E}_e^-(\gamma_{PQ})$, Lemma 4.25 and Corollary 4.31 allow us to continue the Riemann solution for the preceding \mathbf{R} -region with a fast e -rarefaction, characteristic with the b -shock. The solution is:

$$\mathbf{L} \xrightarrow{R_e^s} \widehat{\mathbf{M}}_1 \xrightarrow{S_b^f} \widehat{\mathbf{M}}_2 \xrightarrow{R_e^f} \mathbf{R}, \quad (6.11)$$

where $\widehat{\mathbf{M}}_1 \in \gamma_{PQ}$ and $\widehat{\mathbf{M}}_2 \in \mathcal{E}_e^-(\gamma_{PQ})$.

Riemann solution for \mathcal{R}_6^+

In the transition from the forward \mathbf{R} -region \mathcal{R}_5^+ to the forward \mathbf{R} -region \mathcal{R}_6^+ we crossed the coincidence locus \mathcal{C} . Furthermore, this region is bounded by the isotherms $\{T = T^Q\}$ and $\{T = T^P\}$. The Riemann solution is a concatenation of the same type of Riemann solution found for \mathbf{w}^L in region \mathcal{R}_5^+ with a fast b -wave. The solution is:

$$\mathbf{L} \xrightarrow{R_e^s} \widehat{\mathbf{M}}_1 \xrightarrow{S_b^f} \widehat{\mathbf{M}}_2 \xrightarrow{R_e^f} \widehat{\mathbf{M}}_3 \xrightarrow{R_b^f} \mathbf{R}. \quad (6.12)$$

where $\widehat{\mathbf{M}}_3 \in \mathcal{C}$.

Further Riemann solutions

The subdivision into forward \mathbf{R} -regions illustrated in Figure 6.2 suggests that it is not possible to extend the construction of Riemann solutions for \mathbf{w}^R states below wave curve $\mathcal{W}_+^f(\mathbf{w}^O)$ using only waves defined within \mathbf{TP} .

This key observation leads us to consider the use of waves from other thermodynamical configurations (the single phase liquid region in our case), in addition to those defined inside the two phase region, in order to obtain the complete Riemann solution.

6.2 Elementary waves in the SPL

In Subsection 3.5.2 we derived the system of conservation laws:

$$\left\{ \begin{array}{l} \varphi \frac{\partial}{\partial t} \rho_{ov} + \frac{\partial}{\partial x} (u \rho_{ov}) = 0, \\ \varphi \frac{\partial}{\partial t} \rho_{od} + \frac{\partial}{\partial x} (u \rho_{od}) = 0, \\ \varphi \frac{\partial}{\partial t} (\widehat{H}_r + H_o) + \frac{\partial}{\partial x} (u H_o) = 0, \end{array} \right. \quad (6.13)$$

and introduced the natural parametrization of the single phase liquid state space:

$$\mathbf{SPL} = \{ (T, \rho_{od}) \mid T \geq T_{bV} \text{ and } x_{od}^{eq}(T) \leq x_{od} \leq 1 \}. \quad (6.14)$$

System (6.13) can be written in compact form as:

$$\partial_t G(\mathbf{w}) + \partial_x u F(\mathbf{w}) = 0, \quad (6.15)$$

where:

$$G(T, \rho_{od}) = \begin{pmatrix} \rho_V \\ \rho_{od} \\ \widehat{H}_r + H_o \end{pmatrix} \quad \text{and} \quad F(T, \rho_{od}) = \begin{pmatrix} \rho_V \\ \rho_{od} \\ H_o \end{pmatrix}. \quad (6.16)$$

Multiplying Equation (6.13a) by $1/\rho_V$, Equation (6.13b) by $1/\rho_D$, adding the results and using the ideal mixture law (3.2) we get $\partial_x u = 0$, so u is constant in space. Therefore, the system (6.13) simplifies further to:

$$\left\{ \begin{array}{l} \varphi \frac{\partial}{\partial t} \rho_{od} + u \frac{\partial}{\partial x} \rho_{od} = 0, \\ \varphi \frac{\partial}{\partial t} (\widehat{H}_r + H_o) + u \frac{\partial}{\partial x} H_o = 0, \\ \partial_x u = 0. \end{array} \right. \quad (6.17)$$

We get immediately the (compositional) characteristic speed and its eigenvector:

$$\lambda_c = \frac{u}{\varphi} \quad \text{and} \quad \vec{r}_c = (0, 1)^T, \quad (6.18)$$

and because of the affine linear dependence of the enthalpies on the temperature, see Table A.1 and Equations (3.18), (A.1), (A.2), (A.3), the (thermal) eigenpair is:

$$\lambda_t = \frac{u}{\varphi} \frac{\partial_T H_o}{\partial_T H_o + \partial_T H_r} = \frac{u}{\varphi} \frac{\rho_V c_{oV}}{\rho_V c_{oV} + C_r} \quad \text{and} \quad \vec{r}_t = (1, 0)^T. \quad (6.19)$$

Since both the flux and the accumulation functions in (6.17) are linear, in the **SPL** the Riemann solution is trivial. It is a genuine thermal contact C_t followed by a genuine compositional contact C_c , since $\lambda_t < \lambda_c$.

Since light and dead oils can only form a liquid if the amount of dead oil in the mixture satisfies $x_{od}^{eq}(T) \leq x_{od}$, see Equation 6.14, it is clear that if we fix a $\mathbf{w}^L = (T^L, x_{od}^L)$ state we can only construct Riemann solutions fully contained within **SPL** for $\mathbf{w}^R = (T^R, x_{od}^R)$ states that satisfy:

$$\{T^R \leq T^* \mid T^* \text{ defined by } x_{od}^L = x_{od}^{eq}(T^*)\}. \quad (6.20)$$

This is completely analogous to the situation in the previous subsection.

6.3 Shock waves between regions

In this section we consider discontinuous waves between the single phase liquid region and the two phase region. Familiarity with Sections 3.2.1 and 3.5 is assumed.

We define the extended accumulation function:

$$G^* = \begin{cases} G_{\mathbf{TP}}, & \text{for } \mathbf{w} \in \mathbf{TP}, \\ G_{\mathbf{SPL}}, & \text{for } \mathbf{w} \in \mathbf{SPL}, \end{cases} \quad (6.21)$$

where $G_{\mathbf{TP}}$ is given by Equation (4.4a) and $G_{\mathbf{SPL}}$ is given by Equation (6.16a), as well as the extended flux function:

$$F^* = \begin{cases} F_{\mathbf{TP}}, & \text{for } \mathbf{w} \in \mathbf{TP}, \\ F_{\mathbf{SPL}}, & \text{for } \mathbf{w} \in \mathbf{SPL}, \end{cases} \quad (6.22)$$

where $F_{\mathbf{TP}}$ is given by Equation (4.4b) and $F_{\mathbf{SPL}}$ is given by Equation (6.16b). Since the single phase liquid region and the two phase region share the same boundary:

$$\Omega_{\mathbf{TP}} \cap \Omega_{\mathbf{SPL}} = \left\{ (s_o, T, \rho_{od}) \mid (s_o = 1, T \geq T_{bV}, \rho_{od} = \rho_{od}(T)) \right\}, \quad (6.23)$$

see Equations (3.28), (3.34), (3.3) and (3.5), the extended flux and accumulation functions (6.21), (6.22) are continuous up to the boundary (6.23) (they are smooth inside \mathbf{TP} and \mathbf{SPL}). The interplay between the two phase and the single phase liquid situations is illustrated in Figure 6.3.

The Rankine Hugoniot condition, Equation (2.10), is written as:

$$u^+ F^*(\mathbf{w}^+) - u^- F^*(\mathbf{w}^-) - \sigma (G^*(\mathbf{w}^+) - G^*(\mathbf{w}^-)) = 0, \quad (6.24)$$

where \mathbf{w}^- , \mathbf{w}^+ are allowed to be either in \mathbf{TP} or in \mathbf{SPL} .

Both the extended accumulation and the extended flux are smooth in a neighborhood of any point in the interior of \mathbf{TP} . For any base state of the Hugoniot locus between \mathbf{L} -regions or \mathbf{R} -regions that lie in the interior of \mathbf{TP} we can provide a smooth parametrization of the shock curve. Thus, the Bethe-Wendroff Theorem 4.13 holds in such neighborhoods. If this parametrization crosses the boundary defined in Equation (6.23), the Bethe-Wendroff Theorem may not hold.

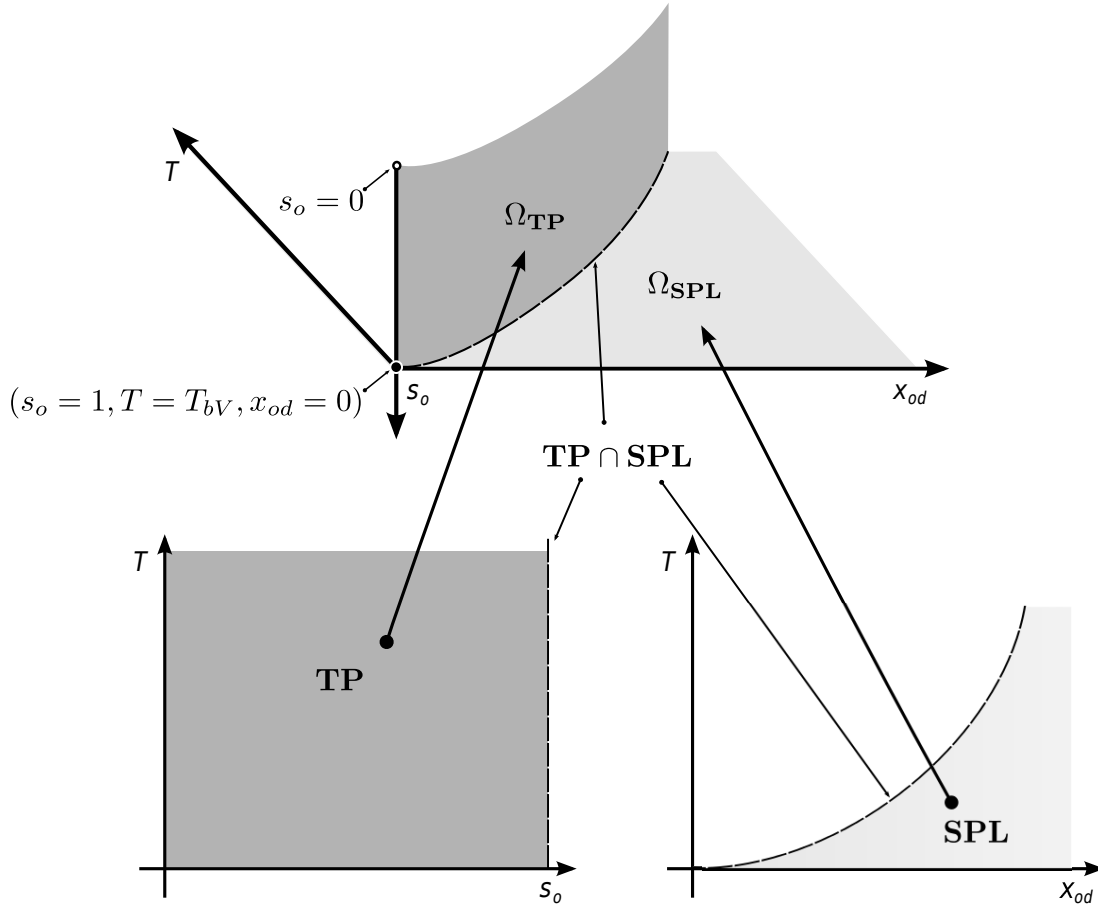


Figure 6.3: Top: relative positions of the two phase and single phase liquid physical configurations. Their parameterizations are shown at the bottom.

6.3.1 Shock waves from TP to SPL

Here we consider the case where \mathbf{w}^- lies in **TP** and $\mathbf{w}^+ = (T^+, x_{od}^+)$ is allowed to vary in **SPL**. We rewrite Equation 6.24 explicitly as:

$$\left\{ \begin{array}{l} \sigma [\rho_V - G_1^-] - u^+ \rho_V + u^- F_1^- = 0, \\ \sigma [\rho_{od}^+ - G_2^-] - u^+ \rho_{od}^+ + u^- F_2^- = 0, \\ \sigma [H_o^+ + H_r^+ - G_3^-] - u^+ H_o^+ + u^- F_3^- = 0, \end{array} \right. \quad (6.25)$$

where G^- , F^- are given by Equation (4.4) and the subscripts $i \in \{1, 2, 3\}$ denote their components.

We will show that the Hugoniot locus inside the **SPL** for a fixed \mathbf{w}^- state inside **TP** is

generically a hyperbola. It degenerates in the cases $\mathbf{w}^- \in \{s_o = 1\}$ and $\mathbf{w}^- \in \mathcal{E}_e^-(s_o = 1)$, as shown in Figure 6.4 and in the proposition that follows.

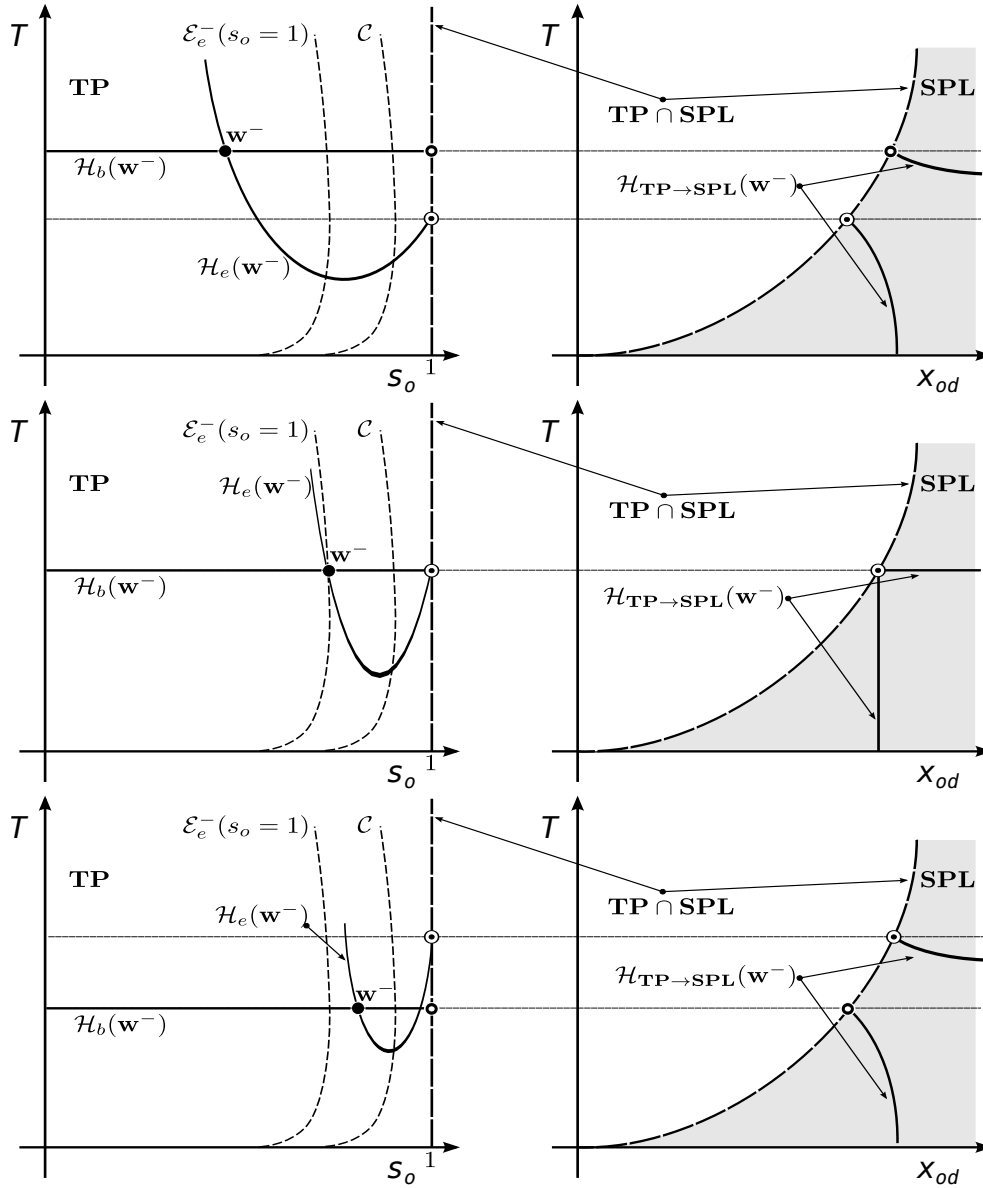


Figure 6.4: Change in the $\mathbf{TP} \rightarrow \mathbf{SPL}$ branch of the Hugoniot locus when $\mathbf{w}^L \in \mathbf{TP}$ crosses the extension of the boundary $\mathcal{E}_e^-(s_o = 1)$.

Proposition 6.8 (Characterization of shock curves $\mathbf{TP} \rightarrow \mathbf{SPL}$). *The shock curve inside \mathbf{SPL} for a left state in \mathbf{TP} is a hyperbola. Its asymptotes are parallel to the axis of the parametrization of the single phase liquid state space, (T, x_{od}) . This locus bifurcates for $\mathbf{w}^- \in \{s_o^- = 1\}$ and $\mathbf{w}^- \in \mathcal{E}_e^-(\{s_o^- = 1\})$.*

Proof. The explicit formulae for enthalpies H_r and H_o are given in equations (3.18), (A.1), (A.2) and (A.3). Using these equations and defining $\tilde{T} = T - \bar{T}$, we rewrite Equation (6.25) as:

$$\begin{pmatrix} [\rho_V - G_1^-] & -\rho_V & F_1^- \\ [\rho_{od}^+ - G_2^-] & -\rho_{od}^+ & F_2^- \\ [(\zeta + C_r)\tilde{T}^+ - G_3^-] & -\zeta\tilde{T}^+ & F_3^- \end{pmatrix} \begin{pmatrix} \sigma \\ u^+ \\ u^- \end{pmatrix} = 0, \quad (6.26)$$

where $\zeta = \rho_V c_{oV}$. The pairs $(\tilde{T}^+, \rho_{od}^+)$ for which the matrix in Equation (6.26) has a non-trivial kernel satisfy:

$$A\rho_{od}^+\tilde{T}^+ + B\rho_{od}^+ + C\tilde{T}^+ + D = 0, \quad (6.27)$$

where:

$$\begin{cases} A = C_r F_1^-, \\ B = G_1^- F_3^- - F_1^- G_3^-, \\ C = \zeta(G_2^- F_1^- - F_2^- G_1^-) - \rho_V C_r F_2^-, \\ D = \rho_V(G_3^- F_2^- - F_3^- G_2^-). \end{cases} \quad (6.28)$$

Under the change of variables $\rho_{od}^+ = Y + Z$, $\tilde{T}^+ = Y - Z$, Equation (6.27) becomes:

$$\left(AY + \frac{B+C}{2}\right)^2 - \left(AZ + \frac{C-B}{2}\right)^2 + AD - BC = 0, \quad (6.29)$$

which is generically a hyperbola (since $A > 0$) with asymptotes parallel to the axes $\{T = T_{bV}\}$ and $\{\rho_{od} = 0\}$. A computation shows that $AD - BC$ in (6.29) vanishes for $\mathbf{w}^- \in \{s_o = 1\}$, making the Hugoniot locus defined in (6.27) bifurcate. The bifurcation in the Hugoniot locus (6.27) for $\mathbf{w}^- \in \mathcal{E}_e^-(\{s_o = 1\})$ follows from the Triple Shock Rule 4.10, Proposition 4.6 and continuity of the extended accumulations and fluxes. \square

6.3.2 Shock waves from SPL to TP

Here we consider the case where \mathbf{w}^- lies in **SPL** and $\mathbf{w}^+ = (s_o^+, T^+)$ is allowed to vary in **TP**. We rewrite Equation 6.24 explicitly as:

$$\left\{ \begin{array}{l} \sigma [\alpha^+ s_o^+ + \rho_{gV}^+ - G_1^-] - u^+(\alpha^+ f_o^+ + \rho_{gV}^+) + u^- F_1^- = 0, \\ \sigma [\beta^+ s_o^+ - G_2^-] - u^+ \beta^+ f_o^+ + u^- F_2^- = 0, \\ \sigma [\gamma^+ s_o^+ + H_g^+ + H_r^+ - G_3^-] - u^+(\gamma^+ f_o^+ + H_g^+) + u^- F_3^- = 0. \end{array} \right. \quad (6.30)$$

Notice that G^- and F^- are given by evaluating Equation (6.16) at \mathbf{w}^- . The subscripts $i \in \{1, 2, 3\}$ denote their components. An illustration of this locus is given in Figure 6.5.

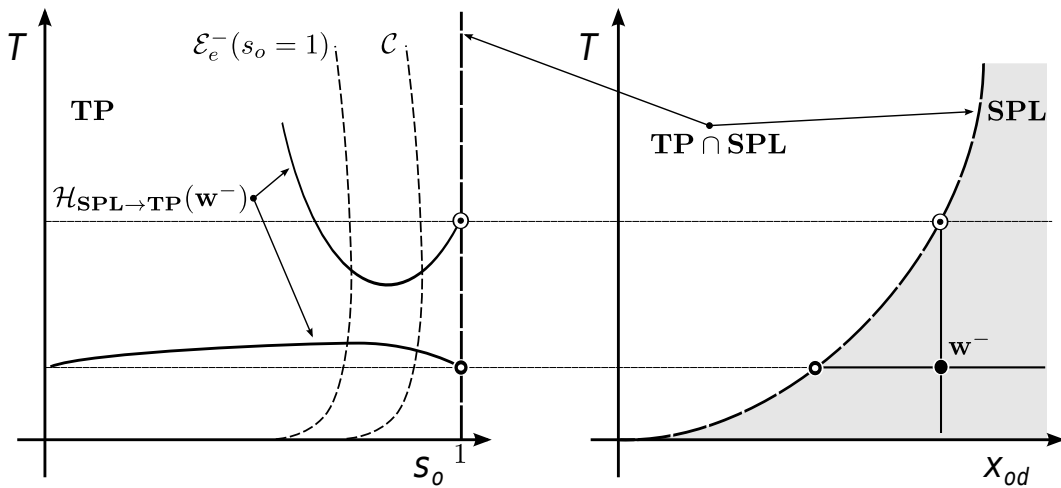


Figure 6.5: **TP** extension of the Hugoniot locus for an \mathbf{w}^L state in **SPL**.

The remarkable similarity between Equations (6.30) and (4.43) yields the propositions:

Proposition 6.9 *Let $(s_o^+, T^+) = \mathbf{w}^+ \in \mathbf{TP}$, $\mathbf{w}^- \in \mathbf{SPL}$ and $\mathbf{w}^+ \in \mathcal{H}(\mathbf{w}^-)$ be such that the rows of the matrix in the Rankine-Hugoniot relation (6.30) for \mathbf{w}^- , \mathbf{w}^+ are not parallel. Then the rescaled speed $\mathbf{U}(\mathbf{w}^-, \mathbf{w}^+)$, defined in Equation 4.41, is a function of \mathbf{w}^- and T^+ .*

Proposition 6.10 *Assume that $\mathbf{w}^b = (s_o^b, T^b)$, $\mathbf{w}^c = (s_o^c, T^c)$ satisfy $\mathbf{w}^b, \mathbf{w}^c \in \mathcal{H}(\mathbf{w}^a)$, $\mathbf{w}^a \in \mathbf{SPL}$ and $T^b = T^c = T$. Let us use the notation $u^b = \mathbf{U}(\mathbf{w}^a, \mathbf{w}^b)$ and $u^c = \mathbf{U}(\mathbf{w}^a, \mathbf{w}^c)$ for Darcy speeds and $P^a = (\mathbf{w}^a, u^a)$, $P^b = (\mathbf{w}^b, u^b)$ and $P^c = (\mathbf{w}^c, u^c)$ for points. If the conditions of Proposition 6.9 and Theorem 4.10 are satisfied, then:*

1. $\mathbf{U}(\mathbf{w}^a, \mathbf{w}^b) = \mathbf{U}(\mathbf{w}^a, \mathbf{w}^c)$,
2. $(\mathbf{w}^c, u^c) \in \mathcal{H}(\mathbf{w}^b)$,
3. $\sigma(P^a; P^b) = \sigma(P^b; P^c) = \sigma(P^c; P^a)$.

The proofs are similar to those of Proposition 4.11 and Proposition 4.12, so they will be omitted.

Chapter 7

Riemann Problem II between TP and SPL

In this chapter we give two representative sets of Riemann solutions for \mathbf{w}^L and \mathbf{w}^R states chosen near the boundary between **SPL**, the single phase liquid region and **TP**, the two phase liquid region. Indeed, we solved the Riemann problem for all cases.

7.1 Riemann solutions for L in SPL

The state $\mathbf{L} = (T^L, x_{od}^L)$ lies in **SPL**, see Figure 7.1. We denote the isotherm $\{(T, \rho_{od}) \mid T = T^L\}$ as γ_{TL} . The slow forward wave curve $\mathcal{W}_+^f(\mathbf{w}^L)$ emanating from \mathbf{w}^L is written as:

$$C_t \longrightarrow S_{\mathbf{SPL} \rightarrow \mathbf{TP}}^s \longrightarrow R_b^s \longrightarrow S_e^s, \quad (7.1)$$

shown in Figure 7.1 as the concatenation of the segments γ_{TL} , $\mathcal{H}_{\mathbf{SPL} \rightarrow \mathbf{TP}}(\mathbf{w}^L)$, γ_{GQ} and $\mathcal{E}_b^-(QG)$. The wave curve $\mathcal{W}_+^f(\mathbf{w}^L)$ is necessary to solve the Riemann problem for \mathbf{w}^R states the temperatures of which satisfy the relationship:

$$\{T^R \geq T^* \mid T^* \text{ defined by } x_{od}^L = x_{od}^{eq}(T^*)\}, \quad (7.2)$$

see Subsections 3.5.2 and 6.2.

We denote the state between the $S_{\mathbf{SPL} \rightarrow \mathbf{TP}}^s$ and R_s^b waves as \mathbf{w}^G . Let us denote as \mathbf{w}^P the intersection of the wave curve $\mathcal{W}_+^f(\mathbf{w}^L)$ with the boundary $s_o = 1$, as \mathbf{w}^Q the intersection of $\mathcal{W}_+^f(\mathbf{w}^L)$ with the coincidence locus \mathcal{C} ; similarly, let \mathbf{w}^O be the intersection

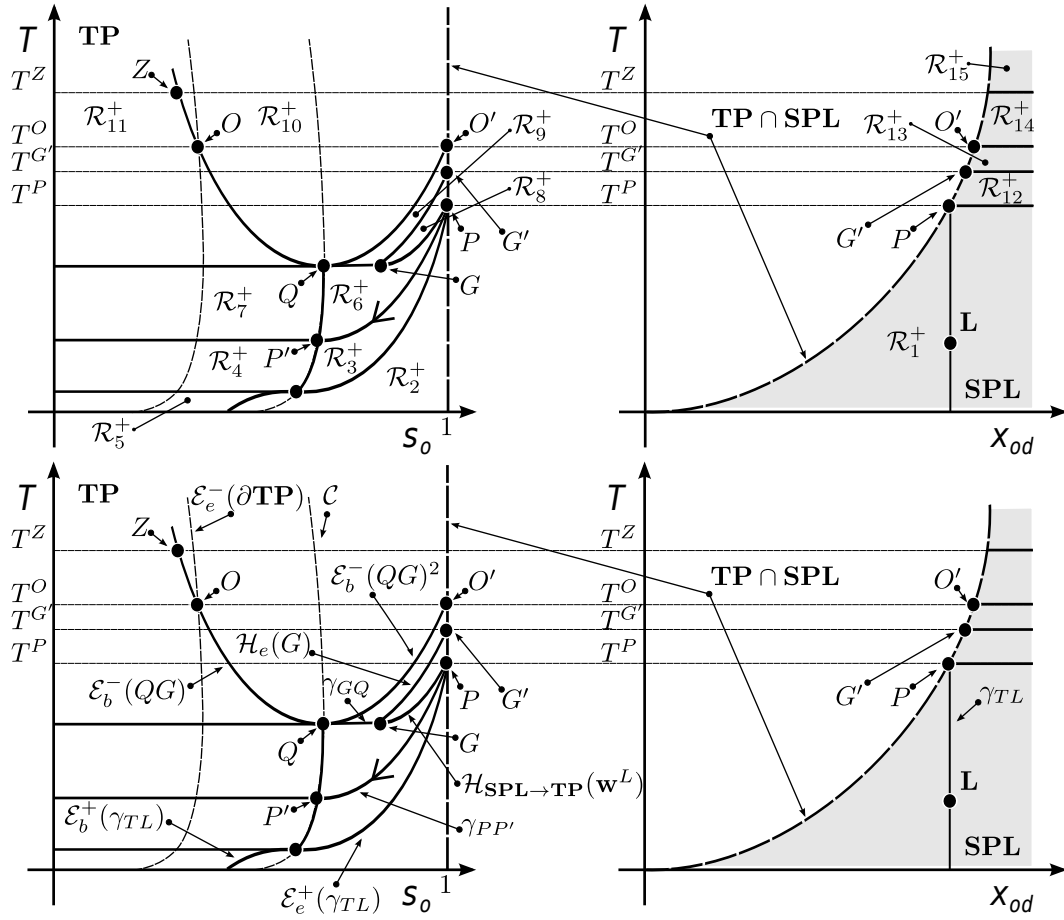


Figure 7.1: Up: forward **R**-regions for **L** in **SPL**. Down: boundaries. Left: regions and boundaries inside **TP**. Right: regions and boundaries inside **SPL**. The single phase liquid region is shaded.

of the wave curve $\mathcal{W}_+^f(\mathbf{w}^L)$ with the extension of the boundary:

$$\mathcal{E}_{\partial\mathbf{TP}} = \mathcal{E}_e^-(\{s_o = 1\}). \quad (7.3)$$

The double extension $\mathcal{E}_b^-(QO)^2$, see Definition 5.5, will delimit the set of admissible fast b -shocks that reach the right side of the coincidence locus.

The **R**-regions induced by fast waves reaching **TP** are bounded by the right extensions $\mathcal{E}_b^+(\gamma_{TL})$ and $\mathcal{E}_e^+(\gamma_{TL})$. We record for later use the fast forward wave curve $\mathcal{W}_+^f(\mathbf{P})$ emanating from point \mathbf{w}^P :

$$R_e^f \longrightarrow R_b^f. \quad (7.4)$$

Riemann solution for \mathcal{R}_1^+

Near the state \mathbf{w}^L in \mathbf{SPL} the Riemann solution is:

$$\mathbf{L} \xrightarrow{C_t} \mathbf{M} \xrightarrow{C_c} \mathbf{R}, \quad (7.5)$$

where $\mathbf{M} \in \gamma_{TL}$.

Riemann solution for \mathcal{R}_2^+

In the region \mathcal{R}_2^+ the states \mathbf{w}^R lie in \mathbf{TP} . This region is bounded by the right extensions $\mathcal{E}_b^+(\gamma_{TL})$, $\mathcal{E}_e^+(\gamma_{TL})$, as well as by the boundary of the \mathbf{TP} region. The Riemann solution is:

$$\mathbf{L} \xrightarrow{C_t} \mathbf{M} \xrightarrow{S_{\mathbf{SPL} \rightarrow \mathbf{TP}}^f} \mathbf{R}, \quad (7.6)$$

where $\mathbf{M} \in \gamma_{TL}$.

Riemann solution for \mathcal{R}_3^+

The region \mathcal{R}_3^+ is bounded by the coincidence locus, by the right extension $\mathcal{E}_e^+(\gamma_{TL})$ and by the wave curve $\mathcal{W}_+^f(\mathbf{P})$. The Riemann solution is given by:

$$\mathbf{L} \xrightarrow{C_t} \mathbf{M}_1 \xrightarrow{S_{\mathbf{SPL} \rightarrow \mathbf{TP}}^f} \widehat{\mathbf{M}}_2 \xrightarrow{R_e^f} \mathbf{R}, \quad (7.7)$$

where the constant state \mathbf{M}_1 lies on γ_{TL} and the intermediate state $\widehat{\mathbf{M}}_2$ lies on the intersection of extension $\mathcal{E}_e^+(\gamma_{TL})$ with the slow branch of the Hugoniot locus from \mathbf{SPL} to \mathbf{TP} emanating from \mathbf{M}_1 .

Riemann solution for \mathcal{R}_4^+

In the transition from region \mathcal{R}_3^+ to region \mathcal{R}_4^+ the \mathbf{w}^R state crossed the coincidence locus. The fast waves in the preceding region are succeeded by a b -rarefaction. The Riemann solution is:

$$\mathbf{L} \xrightarrow{C_t} \mathbf{M}_1 \xrightarrow{S_{\mathbf{SPL} \rightarrow \mathbf{TP}}^f} \widehat{\mathbf{M}}_2 \xrightarrow{R_e^f} \widehat{\mathbf{M}}_3 \xrightarrow{R_b^f} \mathbf{R}, \quad (7.8)$$

where the state $\widehat{\mathbf{M}}_3$ lies on the coincidence locus \mathcal{C} . The descriptions of \mathbf{M}_1 and $\widehat{\mathbf{M}}_2$ is similar to the one given in \mathbf{R} -region \mathcal{R}_3^+ .

Riemann solution for \mathcal{R}_5^+

The region \mathcal{R}_5^+ lies below the region \mathcal{R}_4^+ , on the right side of extension $\mathcal{E}_b^+(\gamma_{TL})$. Notice that the region \mathcal{R}_5^+ is adjacent to the region \mathcal{R}_2^+ . The waves in region \mathcal{R}_2^+ are succeeded by a fast b -rarefaction. The Riemann solution is given by:

$$\mathbf{L} \xrightarrow{C_t} \mathbf{M}_1 \xrightarrow{S_{\text{SPL} \rightarrow \text{TP}}^f} \widehat{\mathbf{M}}_2 \xrightarrow{R_b^f} \mathbf{R}, \quad (7.9)$$

where $\widehat{\mathbf{M}}_2$ lies on $\mathcal{E}_b^+(\gamma_{TL})$.

Riemann solution for \mathcal{R}_6^+

The region \mathcal{R}_6^+ is bounded by the wave curves $\mathcal{W}_+^s(\mathbf{w}^L)$, $\mathcal{W}_+^f(\mathbf{P})$ and by the coincidence locus. The solution is:

$$\mathbf{L} \xrightarrow{S_{\text{SPL} \rightarrow \text{TP}}^s} \mathbf{M}_1 \xrightarrow{R_e^f} \mathbf{R}, \quad (7.10)$$

where $\mathbf{M}_1 \in \mathcal{W}_+^s(\mathbf{w}^L)$.

Riemann solution for \mathcal{R}_7^+

In the transition from region \mathcal{R}_6^+ to region \mathcal{R}_7^+ the state \mathbf{w}^R crossed the coincidence locus. The waves in region \mathcal{R}_6^+ are succeeded by a fast b -rarefaction. The Riemann solution is:

$$\mathbf{L} \xrightarrow{S_{\text{SPL} \rightarrow \text{TP}}^s} \mathbf{M}_1 \xrightarrow{R_e^f} \widehat{\mathbf{M}}_2 \xrightarrow{R_b^f} \mathbf{R}, \quad (7.11)$$

where $\widehat{\mathbf{M}}_2$ lies on the coincidence locus \mathcal{C} .

Riemann solution for \mathcal{R}_8^+

The region \mathcal{R}_8^+ is bounded by the wave curve $\mathcal{W}_+^s(\mathbf{w}^R)$, by the e -branch of the Hugoniot locus emanating from \mathbf{w}^G and by the boundary $\{s_o = 1\}$. The Riemann solution in this region is given as:

$$\mathbf{L} \xrightarrow{S_{\text{SPL} \rightarrow \text{TP}}^s} \mathbf{M}_1 \xrightarrow{S_e^f} \mathbf{R}, \quad (7.12)$$

where \mathbf{M}_1 lies on $\mathcal{H}_{\text{SPL} \rightarrow \text{TP}}(\mathbf{w}^L)$.

Riemann solution for \mathcal{R}_9^+

The region \mathcal{R}_9^+ is bounded by the branch $\mathcal{H}_e(\mathbf{w}^G)$, the segment of rarefaction γ_{GQ} and by the double extension $\mathcal{E}_b^-(QO)^2$. The solution is:

$$\mathbf{L} \xrightarrow{S_{\mathbf{SPL} \rightarrow \mathbf{TP}}^s} \widehat{\mathbf{M}}_1 \xrightarrow{R_b^s} \mathbf{M}_2 \xrightarrow{S_e^f} \mathbf{R}, \quad (7.13)$$

where $\widehat{\mathbf{M}}_1$ coincides with state \mathbf{w}^G in Figure 7.1 and \mathbf{M}_2 lies on the segment of rarefaction γ_{QG} .

Riemann solution for \mathcal{R}_{10}^+

The region \mathcal{R}_{10}^+ lies on the right side of the extension $\mathcal{E}_b^-(\gamma_{QG})$, above the double extension $\mathcal{E}_b^-(QO)^2$, on the left side of the boundary $\{s_o = 1\}$. The solution is:

$$\mathbf{L} \xrightarrow{S_{\mathbf{SPL} \rightarrow \mathbf{TP}}^s} \widehat{\mathbf{M}}_1 \xrightarrow{R_b^s} \widehat{\mathbf{M}}_2 \xrightarrow{S_e^s} \mathbf{M}_3 \xrightarrow{S_b^f} \mathbf{R}, \quad (7.14)$$

where $\widehat{\mathbf{M}}_1$ coincides with state \mathbf{w}^G in Figure 7.1, \mathbf{M}_2 lies on the segment of rarefaction γ_{QG} and \mathbf{M}_3 lies on the extension $\mathcal{E}_b^-(\gamma_{QG})$.

Riemann solution for \mathcal{R}_{11}^+

The region \mathcal{R}_{11}^+ lies on the left side of extension $\mathcal{E}_b^-(\gamma_{QG})$, above the isotherm $T = T^Q$. The solution is:

$$\mathbf{L} \xrightarrow{S_{\mathbf{SPL} \rightarrow \mathbf{TP}}^s} \widehat{\mathbf{M}}_1 \xrightarrow{R_b^s} \widehat{\mathbf{M}}_2 \xrightarrow{S_e^s} \mathbf{M}_3 \xrightarrow{R_b^f} \mathbf{R}, \quad (7.15)$$

where $\widehat{\mathbf{M}}_1$ coincides with state \mathbf{w}^G in Figure 7.1, \mathbf{M}_2 lies on the segment of rarefaction γ_{QG} and \mathbf{M}_3 lies on the extension $\mathcal{E}_b^-(\gamma_{QG})$.

Riemann solution for \mathcal{R}_{12}^+

The region \mathcal{R}_{12}^+ lies between the isotherm $T = T^P$ and the isotherm $T^{G'}$ in \mathbf{SPL} . The region \mathcal{R}_{12}^+ is adjacent to the region \mathcal{R}_8^+ , see Figure 6.3. The waves in region \mathcal{R}_8^+ are followed by a compositional contact discontinuity. The Riemann solution is given by:

$$\mathbf{L} \xrightarrow{S_{\mathbf{SPL} \rightarrow \mathbf{TP}}^s} \mathbf{M}_1 \xrightarrow{S_e^f} \mathbf{M}_2 \xrightarrow{C_c} \mathbf{R}, \quad (7.16)$$

where \mathbf{M}_2 lies on the boundary $\{(s_o, T) \in \mathbf{TP} \mid s_o = 1, T^P \leq T \leq T^{G'}\}$.

Riemann solution for \mathcal{R}_{13}^+

The region \mathcal{R}_{13}^+ is bounded by the isotherm $T = T^O$ and by the isotherm $T = T^{G'}$ in \mathbf{SPL} . Region \mathcal{R}_{13}^+ is adjacent to region \mathcal{R}_9^+ . The waves in region \mathcal{R}_9^+ are followed by a compositional contact discontinuity. The Riemann solution is:

$$\mathbf{L} \xrightarrow{S_{\mathbf{SPL} \rightarrow \mathbf{TP}}^s} \widehat{\mathbf{M}}_1 \xrightarrow{R_b^s} \mathbf{M}_2 \xrightarrow{S_e^f} \mathbf{M}_3 \xrightarrow{C_c} \mathbf{R}, \quad (7.17)$$

where \mathbf{M}_3 lies on the boundary $\{(s_o, T) \in \mathbf{TP} \mid s_o = 1, T^{G'} \leq T \leq T^O\}$.

Riemann solution for \mathcal{R}_{14}^+

The region \mathcal{R}_{14}^+ is bounded by the isotherm $T = T^O$ and by the isotherm $T = T^Z$. State $\mathbf{w}^Z \in \mathcal{E}$ is such that the shock speed from \mathbf{w}^Z to state $\mathbf{w}^{Z'} \in \{s_o = 1\} \cap \{T = T^Z\}$ has the same characteristic speed as the compositional speed, defined in Equation (6.18). Region \mathcal{R}_{14}^+ is adjacent to the region \mathcal{R}_{10}^+ . The Riemann solution is:

$$\mathbf{L} \xrightarrow{S_{\mathbf{SPL} \rightarrow \mathbf{TP}}^s} \widehat{\mathbf{M}}_1 \xrightarrow{R_b^s} \widehat{\mathbf{M}}_2 \xrightarrow{S_e^s} \mathbf{M}_3 \xrightarrow{S_b^f} \mathbf{M}_4 \xrightarrow{C_c} \mathbf{R}, \quad (7.18)$$

where \mathbf{M}_4 lies on the boundary $\{(s_o, T) \in \mathbf{TP} \mid s_o = 1, T^O \leq T \leq T^Z\}$.

Riemann solution for \mathcal{R}_{15}^+

The region \mathcal{R}_{15}^+ lies above the isotherm $T = T^Z$ in **SPL** and is adjacent to the region \mathcal{R}_{10}^+ in physical space. The Riemann solution is given by:

$$\mathbf{L} \xrightarrow{S_{\mathbf{SPL} \rightarrow \mathbf{TP}}^s} \widehat{\mathbf{M}}_1 \xrightarrow{R_b^s} \widehat{\mathbf{M}}_2 \xrightarrow{S_e^s} \mathbf{M}_3 \xrightarrow{S_{\mathbf{TP} \rightarrow \mathbf{SPL}}^f} \mathbf{R}, \quad (7.19)$$

where $\widehat{\mathbf{M}}_1$ coincides with state \mathbf{w}^G in Figure 7.1, \mathbf{M}_2 lies on the segment of rarefaction γ_{GQ} and \mathbf{M}_3 lies on the extension $\mathcal{E}_b^-(\gamma_{GQ})$.

7.2 Riemann solutions for **L** in **TP**

In this section we will complete the Riemann solution given in Subsection 6.1.2, repeating the details for readability. We will focus on \mathbf{w}^L states on the right side of the exceptional locus \mathcal{E} between the b inflection locus (Equation (4.46)) and the extension of the boundary $\{s_o = 1\}$. The subdivision of state space into forward **R**-regions is shown in Figure 7.2.

States \mathbf{w}^R above \mathbf{w}^L are reached through a slow e -shock, followed by a fast b -wave. This construction holds for high temperatures. The wave responsible for reaching states \mathbf{w}^R below but nearby \mathbf{w}^L is the e -rarefaction.

The rarefaction curve emanating from \mathbf{w}^L crosses the extension of the boundary:

$$\mathcal{E}_{\partial \mathbf{TP}} = \mathcal{E}_e^-(\{s_o = 1\}), \quad (7.20)$$

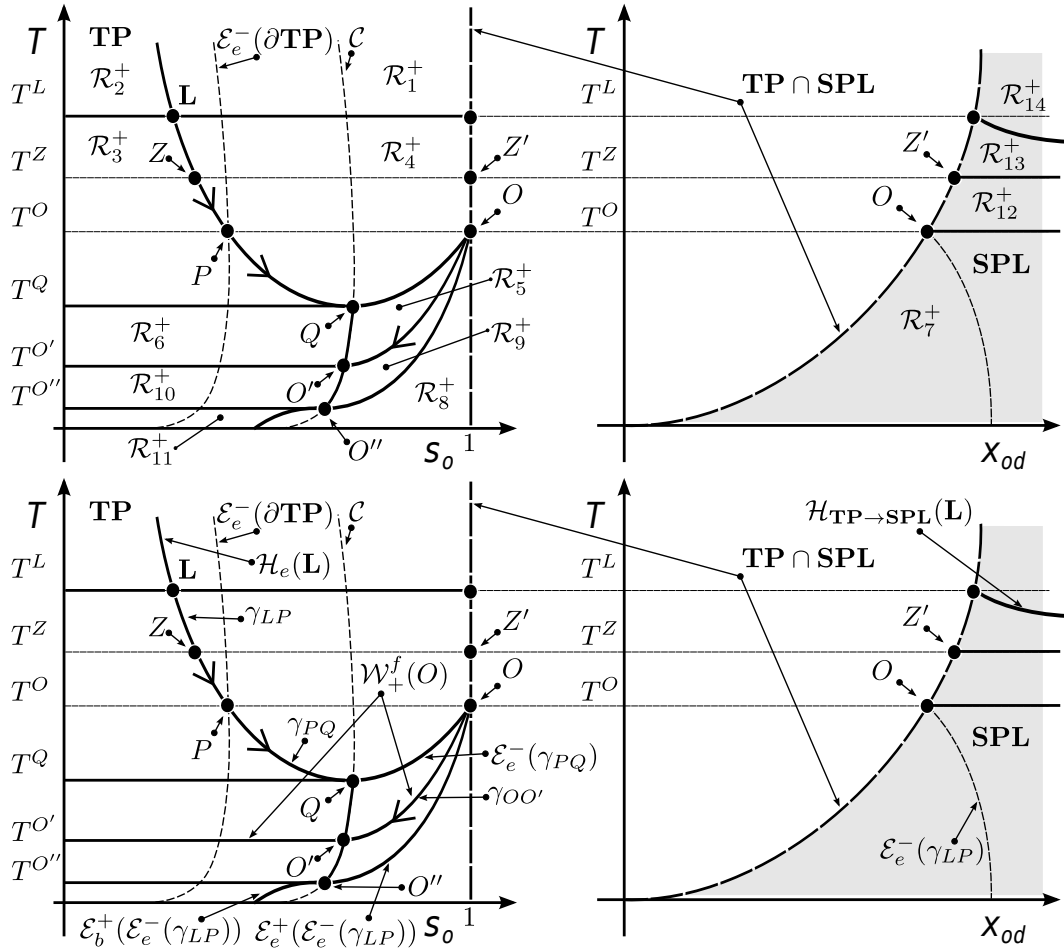


Figure 7.2: Up: forward \mathbf{R} -regions for \mathbf{L} in \mathbf{TP} , between the Buckley-Leverett inflection locus and the extension of the boundary $\mathcal{E}_e^-(\partial\mathbf{TP})$. Down: boundaries. Left: regions and boundaries inside \mathbf{TP} . Right: regions and boundaries inside \mathbf{SPL} . The single phase liquid region is shaded.

at point \mathbf{w}^P and ends at point \mathbf{w}^Q when it intersects the coincidence locus \mathcal{C} , which is also an inflection for the e -rarefaction. We will denote by γ_{PQ} the portion of the rarefaction curve emanating from \mathbf{w}^L between points \mathbf{w}^P and \mathbf{w}^Q , with which we can define the extension $\mathcal{E}_e^-(\gamma_{PQ})$. This extension determines the locus in which fast b -shocks emanating from γ_{PQ} become slow, by Lemma 4.25. We denote by \mathbf{w}^O the intersection point of the isotherm $\{T = T^P\}$ with the boundary $\{s_0 = 1\}$. The segment of the fast forward wave curve $\mathcal{W}_+^f(\mathbf{w}^O)$ emanating from \mathbf{w}^O is an e -rarefaction followed by a b -rarefaction, which we write for later use:

$$R_e^f \longrightarrow R_b^f. \quad (7.21)$$

Inside \mathbf{SPL} , the left extension locus of the rarefaction curve γ_{LQ} is denoted as $\mathcal{E}_e^-(\gamma_{LQ})$.

This extension will be used to construct Riemann solutions for $\mathbf{w}^R = (T^R, x_{od}^R)$ states (in **SPL**) such that $T^R \leq T^O$.

The fast branch of the Hugoniot locus from **SPL** to **TP** together with the right extensions of $\mathcal{E}_e^-(\gamma_{LQ})$ inside **TP**, *i.e.*, $\mathcal{E}_b^+(\mathcal{E}_e^-(\gamma_{LQ}))$ and $\mathcal{E}_e^+(\mathcal{E}_e^-(\gamma_{LQ}))$ will be used to construct Riemann solutions for $\mathbf{w}^R = (s_o^R, T^R)$ states (in **TP**) such that $T^R \leq T^O$, filling the gap left in Subsection 6.1.2.

Riemann solution for \mathcal{R}_1^+

The region \mathcal{R}_1^+ lies on the right side of $\mathcal{H}_e(\mathbf{w}^L)$, the e -branch of the Hugoniot locus emanating from \mathbf{w}^L , above $\{T = T^L\}$. The solution is given by the Lax construction:

$$\mathbf{L} \xrightarrow{S_e^s} \mathbf{M} \xrightarrow{S_b^f} \mathbf{R}, \quad (7.22)$$

where $\mathbf{M} \in \mathcal{H}_e(\mathbf{w}^L) \cap \{T = T^R\}$. In the text that follows we will omit the definition of constant states given by the Lax construction.

Riemann solution for \mathcal{R}_2^+

The region \mathcal{R}_2^+ lies on the left side of $\mathcal{H}_e(\mathbf{w}^L)$, the e -branch of the Hugoniot locus emanating from \mathbf{w}^L , above $\{T = T^L\}$. The solution is:

$$\mathbf{L} \xrightarrow{S_e^s} \mathbf{M} \xrightarrow{R_b^f} \mathbf{R}. \quad (7.23)$$

Riemann solution for \mathcal{R}_3^+

The region \mathcal{R}_3^+ lies on the left side of the e -rarefaction emanating from \mathbf{w}^L , between the isotherms $\{T = T^L\}$ and $\{T = T^Q\}$. The solution is:

$$\mathbf{L} \xrightarrow{R_e^s} \mathbf{M} \xrightarrow{R_b^f} \mathbf{R}. \quad (7.24)$$

Riemann solution for \mathcal{R}_4^+

The region \mathcal{R}_4^+ lies on the right side of the e -rarefaction emanating from \mathbf{w}^L . It is bounded by the aforementioned rarefaction, by the extension $\mathcal{E}_e^-(\gamma_{PQ})$, by the boundary $\{(s_o, T) \in \mathbf{TP} \mid s_o = 1, T^O \leq T \leq T^L\}$ and by the isotherm $T = T^L$. This is the last region in our description to benefit from the Lax construction:

$$\mathbf{L} \xrightarrow{R_e^s} \mathbf{M} \xrightarrow{S_b^f} \mathbf{R}. \quad (7.25)$$

Riemann solution for \mathcal{R}_5^+

The region \mathcal{R}_5^+ is bounded by the extension $\mathcal{E}_e^-(\gamma_{PQ})$, by the coincidence locus \mathcal{C} and by γ_{PQ} , a segment of the rarefaction emanating from \mathbf{w}^L . The construction of extension $\mathcal{E}_e^-(\gamma_{PQ})$, (see Lemma 4.25 and Corollary 4.31) allows us to continue the Riemann solution in the preceding \mathbf{R} -region with a fast e -rarefaction, characteristic with the b -shock. The solution is:

$$\mathbf{L} \xrightarrow{R_e^s} \widehat{\mathbf{M}}_1 \xrightarrow{S_b^f} \widehat{\mathbf{M}}_2 \xrightarrow{R_e^f} \mathbf{R}, \quad (7.26)$$

where $\widehat{\mathbf{M}}_1 \in \gamma_{PQ}$ and $\widehat{\mathbf{M}}_2 \in \mathcal{E}_e^-(\gamma_{PQ})$.

Riemann solution for \mathcal{R}_6^+

In the transition from the forward \mathbf{R} -region \mathcal{R}_5^+ to the forward \mathbf{R} -region \mathcal{R}_6^+ the coincidence locus \mathcal{C} was crossed. Furthermore, this region is bounded by the isotherms $\{T = T^Q\}$ and $\{T = T^P\}$. The Riemann solution is a concatenation of the same type of Riemann solution found for \mathbf{w}^L in region \mathcal{R}_5^+ with a fast b -wave. The solution is:

$$\mathbf{L} \xrightarrow{R_e^s} \widehat{\mathbf{M}}_1 \xrightarrow{S_b^f} \widehat{\mathbf{M}}_2 \xrightarrow{R_e^f} \widehat{\mathbf{M}}_3 \xrightarrow{R_b^f} \mathbf{R}, \quad (7.27)$$

where $\widehat{\mathbf{M}}_3 \in \mathcal{C}$.

Riemann solution for \mathcal{R}_7^+

The region \mathcal{R}_7^+ lies inside \mathbf{SPL} , below the isotherm $T = T^O$. The Riemann solution is:

$$\mathbf{L} \xrightarrow{R_e^s} \widehat{\mathbf{M}}_1 \xrightarrow{S_{\mathbf{TP} \rightarrow \mathbf{SPL}}^s} \mathbf{M}_2 \xrightarrow{C_c} \mathbf{R}, \quad (7.28)$$

where $\widehat{\mathbf{M}}_1 \in \gamma_{LP}$ and $\mathbf{M}_2 \in \mathcal{E}_e^-(\gamma_{LP})$.

Riemann solution for \mathcal{R}_8^+

The region \mathcal{R}_8^+ lies in \mathbf{TP} ; it is adjacent to region \mathcal{R}_7^+ . It is bounded by the two extensions $\mathcal{E}_b^+(\mathcal{E}_e^-(\gamma_{LQ}))$ and $\mathcal{E}_e^+(\mathcal{E}_e^-(\gamma_{LQ}))$. The Riemann solution is:

$$\mathbf{L} \xrightarrow{R_e^s} \widehat{\mathbf{M}}_1 \xrightarrow{S_{\mathbf{TP} \rightarrow \mathbf{SPL}}^s} \mathbf{M}_2 \xrightarrow{S_{\mathbf{SPL} \rightarrow \mathbf{TP}}^f} \mathbf{R}, \quad (7.29)$$

where $\widehat{\mathbf{M}}_1 \in \gamma_{LP}$ and $\mathbf{M}_2 \in \mathcal{E}_e^-(\gamma_{LP})$.

Riemann solution for \mathcal{R}_9^+

The region \mathcal{R}_9^+ is bounded by the coincidence locus \mathcal{C} , the rarefaction $\gamma_{OO'}$ emanating from \mathbf{w}^O and by the extension $\mathcal{E}_e^+(\mathcal{E}_e^-(\gamma_{LQ}))$. The Riemann solution is a concatenation of the same type of solution for region \mathcal{R}_8^+ followed by a fast e -rarefaction:

$$\mathbf{L} \xrightarrow{R_e^s} \widehat{\mathbf{M}}_1 \xrightarrow{S_{\mathbf{TP} \rightarrow \mathbf{SPL}}^s} \mathbf{M}_2 \xrightarrow{S_{\mathbf{SPL} \rightarrow \mathbf{TP}}^f} \widehat{\mathbf{M}}_3 \xrightarrow{R_e^f} \mathbf{R}, \quad (7.30)$$

where $\widehat{\mathbf{M}}_3$ lies on the intersection of the fast branch of the Hugoniot locus from **SPL** to **TP** emanating from \mathbf{M}_2 with extension $\mathcal{E}_e^+(\mathcal{E}_e^-(\gamma_{LQ}))$.

Riemann solution for \mathcal{R}_{10}^+

In the transition from region \mathcal{R}_9^+ to region \mathcal{R}_{10}^+ the coincidence locus was crossed. The Riemann solution is:

$$\mathbf{L} \xrightarrow{R_e^s} \widehat{\mathbf{M}}_1 \xrightarrow{S_{\mathbf{TP} \rightarrow \mathbf{SPL}}^s} \mathbf{M}_2 \xrightarrow{S_{\mathbf{SPL} \rightarrow \mathbf{TP}}^f} \widehat{\mathbf{M}}_3 \xrightarrow{R_e^f} \widehat{\mathbf{M}}_4 \xrightarrow{R_b^f} \mathbf{R}, \quad (7.31)$$

where $\widehat{\mathbf{M}}_4$ lies on the coincidence locus \mathcal{C} .

Riemann solution for \mathcal{R}_{11}^+

The region \mathcal{R}_{11}^+ is adjacent to region \mathcal{R}_8^+ in **TP**. It lies on the right side of extension $\mathcal{E}_b^+(\mathcal{E}_e^-(\gamma_{LQ}))$, below isotherm $T = T^{O''}$. The solution is:

$$\mathbf{L} \xrightarrow{R_e^s} \widehat{\mathbf{M}}_1 \xrightarrow{S_{\mathbf{TP} \rightarrow \mathbf{SPL}}^s} \mathbf{M}_2 \xrightarrow{S_{\mathbf{SPL} \rightarrow \mathbf{TP}}^f} \widehat{\mathbf{M}}_3 \xrightarrow{R_b^f} \mathbf{R}, \quad (7.32)$$

where $\widehat{\mathbf{M}}_3$ lies on $\mathcal{E}_b^+(\mathcal{E}_e^-(\gamma_{LQ}))$.

Riemann solution for \mathcal{R}_{12}^+

The region \mathcal{R}_{12}^+ lies in the **SPL**, it is adjacent to regions \mathcal{R}_4^+ and \mathcal{R}_7^+ . It is bounded by the isotherms $T = T^O$ and $T = T^Z$. The Riemann solution is:

$$\mathbf{L} \xrightarrow{R_e^s} \mathbf{M}_1 \xrightarrow{S_b^f} \mathbf{M}_2 \xrightarrow{C_e} \mathbf{R}, \quad (7.33)$$

where $\mathbf{M}_2 \in \{(s_o, T) \in \mathbf{TP} \mid s_o = 1, T^O \leq T \leq T^L\}$.

Riemann solution for \mathcal{R}_{13}^+

The region \mathcal{R}_{13}^+ is adjacent to region \mathcal{R}_4^+ and lies below $\mathcal{H}_{\mathbf{SPL} \rightarrow \mathbf{TP}}(\mathbf{w}^L)$, the fast branch of the Hugoniot locus from **TP** to **SPL** emanating from \mathbf{w}^L , and above the isotherm

$T = T^Z$. The shock speed between the pair $\mathbf{w}^Z, \mathbf{w}^{Z'}$ (shown in Figure 7.2) equals the compositional characteristic speed in \mathbf{SPL} , defined in Equation (6.18). The Riemann solution is:

$$\mathbf{L} \xrightarrow{R_e^s} \mathbf{M} \xrightarrow{S_{\mathbf{TP} \rightarrow \mathbf{SPL}}^f} \mathbf{R}, \quad (7.34)$$

where \mathbf{M} lies at the e -rarefaction emanating from \mathbf{w}^L .

Riemann solution for \mathcal{R}_{14}^+

The region \mathcal{R}_{14}^+ is adjacent to region \mathcal{R}_1^+ and lies above $\mathcal{H}_{\mathbf{TP} \rightarrow \mathbf{SPL}}(\mathbf{w}^L)$, which is the fast branch of the Hugoniot locus from \mathbf{TP} to \mathbf{SPL} emanating from \mathbf{w}^L . The solution is:

$$\mathbf{L} \xrightarrow{S_e^s} \mathbf{M} \xrightarrow{S_{\mathbf{TP} \rightarrow \mathbf{SPL}}^f} \mathbf{R}, \quad (7.35)$$

where \mathbf{M} lies at $\mathcal{H}_e(\mathbf{w}^L)$.

Bibliography

- [1] A. V. Azevedo, A. J. de Souza, F. Furtado, D. Marchesin, and B. Plohr. The solution by the wave curve method of three-phase flow in virgin reservoirs. *Transp. Porous Media*, 83(1):99–125, 2010.
- [2] K. Aziz. *Petroleum Reservoir Simulation*. Applied Science Publishers, London, 1979.
- [3] H. A. Bethe. On the theory of shock waves for an arbitrary equation of state [Rep. No. 545, Serial No. NDRC-B-237, Office Sci. Res. Develop., U. S. Army Ballistic Research Laboratory, Aberdeen Proving Ground, MD, 1942]. In *Classic Papers in Shock Compression Science*, High-press. Shock Compression Condens. Matter, pages 421–492. Springer, New York, 1998.
- [4] J. Bruining and D. Marchesin. Maximal oil recovery by simultaneous condensation of alkane and steam. *Phys. Rev. E*, 75(3):036312, Mar 2007.
- [5] J. Bruining, D. N. Dietz, A. Emke, G. Metselaar, and J. W. Scholten. Improved recovery of heavy oil by steam with added distillables. In *Proceedings of the 3rd European Meeting on Improved Oil Recovery*, pages 371–378, Rome, 1985.
- [6] J. Bruining, D. W. van Batenburg, H. J. de Haan, R. Quak, and C. T. S. Palmgren. The efficiency of the distillation mechanisms to enhance steamdrive recovery. In *Proceedings of the 4th Symposium on Enhanced Oil Recovery*, pages 887–898, Hamburg, 1987.
- [7] J. Bruining, D. Marchesin, and C. J. Van Duijn. Steam injection into water-saturated porous rock. *Comput. Appl. Math.*, 22(3):359–395, 2003.
- [8] S. E. Buckley and M. C. Leverett. Mechanism of fluid displacement in sands. *Trans. AIME*, 146:187–196, 1942.
- [9] J. D. Cole. On a quasi-linear parabolic equation occurring in aerodynamics. *Quart. Appl. Math.*, 9:225–236, 1951.

-
- [10] J. G. Conlon. A theorem in ordinary differential equations with an application to hyperbolic conservation laws. *Adv. in Math.*, 35(1):1–18, 1980.
- [11] A. Corey, C. Rathjens, J. Henderson, and M. Wyllie. Three-phase relative permeability. *Trans. AIME*, 207:349–351, 1956.
- [12] R. Courant and K. O. Friedrichs. *Supersonic Flow and Shock Waves*. Interscience Publishers, Inc., New York, 1948.
- [13] C. M. Dafermos. *Hyperbolic Conservation Laws in Continuum Physics*, volume 325 of *Grundlehren der Mathematischen Wissenschaften [Fundamental Principles of Mathematical Sciences]*. Springer-Verlag, Berlin, second edition, 2005.
- [14] A. J. de Souza. Stability of singular fundamental solutions under perturbations for flow in porous media. *Mat. Apl. Comput.*, 11(2):73–115, 1992.
- [15] A. J. de Souza and D. Marchesin. Conservation laws possessing contact characteristic fields with singularities. *Acta Appl. Math.*, 51(3):353–364, 1998.
- [16] A. J. de Souza and D. Marchesin. Resonances for a contact wave in systems of conservation laws. *Comput. Appl. Math.*, 17(3):317–341, 1998.
- [17] P. Duhem. *Recherches Sur l'Hydrodynamique*. Nouvelle édition. Avec une préface de J. Kampé de Fériet. Publ. Sci. Tech. Ministère de l'Air, Hors Série, Paris, 1961.
- [18] S. M. Farouq Ali and B. Abad. Bitumen recovery from oil sands, using solvent in conjunction with steam. *J. Cdn. Pet. Tech.*, 15(3):80–90, 1976.
- [19] F. Furtado. *Structural stability of nonlinear waves for conservation laws*. PhD thesis, NYU, 1989.
- [20] I. M. Gel'fand. Some problems in the theory of quasilinear equations. *Amer. Math. Soc. Transl. (2)*, 29:295–381, 1963.
- [21] D. Gilbarg. The existence and limit behavior of the one-dimensional shock layer. *Amer. J. Math.*, 73:256–274, 1951.
- [22] J. Glimm. Solutions in the large for nonlinear hyperbolic systems of equations. *Comm. Pure Appl. Math.*, 18:697–715, 1965.
- [23] E. Hopf. The partial differential equation $u_t + uu_x = \mu u_{xx}$. *Comm. Pure Appl. Math.*, 3:201–230, 1950.

-
- [24] H. Hugoniot. On the propagation of motion in bodies and in perfect gases in particular. II [J. Éc. Polytech. **58** (1889), 1–125]. In *Classic Papers in Shock Compression Science*, High-press. Shock Compression Condens. Matter, pages 245–358. Springer, New York, 1998.
- [25] E. L. Isaacson, D. Marchesin, and B. J. Plohr. Transitional waves for conservation laws. *SIAM J. Math. Anal.*, 21(4):837–866, 1990.
- [26] E. L. Isaacson, D. Marchesin, B. J. Plohr, and J. B. Temple. Multiphase flow models with singular Riemann problems. *Mat. Apl. Comput.*, 11(2):147–166, 1992.
- [27] L. W. Lake. *Enhanced Oil Recovery*. Prentice Hall, 1st edition, 1996.
- [28] W. Lambert. *Riemann solutions of balance system with phase change for thermal flow in porous media*. PhD thesis, IMPA, 2006.
- [29] W. Lambert and D. Marchesin. The Riemann problem for multiphase flows in porous media with mass transfer between phases. *J. Hyperbolic Differ. Equ.*, 6(4):725–751, 2009.
- [30] W. Lambert, D. Marchesin, and J. Bruining. On the Riemann solutions of the balance equations for steam and water flow in a porous medium. *Methods Appl. Anal.*, 12(3):325–348, 2005.
- [31] W. Lambert, D. Marchesin, and J. Bruining. The Riemann solution for the injection of steam and nitrogen in a porous medium. *Transp. Porous Media*, 81(3):505–526, 2010.
- [32] P. D. Lax. Hyperbolic systems of conservation laws II. *Comm. Pure Appl. Math.*, 10:537–566, 1957.
- [33] T. P. Liu. The Riemann problem for general 2×2 conservation laws. *Trans. Amer. Math. Soc.*, 199:89–112, 1974.
- [34] T. P. Liu. The Riemann problem for general systems of conservation laws. *J. Differential Equations*, 18:218–234, 1975.
- [35] A. Majda and R. L. Pego. Stable viscosity matrices for systems of conservation laws. *J. Differential Equations*, 56(2):229–262, 1985.
- [36] D. Marchesin and B. J. Plohr. Wave structure in WAG recovery. *Society Of Petroleum Engineering Journal*, 6(2):209–219, 2001.

- [37] W. J. Moore. *Physical Chemistry*. Longmans Green and Co Ltd, Prentice Hall, 1962.
- [38] R. Natalini. Recent results on hyperbolic relaxation problems. In *Analysis of Systems of Conservation Laws (Aachen, 1997)*, volume 99 of *Surv. Pure Appl. Math.*, pages 128–198. Chapman & Hall/CRC, Boca Raton, FL, 1999.
- [39] O. A. Oleĭnik. Uniqueness and stability of the generalized solution of the Cauchy problem for a quasi-linear equation. *Uspehi Mat. Nauk*, 14(2 (86)):165–170, 1959.
- [40] W. J. M. Rankine. On the thermodynamic theory of waves of finite longitudinal disturbance [Philos. Trans. **160** (1870), part II, 277–288]. In *Classic Papers in Shock Compression Science*, High-press. Shock Compression Condens. Matter, pages 133–147. Springer, New York, 1998.
- [41] Lord Rayleigh. Aerial plane waves of finite amplitude [Proc. Roy. Soc. London Ser. A **84** (1910), 247–284]. In *Classic Papers in Shock Compression Science*, High-press. Shock Compression Condens. Matter, pages 361–404. Springer, New York, 1998.
- [42] B. Riemann. The propagation of planar air waves of finite amplitude [Abh. Ges. Wiss. Göttingen **8** (1860), 43–65]. In *Classic Papers in Shock Compression Science*, High-press. Shock Compression Condens. Matter, pages 109–128. Springer, New York, 1998.
- [43] W. Rudin. *Principles of Mathematical Analysis*. McGraw-Hill Book Co., New York, third edition, 1976. International Series in Pure and Applied Mathematics.
- [44] S. Schecter, D. Marchesin, and B. J. Plohr. Structurally stable Riemann solutions. *J. Differential Equations*, 126(2):303–354, 1996.
- [45] S. Schecter, B. J. Plohr, and D. Marchesin. Classification of codimension-one Riemann solutions. *J. Dynam. Differential Equations*, 13(3):523–588, 2001.
- [46] J. Smoller. *Shock Waves and Reaction-Diffusion Equations*, volume 258 of *Grundlehren der Mathematischen Wissenschaften [Fundamental Principles of Mathematical Sciences]*. Springer-Verlag, New York, second edition, 1994.
- [47] G. G. Stokes. On a difficulty in the theory of sound [Philos. Mag. **xxxiii** (1848), 349–356; *mathematical and physical papers, vol. ii*, Cambridge Univ. Press, Cambridge, 1883]. In *Classic Papers in Shock Compression Science*, High-press. Shock Compression Condens. Matter, pages 71–79. Springer, New York, 1998.

-
- [48] H. L. Stone. Probability model for estimating three-phase relative permeability. *J. Petr. Tech.*, pages 214–218, 1970.
- [49] G. I. Taylor. The conditions necessary for discontinuous motion in gases [Proc. Roy. Soc. London Ser. A **84** (1910), 371–377]. In *Classic Papers in Shock Compression Science*, High-press. Shock Compression Condens. Matter, pages 409–416. Springer, New York, 1998.
- [50] B. Temple. Systems of conservation laws with coinciding shock and rarefaction waves. *Contemporary Mathematics*, 17:141–151, 1983.
- [51] W. S. Tortike and S. M. Farouq Ali. Saturated-steam-property functional correlations for fully implicit thermal reservoir simulation. *Society Of Petroleum Engineering Journal*, 4(4):471–474, 1989.
- [52] R. C. Weast. *CRC Handbook of Chemistry and Physics*. CRC Press, Inc., 58th edition, 1978.
- [53] H. Weyl. Shock waves in arbitrary fluids [Commun. Pure Appl. Math. **ii** (1949), no. 2-3, 103–122]. In *Classic Papers in Shock Compression Science*, High-press. Shock Compression Condens. Matter, pages 497–519. Springer, New York, 1998.
- [54] K. Zumbrun and P. Howard. Pointwise semigroup methods and stability of viscous shock waves. *Indiana Univ. Math. J.*, 47(3):741–871, 1998.
- [55] K. Zumbrun and P. Howard. Errata to: “Pointwise semigroup methods, and stability of viscous shock waves” [Indiana Univ. Math. J. **47** (1998), no. 3, 741–871; MR1665788 (99m:35157)]. *Indiana Univ. Math. J.*, 51(4):1017–1021, 2002.

Appendix A

Physical quantities

A.1 Physical quantities, symbols and values

In this appendix we describe the quantities used in the computation and empirical expressions for the various functions parameter values and units. For convenience we express the heat capacity of the rock C_r in terms of energy per unit volume of *porous medium* per unit temperature, *i.e.*, the factor $1 - \varphi$ is already included in the rock density. All other densities and concentrations are expressed in terms of mass per unit volume of the phase. All enthalpies per unit mass are with respect to the enthalpies at the reference temperature of the components in their standard form. All heat capacities are at constant pressure. All enthalpies in their standard form are zero at the reference temperature.

<i>Physical quantity</i>	<i>Symbol</i>	<i>Value</i>	<i>Unit</i>
Absolute porous rock permeability	k	1.0×10^{-12}	[m ²]
Volatile, dead oil molar weights	M_V, M_D	0.10021, 0.4	[kg/mole]
Total pressure	p^{tot}	1.0135×10^5	[Pa]
Reservoir, injection temperature	T^{ref}, T^{inj}	350, 440	[K]
Boiling point of volatile, dead oil	T_b^V, T_b^d	371.57, ∞	[K]
Volatile, dead oil heat capacities	c_{oV}, c_{oD}	2121, $c_{oV}\rho_V/\rho_D$	[J/kg/K]
Log of volatile oil viscosity	μ_{ov}	$-11.145 + \frac{981.25}{T}$	[Pa s]
Log of dead oil viscosity	μ_{od}	$-13.80 + \frac{3780}{T}$	[Pa s]
Universal gas constant	R	8.31	[J/mole/K]
Pure volatile, dead oil densities	ρ_V, ρ_D	683, 800	[kg/m ³]
Rock porosity	φ	0.38	[m ³ /m ³]

A.1.1 Temperature dependent variables.

We use references Tortike and Farouq Ali [51] and Weast [52] to obtain all the temperature dependent properties below.

The rock enthalpy C_r can be expressed as

$$\begin{aligned} H_r &= C_r (T - \bar{T}), \\ C_r &= (1 - \varphi) \times 3.274 \times 10^6 = 2.03 \times 10^6 \quad J/m^3/K. \end{aligned} \quad (\text{A.1})$$

A conventional choice for the reference temperature is $\bar{T} = 298.15K$. The volatile oil enthalpy $h_{oV}[J/kg]$ and the dead oil enthalpy $h_{oD}[J/kg]$ as a function of temperature are approximated by

$$h_{oV}(T) = c_{oV}(T - \bar{T}), \quad (\text{A.2})$$

$$h_{oD}(T) = c_{oD}(T - \bar{T}). \quad (\text{A.3})$$

where c_{oV} and c_{oD} can be found in Table A.1. The enthalpies are chosen so that the enthalpy of oil per unit volume is independent of composition. Therefore the heat capacity of the oleic phase per unit volume can also be defined independently of composition.

The volatile oil vapor enthalpy $h_{gV}[J/kg]$ as a function of temperature is approximated by

$$h_{gV}(T) = c_{gV}(T - \bar{T}) + \Lambda_V(\bar{T}). \quad (\text{A.4})$$

The enthalpies $h_{oV}(T)$, $h_{oD}(T)$ vanish at the reference temperature $\bar{T} = 298.15K$.

For the evaporation heat $\Lambda_V(T)[J/kg]$ we use Trouton's rule [52]:

$$\Lambda_V(T) = 88.0 \times T_b^V / M_V - (c_{oV} - c_{gV})(T - T_b^V). \quad (\text{A.5})$$

The viscosities of liquid volatile oil μ_{ov} and liquid dead oil μ_{od} can be found from Table A.1. For simplicity, the viscosity of the oil mixture is approximated by:

$$\mu_{mix} = \frac{\rho_{ov}}{\rho_V} \mu_{ov} + \frac{\rho_{od}}{\rho_D} \mu_{od}. \quad (\text{A.6})$$

We assume that that the viscosity of the gas is independent of composition

$$\mu_g = 1.8264 \times 10^{-5} \left(\frac{T}{300} \right)^{0.6}. \quad (\text{A.7})$$